NASA CR-174789

SYSTEM DESIGN AND INTEGRATION OF THE LARGE-SCALE ADVANCED PROP-FAN

By: Brian P. Huth

HAMILTON STANDARD DIVISION

UNITED TECHNOLOGIES CORPORATION

PREPARED FOR

NATIONAL AERONAUTICS AND SPACE ADMINISTRATION

NASA-LEWIS RESEARCH CENTER

CONTRACT NAS3-23051

NASA CR-174789

SYSTEM DESIGN AND INTEGRATION OF THE LARGE-SCALE ADVANCED PROP-FAN

By: Brian P. Huth

HAMILTON STANDARD DIVISION

UNITED TECHNOLOGIES CORPORATION

PREPARED FOR

NATIONAL AERONAUTICS AND SPACE ADMINISTRATION

NASA-LEWIS RESEARCH CENTER

CONTRACT NAS3-23051

1. Report No.	2. Government Accession No.	3. Recipient's Catalog No.
CR-174789		

4. Title and Subtitle	5. Report Date
System Design and Integration of the Large-Scale Advanced Prop-Fan	August, 1986
	6. Performing Organization Code

7. Author(s)	8. Performing Organization Report No.
Brian P. Huth	HSER 9333
	10. Work Unit No.

9. Performing Organization Name and Address	11. Contract or Grant No.
Hamilton Standard Division United Technologies Corporation P.O. Box 1000 Windsor Locks, Connecticut 06096	NAS 3-23051
	13. Type of Report and Period Covered Contractor Report

12. Sponsoring Agency Name and Address	14. Sponsoring Agency Code
National Aeronautics and Space Administration Washington, D.C. 20546	

15. Supplementary Notes

Project Manager, Irving E. Summer, Advanced Turbo Prop
Project Office, NASA Lewis Research Center, Cleveland, Ohio 44135

16. Abstract

In recent years, considerable attention has been directed toward improving aircraft fuel consumption. Studies have shown that blades with thin airfoils and aerodynamic sweep extend the inherent efficiency advantage that turboprop propulsion systems have demonstrated to the higher speed to today's aircraft.

Hamilton Standard has designed a 9-foot diameter single-rotation prop-Fan. It is planned to test the hardware on a static test stand, in low speed and high speed wind tunnels and on a research aircraft. The major objective of this testing is to establish the structural integrity of large scale Prop-Fans of advanced construction in addition to the evaluation of aerodynamic performance and the aeroacoustic design.

This report summarizes the coordination efforts performed to ensure smooth operation and assembly of the Prop-Fan. It also provides a summary of the loads used to size the system components, the methodology used to establish material allowables and a review of the key analytical results.

17. Key Words (Suggested by Author(s))	18. Distribution Statement
Prop-Fan Structural Loads	General Release

19. Security Classif. (of this report)	20. Security Classif. (of this page)	21. No. of Pages	22. Price*
Unclassified	Unclassified	102	

* For sale by the National Technical Information Service, Springfield, Virginia 22161

NASA-C-168 (Rev. 10-75)

CONTENTS

SECTION		PAGE
1.0	SUMMARY	1
2.0	INTRODUCTION	3
3.0	SYSTEM DESIGN LOADS	7
3.1	Blade Loads	7
3.2	Blade Retention Loads	11
3.3	Actuator Loads	15
3.4	Trunnion Loads	19
3.5	Hub Loads	21
3.6	Tailshaft Loads	24
3.7	Spinner Loads	25
4.0	FATIGUE ALLOWABLE METHODOLOGY	31
5.0	SYSTEM STRESS SUMMARY	35
5.1	Hub Arm Stresses	35
5.2	Retention Stresses	35
5.3	Blade Trunnion Stresses	42
5.4	Actuator Stresses	42
5.5	Tailshaft Stresses	47
5.6	Spinner Stresses	47
6.0	COMPARISON OF FINAL DESIGN TO DESIGN SPECIFICATIONS	51
6.1	Blade Requirements	51
6.2	Disc/Retention Requirements	51
7.0	HARDWARE COMPATIBILITY	57
8.0	FAILURE MODE AND EFFECTS ANALYSIS	59
9.0	CONCLUSIONS	71
10.0	APPENDIX	73
10.1	Design Requirements for SR-7L Propeller; 267X-7	73

ILLUSTRATIONS

FIGURE		PAGE
2.1	Large Scale Advanced Prop-Fan (LAP)	4
3.1	System Components	8
3.2	Blade Shank Reactions	9
3.3	Blade Shank Constraints	10
3.4	Trunnion/Actuator Interface	13
3.5	Trunnion Pin Loading	14
3.6	Twisting Moment Vs Blade Angle	17
3.7	Hub Loading	22
3.8	Tailshaft Loading (On Cross-Section)	26
3.9	Propeller Modes of Vibration	27
3.10	Spinner Vibratory Modes and Accelerations	29
4.1	Fatigue Allowable Methodology	32
4.2	Typical Fatigue Allowable (Modified Goodman Diagram)	33
5.1	Hub & Retention Peak Stress Locations	36
5.2	Hub & Tailshaft Surface Tensile Stresses (HCF & Overspeed)	37
5.3	Hub & Tailshaft Surface Tensile Stresses (LCF)	38
5.4	Blade Retention Surface Hertzian Contact Stresses (HCF & Overspeed)	40
5.5	Blade Retention Stresses	41
5.6	Octahedral Subsurface Shear Stress (Hub Raceway & Actuator Wear Plate)	43
5.7	Blade Trunnion & Actuator Yoke Stresses (HCF & Overspeed)	44
5.8	Trunnion Peak Stress Location	45
5.9	Trunnion/Actuator Interface (Peak Stress Locations)	45
5.10	Blade Trunnion & Actuator Yoke Stresses (LCF)	46
5.11	Spinner Stresses (Fore & Aft)	48
5.12	Spinner Stresses (Lateral)	49
6.1	Stall Flutter (H.S. Method)	52
6.2	Stall Flutter (Steinman Method)	53
6.3	Blade Critical Speed Margins	54

1.0 Summary

The coordination efforts to ensure the smooth operation and assembly of the Large-Scale Advanced Prop-Fan took place in two phases. The first phase, the coordination of the design loads at the system interfaces, indicated that although the interface loads were not always consistent, they were conservative. The stresses calculated using these loads indicated that all the system components have adequate life for the Large-Scale Advanced Prop-Fan program, when compared to the applicable material allowables. The allowables are more conservative than a "specimen only" ($X-3\sigma$) approach to fatigue allowables, but Hamilton Standard's 50 years of propeller experience indicates that these allowables are realistic.

In the second step of the coordination effort, relating to the physical dimensions of the hardware at the system interfaces, all design layouts were carefully compared to the final assembly layout and the detail drawings. No interference or assembly problems were found.

The final area of the Prop-Fan program requiring coordination was the Failure Mode and Effects Analysis (FMEA). The FMEA analysis was based on function rather than a detailed part analysis in order to isolate significant problems of a system nature. The FMEA is complete and no problems were uncovered.

2.0 Introduction

In recent years, considerable attention has been directed toward improving aircraft fuel consumption. Studies have shown that the inherent efficiency advantage that turboprop propulsion systems have demonstrated at lower cruise speeds may now be extended to the higher speed of today's turbofan and turbojetpowered aircraft. To achieve this goal, new propeller designs which feature more blades with thin airfoils and aerodynamic sweep are required.

Since 1975, Hamilton Standard has been deeply involved with the NASA Lewis Research Center in the development of the advanced turboprop or Prop-Fan. Many aircraft system studies have been accomplished for a variety of subsonic air transport applications and all these studies have shown significant fuel savings with Prop-Fan propulsion. The fuel savings potential of future Prop-Fan powered aircraft is generally 15-20% for commercial applications and 25-35% for military patrol aircraft compared to equal technology turbofan systems, depending upon the specific application, cruise speed, stage length and other requirements.

To date, several propeller models have been designed, manufactured and subjected to a number of tests. A series of small-scale 0.6223 meter (24.5 inch) diameter model tests have been conducted in both UTRC and NASA wind tunnels and on a modified NASA airplane. These tests have shown that propellers with 8-10 swept blades, high tip speeds and high power loadings can offer increased fuel efficiencies at speeds up to 0.8 Mn.

Under the NASA sponsored Large-Scale Advanced Prop-Fan (LAP) Program, Hamilton Standard designed a 2.743 meter (9-foot) dia. single-rotation Prop-Fan (Figure 2.1) and recently completed the process of manufacturing this system. This hardware was tested at Wright Field and in the ONERA S1 wind tunnel in France. The hardware will be used in a follow-on program where it will be run with an engine on a static test stand, and on a research aircraft. The major objective of this testing is to establish the structural integrity of large-scale Prop-Fans of advanced construction in addition to the evaluation of aero-acoustic performance.

As specified under contract NAS3-23051, the Prop-Fan hub, retention and pitch control system design has been coordinated to ensure proper operation within the spinner envelope. The first step was to verify that the design loads used at the various system interfaces were consistent. The retention transfers the blade centrifugal, bending and shear loads to the hub. The trunnion transfers the blade torsional load to the actuator, and the tailshaft transfers the hub loads to the engine shaft. The loads at these interfaces must, therefore, be consistent. Given sufficient time, complete consistency in the design loads would have been possible. However, the demands of the schedule made this impossible. The components had to be designed in parallel, so the final loads were not usually available when needed. Therefore, some of the loads used to size the component interfaces were best estimates based on a preliminary analysis and previous experience.

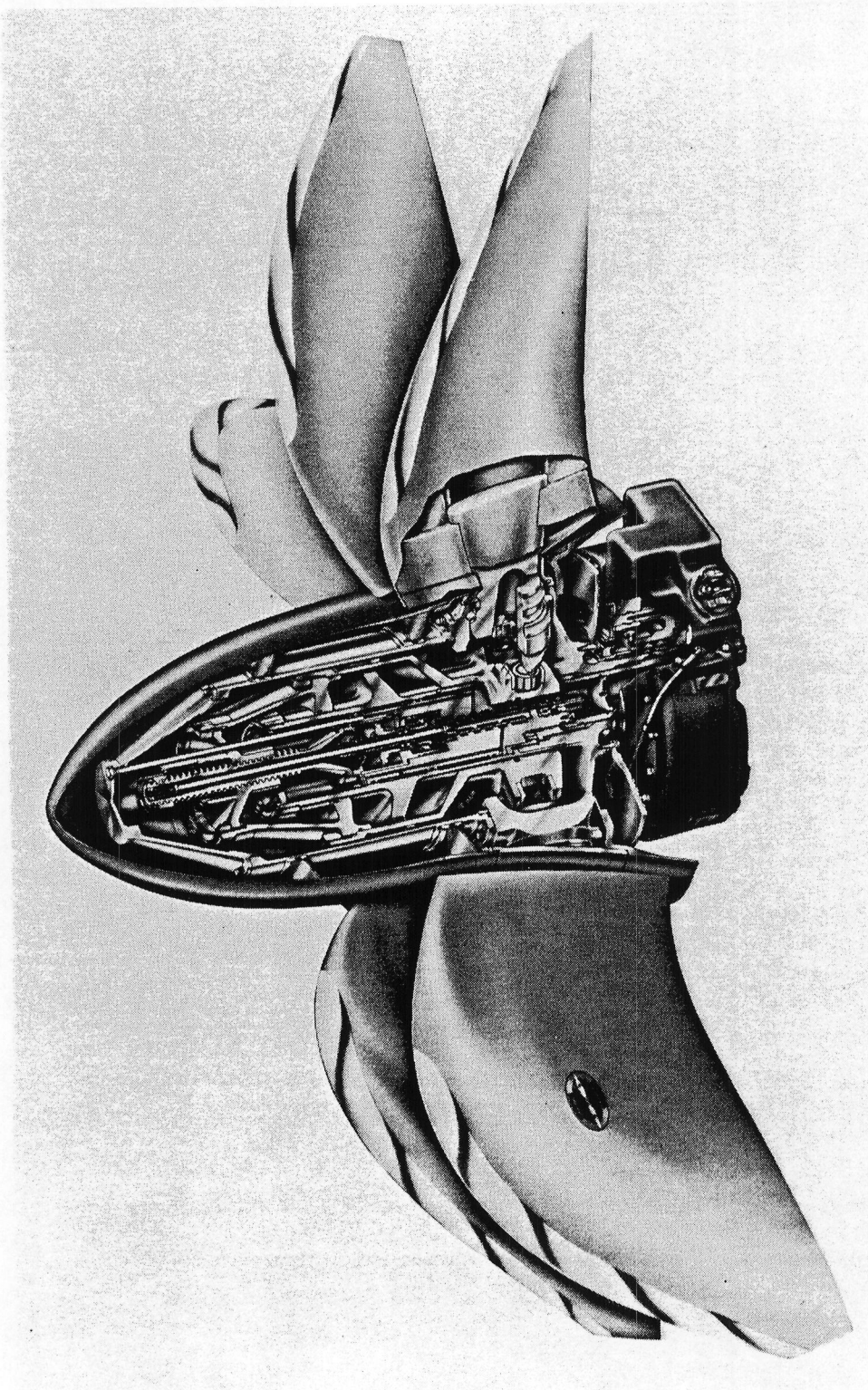

FIGURE 2.1 LARGE SCALE ADVANCED PROP-FAN (LAP)

As the analysis was refined, the loads were revised. As time permitted or if the initial analysis was not conservative, the affected hardware was re-analyzed. If however, the initial load was conservative and the results were acceptable, there was no re-analysis. Thus, the loads used in the analyses were not always consistent but they were conservative.

The second step of the coordination effort related to the physical dimensions of the hardware interfaces. Proper fits and clearances were necessary to ensure smooth operation and assembly of the propeller. A system of formal documents, drawings and design reviews was used to coordinate the flow of information between the design and drafting departments. The system ensured that all design requirements were satisfied.

The final coordination effort was concerned with the interface between the group performing the FMEA (the Operational Effectiveness (OE) group) and the design groups. To perform an accurate FMEA, the OE group needed complete drawings, and a good understanding of how the system operated. The coordination effort ensured the timely transfer of the required information to the OE group.

Nearly all of the results (loads and stresses) reported in this document have been presented in much greater detail in the Design Reports of the individual components. For a more complete discussion of these results, refer to the applicable Design Reports:

1. Large Scale Advanced Prop-Fan (LAP) Blade Design Report, NASA CR174790

2. Large Scale Advanced Prop-Fan (LAP) Hub and Blade Retention Design Report, NASA CR174786

3. Large Scale Advanced Prop-Fan (LAP) Spinner Design Report, NASA CR174785

4. Large Scale Advanced Prop-Fan (LAP) Pitch Change Actuator and Control Design Report, NASA CR174788

3.0 System Design Loads

In this section, the progression of the design loads will be traced through the propeller system (see Figure 3.1). The discussion will be limited to the internal load interfaces. For a complete summary of the loads on a particular component, refer to the applicable component reports. All of the component interfaces, except the spinner/hub interface, were evaluated for low-cycle and high-cycle fatigue and for overstressing at 125% overspeed and 140% overspeed. The loads corresponding to these four cases, and their origins, will be discussed in the following sections. Any inconsistencies in the loads at the system interfaces, will be identified and explained.

3.1 Blade Loads

An external blade definition and the airloads for the important flight conditions were supplied by the aerodynamics group. Using this external definition, a finite element model was created. The airloads were then distributed across the center layer of the finite element grid. BESTRAN, an in-house finite element program, was used to calculate the blade stresses and deflections, as well as the reactions (see Figure 3.2) at the blade retention.

The blade shank was modeled with triangular plate elements to approximate the cylindrical shank configuration. Five spring elements, in the plane of the blade butt-face were used to represent the retention system characteristics. See Figure 3.3. The primary springs controlling most degrees of freedom were attached to the center node (node 4) of the butt-face. A torsional spring of 22.59×10^6 N-M/rad (200.0×10^6 in-lb/rad) and a radial spring of 19.61×10^8 N/M (11.20×10^6 lb/in) were attached to this node. Node 4 was fixed in the in-plane and out-of-plane direction to eliminate all rigid body shear motion.

The nodes that establish the position of the four remaining spring elements did not lie on the shank. All the displacements and rotations at these nodes were tied to node 4, except displacements in the radial direction. Two springs of equal magnitude lie on the out-of-plane (OOP) axis and two lie on the in-plane (IP) axis. The distances between the opposing nodes (610 and 612 out-of-plane, 611 and 613 in-plane) and the radial spring rates at these nodes were carefully chosen to simulate the required rotational spring rates about these axes. A moment about an IP or OOP axis, resolved into radial forces using a 2M/R equivalent, compressed one spring and stretched the other spring to produce the rotation that was consistent with the desired spring rate. The rotational spring rate, $K\theta$, was calculated as follows, $K\theta = M/\theta$. The radial spring rates were, therefore, used to establish the correct rotational spring rates about the in-plane and out-of-plane axes.

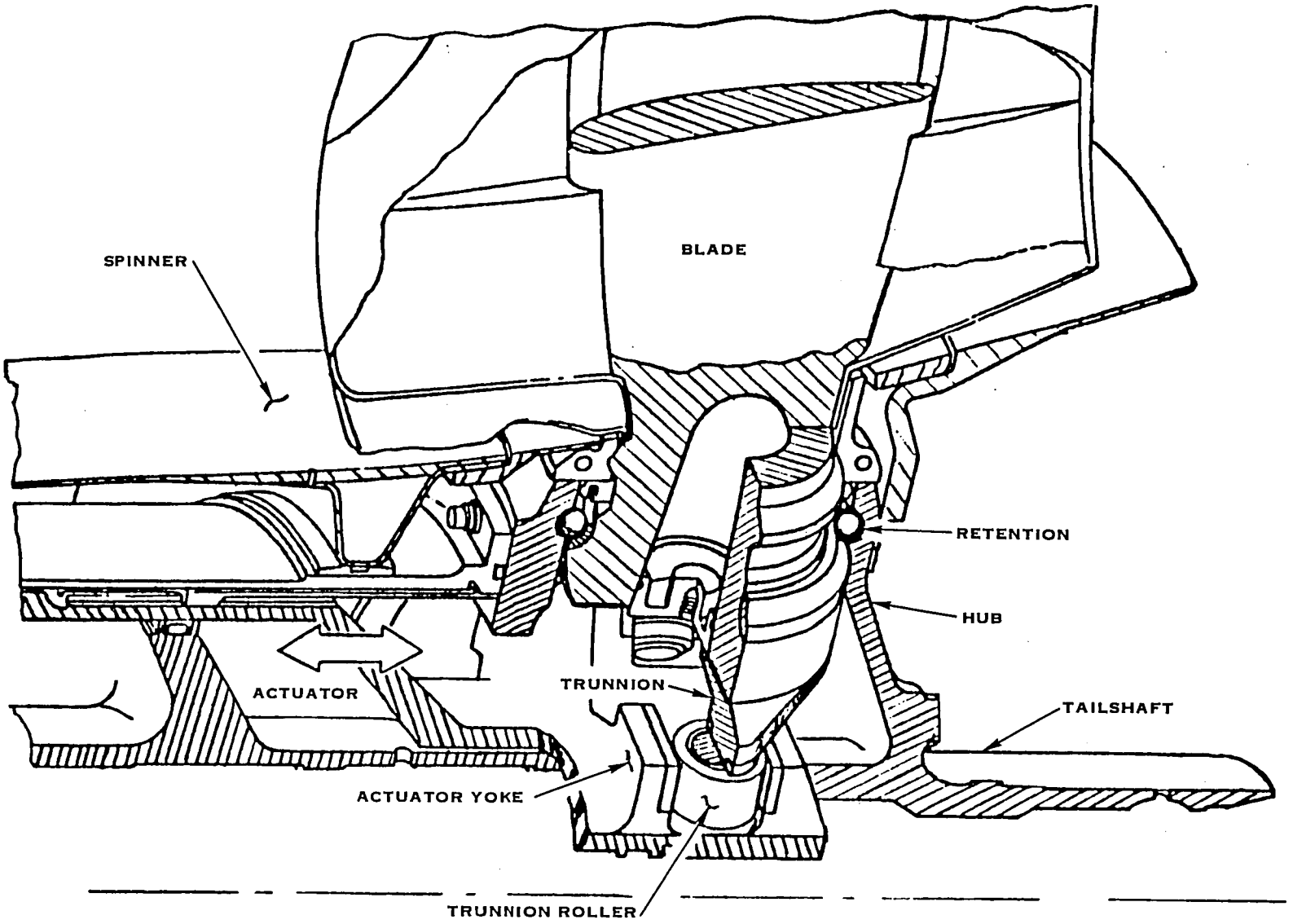

FIGURE 3.1 SYSTEM COMPONENTS

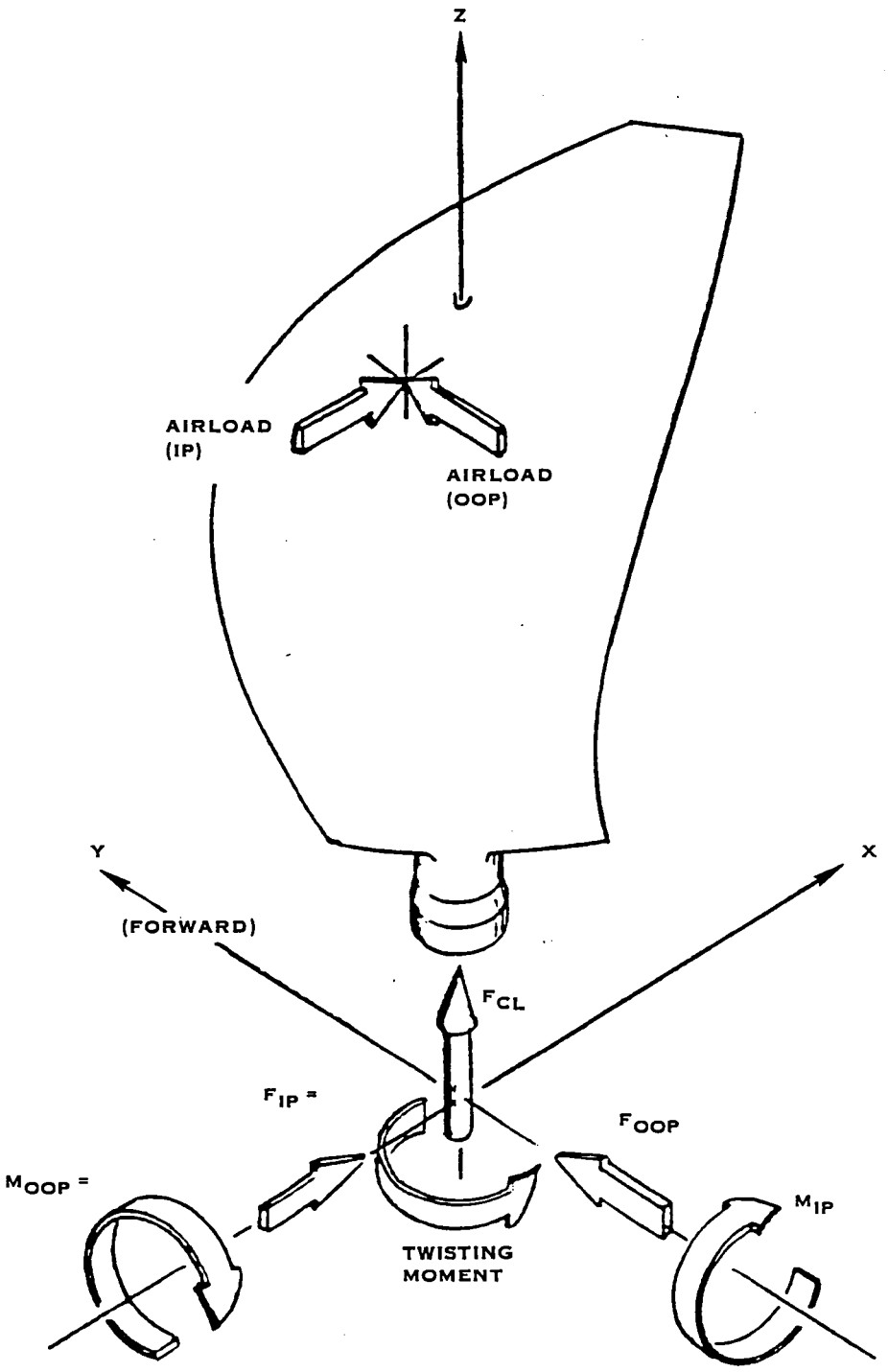

FIGURE 3.2 BLADE SHANK REACTIONS

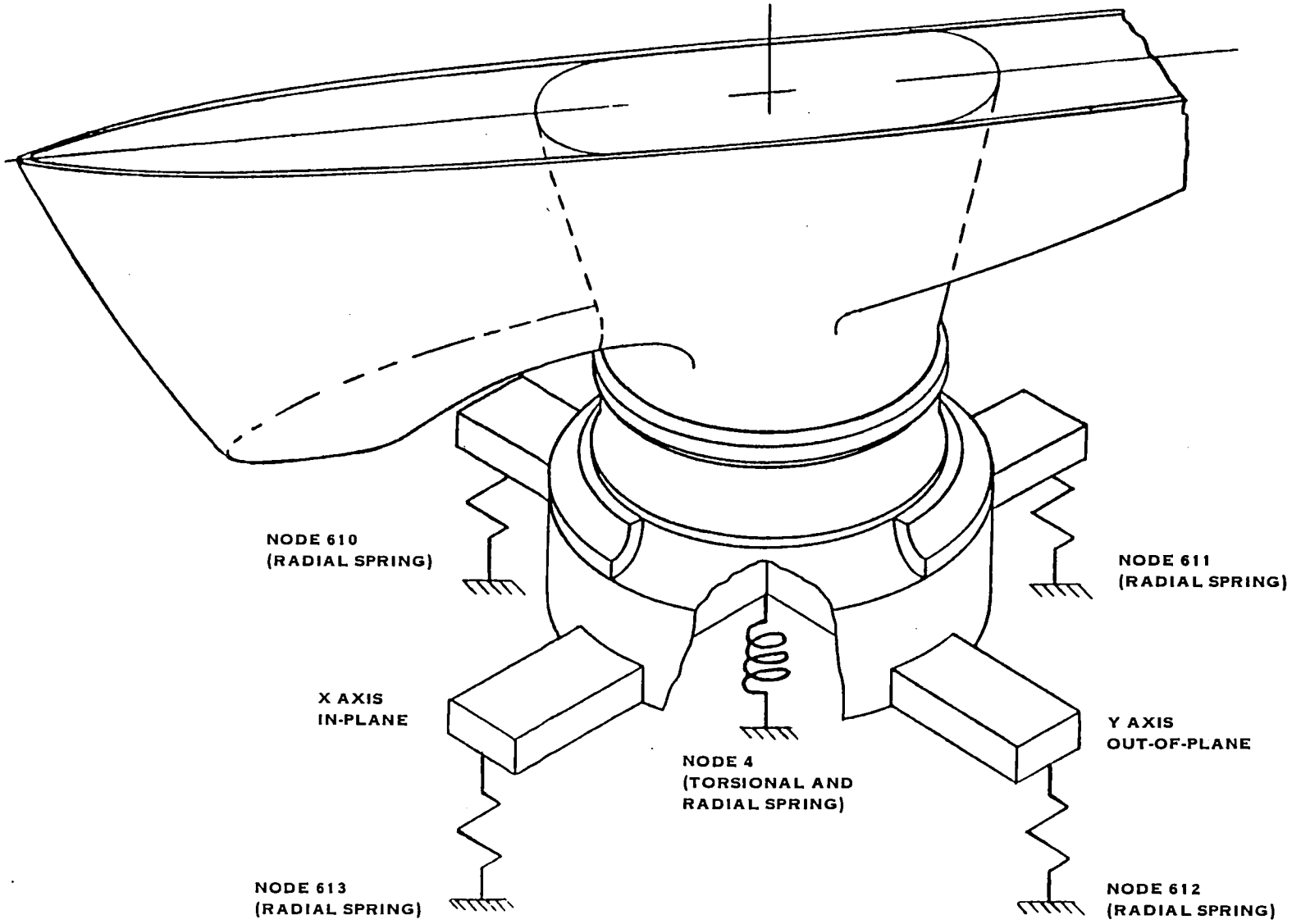

FIGURE 3.3 BLADE SHANK CONSTRAINTS

The radial spring rate at nodes 610 and 612 was 1.88 x 10^8 N/M (1.07 x 10^6 lb/in), which resulted in a rotational OOP spring rate (about the in-plane axis) of 1.51 x 10^6 N-M/RAD (13.41 x 10^6 in-lb/RAD). The IP spring rate (about the out-of-plane axis) was 1.15 x 10^6 N-M/RAD (10.22 x 10^6 in-lb/rad) and was produced by radial spring rates of 1.43 x 10^8 N/M (0.82 x 10^6 lb/in) at nodes 611 and 613. The sum of the five radial springs equaled the total radial spring rate, 26.23 x 10^8 N/M (14.98 x 10^6 lb/in).

The reactions calculated by BESTRAN were used to determine the retention bearing design loads. The following loads were calculated for the 0.2 Mn take-off climb condition. This was the most severe infinite life design condition. The twisting moment from Bestran included the centrifugal twisting moment (CTM) and the aerodynamic twisting moments (ATM) only.

Centrifugal Force - Fc = 353,238 N (79,415 lbs)

Out-of-Plane Moment - Moop = 1,349 $\pm$ 1,960 N-M (11,937 $\pm$ 17,350 in-lbs)

In-Plane Moment - Mip = 1,384 $\pm$ 2,514 N-M (12,248 $\pm$ 22,251 in-lbs)

Out-of-Plane Shear - Foop = 4,132 $\pm$ 4,163 N (929 $\pm$ 936 lbs)

In-Plane Shear - Fip = 8.638 $\pm$ 5,725 N (1,942 $\pm$ 1,287 lbs)

Twisting Moment - TW = 2,174 $\pm$ 239 N-M (19,246 $\pm$ 2,113 in-lbs)

3.2 Blade Retention Loads

The reactions from the BESTRAN analysis had to be adjusted because of differences in the shank modeling relative to the actual hardware. The blade retention was analyzed using a larger centrifugal load, a higher out-of-plane shear load and a higher out-of-plane moment load. The reasons for these increases are explained below.

Although the shank FEA model was an adequate representation of the blade structure down to and including the retention and it's spring rate, it did not reflect the exact shape and mass of all the hardware in the final design. The finite element modeling and most of the analyses had to be completed well in advance of the final retention and pitch change mechanism design. Fortunately, it was possible to analyze the blade without including these components. Therefore, to determine the total centrifugal load on the blade retention, the centrifugal pull on the following items had to be added to, or subtracted from, the load calculated using BESTRAN: 1) the retention bearing (including the balls and inner race), 2) the blade trunnion, trunnion roller and the associated hardware, 3) the shank taper bore (subtracted), 4) the taper bore plug and 5) the blade retaining ring. These adjustments increased the centrifugal load from 353,238 N (79,415 lbs) to 368,694 N (82,890 lbs).

The increased out-of-plane (OOP) retention loads, over those calculated by BESTRAN, were related to the way in which the twisting moments were reacted in the model. As explained in the Blade Loads section, rotations about the pitch change axis were constrained by a fictitious torsional spring at the center node of the BESTRAN shank model. In reality, this motion was prevented by the blade trunnion pin and the pitch change actuator yoke (see Figure 3.4). As shown in Figure 3.5, the trunnion pin was offset 7.62 cm (3.00 in) from the pitch change axis. As the blade tries to rotate about the axis, the pin presses against the yoke and prevents a change in the blade angle setting. The trunnion pin load was, therefore, a function of the total twisting moment (TTM). The total twisting moment is the sum of the centrifugal twisting moment (CTM), the aerodynamic twisting moment (ATM) and the frictional twisting moments (FTM). At mid-stroke, the pin load was equal to the TTM divided by the 7.62 cm (3.00 in) offset (see Figure 3.5). Regardless of the blade angle setting, the trunnion pin force was always in the out-of-plane direction. As the actuator translates fore-and-aft along the engine centerline, the face of the yoke wear plate (see Figure 3.4) remains perpendicular to the out-of-plane axis. As blade angle changes, the trunnion bearing rolls across the yoke face and can only exert a force perpendicular to this face (the OOP direction). The total out-of-plane shear force (Foop in Figure 3.5) was, therefore, the sum of the aerodynamic shear forces (from BESTRAN) and the pin load.

The finite element model was constrained such that all the reactions were calculated at a common radial station. For the retention analysis, it was assumed that this station was coincident with the bearing plane. The bearing plane is defined as the radial location of the center of curvature of the inner race. To simplify the input to the bearing program, the trunnion pin force, which is not actually applied at this location, was resolved into equivalent loads at this location. The trunnion pin reaction occurred 11.05 cm (4.35 in) below the bearing plane (see Figure 3.5). The equivalent loading was an out-of-plane moment equal to 11.05 cm (4.35 in) times the pin load.

Making these adjustments for the 0.2 Mn take-off climb condition, yielded the following results:

Centrifugal Force - Fc = 368,694 N (82,890 lbs)

Out-of-Plane Moment - Moop = 4,178 $\pm$ 1,820 N-M (36,981 $\pm$ 16,111 in-lbs)

In-Plane Moment - Mip = 1,384 $\pm$ 2,513 N-M (12,248 $\pm$ 22,251 in-lbs)

Out-of-Plane Shear - Foop = 32,341 $\pm$ 4,163 N (7,271 $\pm$ 936 lbs)

In-Plane Shear - Fip = 8,638 $\pm$ 5,725 N (1,942 $\pm$ 1,287 lbs)

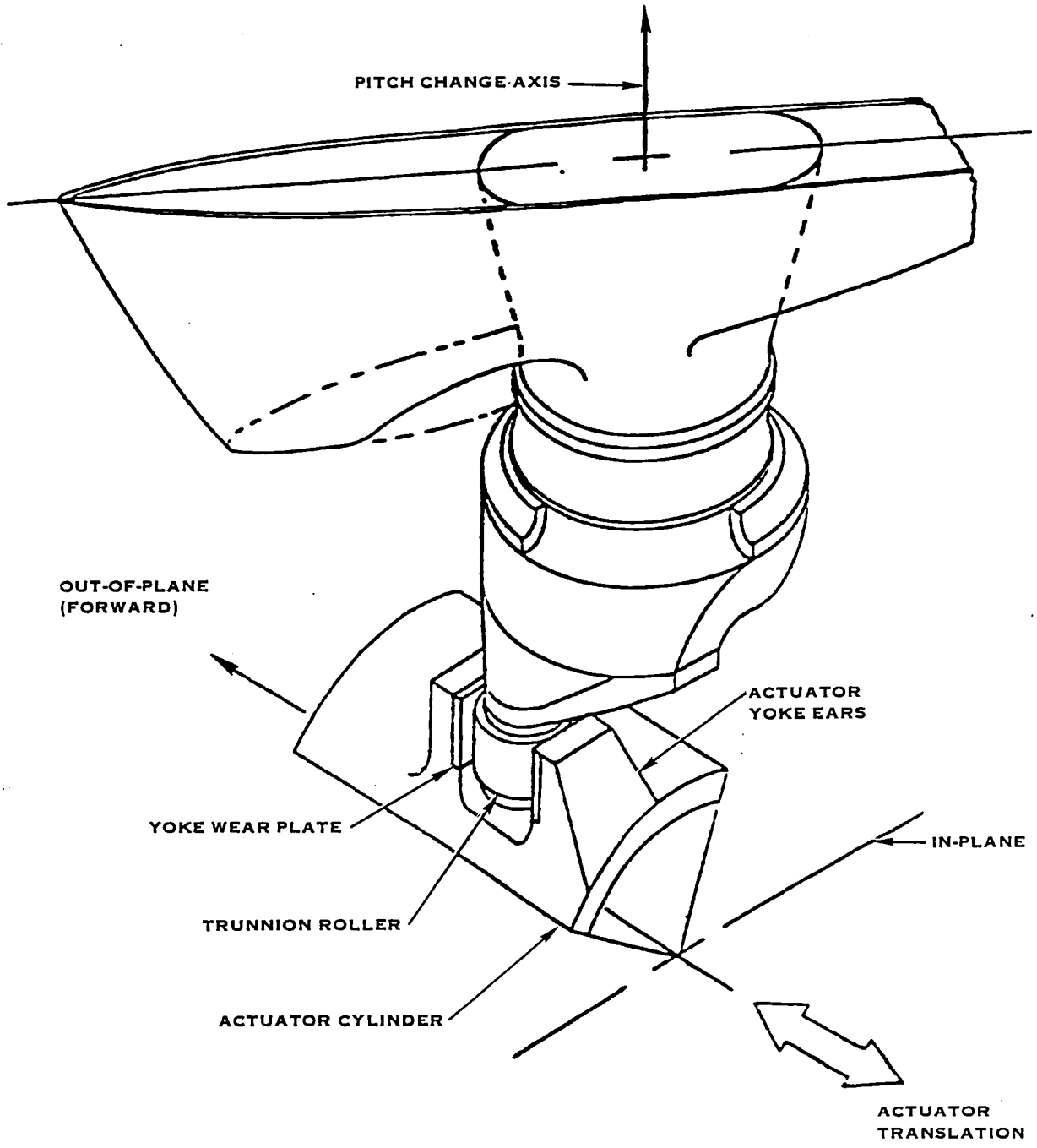

FIGURE 3.4 TRUNNION/ACTUATOR INTERFACE

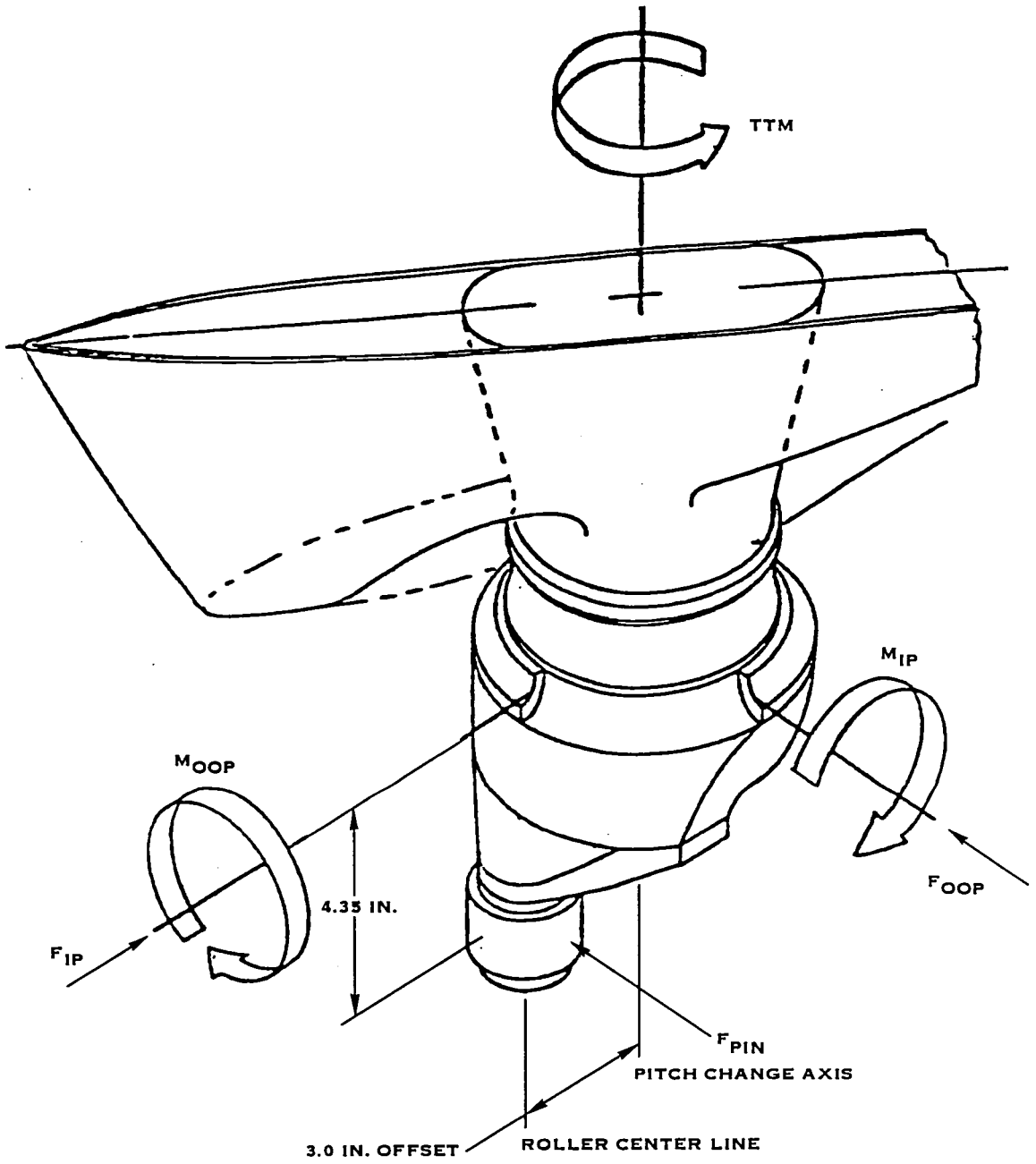

FIGURE 3.5 TRUNNION PIN LOADING

The retention was also analyzed at two overspeed cases, 125% overspeed and 140% overspeed. The significant loads, at these overspeeds, are dependent on the blade angle setting at the time of the overspeed. At a very low blade angle (approaching flat pitch), the steady and cyclic aerodynamic loads are essentially zero. The steady and cyclic body forces are also greatly reduced at these conditions. The retention could therefore be analyzed using only centrifugal load.

However, the blade was analyzed for the overspeed cases at the cruise blade angle of 57.57 degrees. At this blade angle, only the cyclic aerodynamic forces and the cyclic body forces can be neglected. Resolving the BESTRAN reactions into the bearing plane, using the procedure developed for the 0.2 Mn take-off climb condition, produces the following set of retention loads:

125% Overspeed -

Centrifugal Force - Fc = 576,105 N (129,520 lbs)

Out-of-Plane Moment - Moop = 6,266 N-M (55,460 in-lbs)

In-Plane Moment - Mip = 1,537 N-M (13,606 in-lbs)

Out-of-Plane Shear - Foop = 38,902 N (8,746 lbs)

In-Plane Shear - Fip = 8,807 N (1,980 lbs)

140% Overspeed

Centrifugal Force - Fc = 722,622 N (162,460 lbs)

Out-of-Plane Moment - Moop = 7,730 N-M (68,423 in-lbs)

In-Plane Moment - Mip = 1,804 N-M (15,971 in-lbs)

Out-of-Plane Shear - Foop = 48,986 N (11,013 lbs)

In-Plane Shear - Fip = 10,408 N (2,340 lbs)

3.3 Actuator Loads

The pitch change actuator has two basic components, the actuator cylinder and the actuator yoke. The yoke provides the interface between the blades and the pitch change system. This report is only concerned with the system interfaces and, as such, will address only the actuator yoke loads. The yoke consists of essentially two items, the yoke ears, which are an integral part of the actuator cylinder, and the wear plates which are press fit into the yoke ears (see Figure 3.4). These two components were analyzed separately. The yoke ears were analyzed along with the actuator cylinder using H561, a Hamilton Standard finite element shell of revolution program. The subsurface octahedral shear stress in the wear plates was calculated using P248. As explained in the following sections, the same loads were not used in these analyses.

3.3.1 Actuator Wear Plate Loads

For the wear plate analysis, the compressive trunnion pin force on the actuator was calculated directly from the blade total twisting moment (see the Blade Retention section). The blade total twisting moment (TTM) is comprised of three individual components; the centrifugal twisting moment (CTM), the aerodynamic twisting moment (ATM), and the frictional twisting moment (FTM). These four twisting moments are plotted against blade angle on Figure 3.6. All of the load components are propeller speed sensitive. For the wear plate analysis a constant speed, 100% RPM, was assumed.

The ATM is also a function of the flight condition. For most operating conditions, the Prop-Fan ATM is opposite the CTM. Only during a dive, is it additive. Therefore, for conservatism the zero power, sea level dive condition was used in the analysis. This condition produces the highest ATM's reacted by the actuator. These ATM values were supplied by the aerodynamics group for a range of blade angle settings. The ATM curve shown on Figure 3.6 has been multiplied by a 1.20 contingency factor.

To calculate the worst case TTM, the CTM had to be combined with the worst case ATM's. The CTM, at a constant propeller speed, is a function of blade angle only. As shown on Figure 3.6, the CTM peaks at a blade angle setting of approximately 42 degrees. This CTM was derived by modifying the results of the BESTRAN blade analysis at the various conditions analyzed, to subtract out the ATM resulting from the applied airloads at each respective condition. A separate program was written to summarize the ATM at a given flight condition. The ATM was then subtracted from the twisting moment calculated by BESTRAN, for the same flight condition leaving only the centrifugal component. These CTM values were also multiplied by the 1.20 contingency factor and plotted on Figure 3.6.

The FTM is a function of centrifugal load and is, therefore, constant for a given RPM. The FTM was calculated using the following formula: FTM = 0.005 x Centrifugal Load x Bearing Pitch Dia. x 0.500. This component was not multiplied by a contingency factor. The ATM, CTM and FTM were added together to yield the TTM curve shown on Figure 3.6. The peak of the TTM curve occurs at a blade angle of approximately 44 degrees. The individual components of the TTM, at this blade angle, were as follows

TTM = 3,556 N-M (31,474 in-lbs)

CTM = 2,500 x 1.20 = 3,000 N-M (26,556 in-lbs)

ATM = 345 x 1.20 = 414 N-M (3,662 in-lbs)

FTM = 142 N-M (1,256 in-lbs)

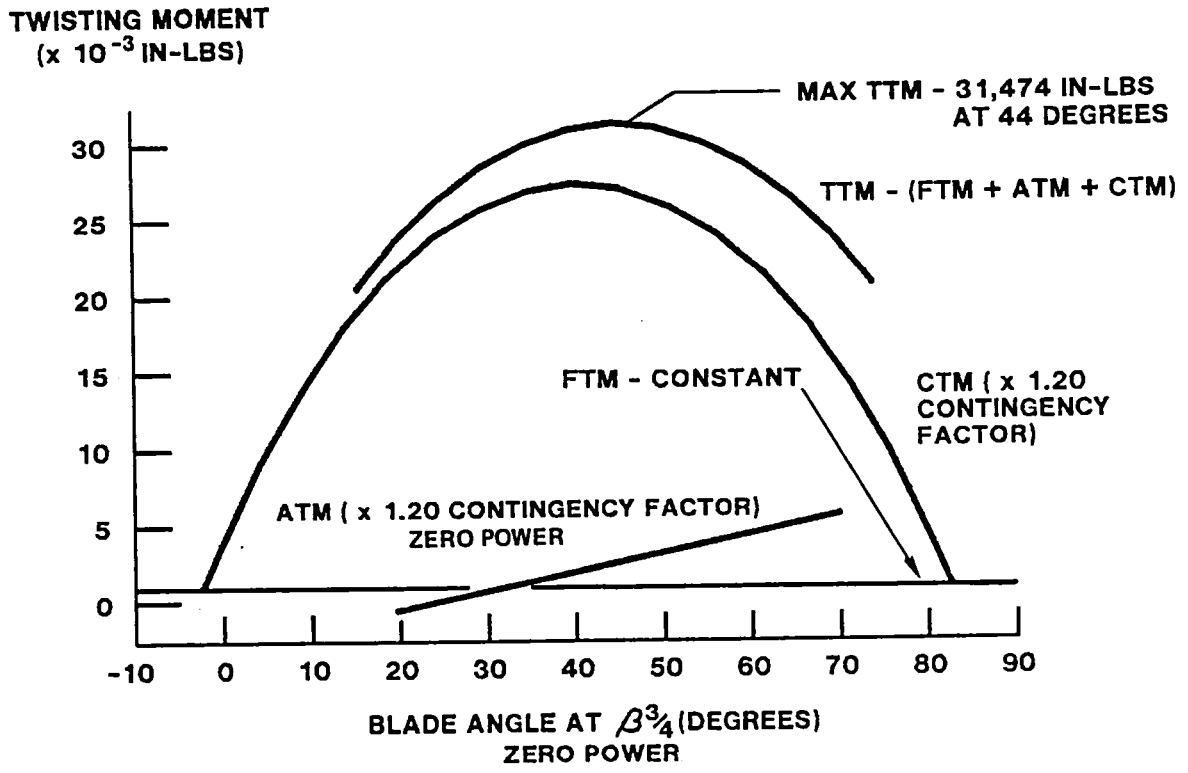

FIGURE 3.6 TWISTING MOMENT VS BLADE ANGLE

From the TTM, the trunnion pin force, which equals the steady compressive load on the wear plates, was calculated. As discussed in the Blade Retention Loads section, the pin load is equal to the TTM divided by the effective distance from the pitch change axis to the trunnion pin centerline. At mid-stroke (blade angle = 38.5 degrees), the effective moment arm is equal to 7.62 cm (3.00 in). As the blade moves away from mid-stroke, the moment arm decreases and the pin force increases. The moment arm is a function of the angular change and is calculated as follows: Effective Moment Arm = 7.62 cm x Cos (38.5 - actual blade angle setting). However, for the wear plate analysis, it was assumed that the blade was at mid-stroke. This simplification is slightly unconservative. Using the actual blade angle at the maximum TTM (44 degrees), would decrease the moment arm to 7.58 cm (2.99 in) and increase the pin load by less than 1%.

Using the full 7.62 cm (3.00 in) moment arm, the maximum steady load on the wear plate was calculated as 46,704 N (10,500 lbs). For the high-cycle fatigue life calculation, it was assumed that the cyclic load on the actuator was equal to 25% of the steady load or 11,676 N (2,625 lbs). Experience has shown this to be a conservative assumption. This appeared to be true of the Prop-Fan blade. The cyclic pin force calculated using the BESTRAN results was only 11% of the steady pin force, for the Take-Off Climb condition, therefore, using 25% was conservative.

The low-cycle fatigue criteria for the Prop-Fan actuator was 10,000 start-stop cycles (zero load, increasing to the maximum load, returning to zero). The loads used for the wear plate LCF analysis were assumed to be one-half the maximum steady load (calculated using the maximum steady TTM), plus or minus one-half the same load. It could be argued that the maximum wear plate load should have been based on the maximum steady load plus the cyclic load, but this is unrealistic. The maximum steady TTM used corresponds to an extreme flight condition; the zero power, sea level dive condition. This condition will not occur 10,000 times during the life of the actuator. A more realistic condition might have been the 0.2 Mn, take-off climb condition. At this condition, the maximum total load (steady plus the cyclic pin load) is 33,955 N (7,634 lbs). The LCF load for this condition, therefore, would have been 16,978 $\pm$ 16,978 N (3,817 $\pm$ 3,817 lbs). The actual load used for the wear plate LCF analysis, 23,352 $\pm$ 23,352 N (5,250 $\pm$ 5,250 lbs), was 28% greater than this load and thus is very conservative. The following table summarized the design loads for the actuator wear plates.

HCF Load (10^8 cycles) = 46,704 $\pm$ 11,676 N (10,500 $\pm$ 2,625 lbs)

LCF Load (5×10^4 cycles) = 23,352 $\pm$ 23,352 N (5,250 $\pm$ 5,250 lbs)

3.3.2 Actuator Yoke Loads

The actuator yoke was analyzed using the loads associated with the actuator pressure spectrum instead of the loads resulting from the blade twisting moments. The yoke was analyzed for both high and low-cycle fatigue. To determine the steady load for the HCF analysis, the maximum actuator

operating pressure was used. The maximum operating pressure is controlled by the pressure relief valve (PRV) pressure. It was conservatively assumed that the actuator would remain at this average pressure while undergoing 10^8 cycles of lesser pressure pulsations. This situation could occur if the retention had failed completely (i.e. the balls and/or races had been crushed) and the blade was unable to change pitch. The cyclic load for the HCF analysis was assumed to be 15% of the PRV pressure. These pressures, 793 N/cm^2 $\pm$ 119 n/cm^2 (1,150 psi $\pm$ 173 psi), were converted to actuator forces by multiplying by the actuator piston area. These forces were divided by the number of blades to get the forces per yoke ear.

The LCF actuator analysis assumed the actuator was subjected to 10,000 start-stop cycles. A start-stop cycle is defined as follows: actuator pressure starts at zero, increases to the high pressure relief valve (HPRV) pressure and returns to zero. This pressure, 948 N/cm^2 (1375 psi), was also converted to an actuator force using the piston area. The steady loads and cyclic loads used in the low-cycle fatigue stress calculation were equal to one-half the maximum load in the cycle (calculated using the HPRV pressure) plus or minus one-half the same load.

It was intended to analyze the actuator yoke at two overspeed loads, 125% and 140% overspeed, but these loads were not included in the actuator pressure spectrum. However, the pressure spectrum did include an actuator proof-test pressure which produced higher yoke loads than either overspeed cases. This load, 102,082 N (22,950 lbs), is 52% greater than the 125% overspeed load and 21% greater than the 140% RPM load. Clearly, if the actuator can survive the proof-test load, it could survive either overspeed loads. The following table summarizes the actuator yoke design loads.

HCF Load (10^8 cycles) = 69,055 $\pm$ 10,512 N (15,525 $\pm$ 2,363 lbs)

LCF Load (10^4 cycles) = 41,281 $\pm$ 41,281 N (9,281 $\pm$ 9,281 lbs)

Proof-Test Load (1 cycle) = 102,082 N (22,950 lbs)

3.4 Blade Trunnion Loads

The blade trunnion was designed in conjunction with the actuator wear plates, so the same methods were used to determine the appropriate TTM's. As discussed in the Actuator Loads section, the max TTM occurred at a blade angle setting of 44 degrees, but for the analysis it was assumed that the trunnion was at mid-stroke. The loads used in the trunnion HCF and LCF analyses for this condition, were the same as those used in the wear plate analyses.

The trunnion was also analyzed for low-cycle and high-cycle fatigue at two additional blade angle settings, the High Speed Cruise angle, 57.57 degrees, and the Take-Off Climb angle, 38.3 degrees. The same methods were used to determine the maximum TTM at the appropriate blade angles. Most of the same assumptions (i.e. cyclic portion of the HCF load equals 25% of the steady

load and the maximum total load used in the LCF analysis equals the maximum steady load) were used to calculate the trunnion loads. The pin loads, however, were calculated using the actual blade angles. The following table contains the pertinent design loads for these conditions.

Condition (blade angle)	HCF Loads	LCF Loads
*Max TTM (38.5 degrees)	53,376 ± 13,344 N (12,000 ± 3,000 lbs)	26,688 ± 26,688 N (6,000 ± 6,000 lbs)
Max TTM (38.5 degrees)	46,704 ± 11,676 N (10,500 ± 2,625 lbs)	23,352 ± 23,352 N (5,250 ± 5,250 lbs)
Cruise (57.4 degrees)	46,254 ± 8,896 N (10,400 ± 2,000 lbs)	23,130 ± 23,130N (5,200 ± 5,200 lbs)
Take-off (38.5 degrees)	49,818 ± 12,454 N (11,200 ± 2,800 lbs)	24,909 ± 24,909N (5,600 ± 5,600 lbs)

*Trunnion loads prior to CTM curve revision.

For the initial trunnion analysis, the steady TTM used was 4,011 N-M (35,500 in-lbs). The TTM curve was subsequently revised downward to reflect a reduction in the CTM curve, and the maximum TTM was reduced to 3,556 N-M (31,474 in-lbs). Some of the trunnion stresses were recalculated at the reduced loads to increase the stress margins. The stresses calculated using the overly conservative TTM curve were not re-evaluated if they resulted in acceptable stress margins.

The trunnion overspeed analyses were performed using the following loads; 67,254 N (15,120 lbs) at 125% RPM and 84,512 N (19,000 lbs) at 140% overspeed. The loads were calculated using the curves shown on Figure 3.6. At the overspeed blade angle, 57.57 degrees, the CTM, ATM and the FTM were 2,655 N-M (23,500 in-lbs), 587 N-M (5,200 in-lbs) and 142 N-M (1,256 in-lbs) respectively. These moments were increased as the square of the prop speed. At 125% RPM the moments were multiplied by 1.563 (1.25^2); at 140% RPM, the factor was 1.960 (1.40^2). The overspeed twisting moments and the resulting pin forces were as follows:

Component	125% RPM	140% RPM
CTM	4,147 N-M (36,710 in-lbs)	5,204 N-M (46,060 in-lbs)
ATM	917 N-M (8,120 in-lbs)	1,151 N-M (10,190 in-lbs)
FTM	-221 N-M (-1,960 in-lbs)	-278 N-M (-2,460 in-lbs)

TTM	4,845 N-M (42,890 in-lbs)	6,077 N-M (53,790 in-lbs)
Fpin	67,254 N (15,120 lbs)	84,512 N (19,000 lbs)

During an overspeed, the actuator is not required to change pitch, so the frictional component (FTM component) reduces the total twisting moment reacted by the trunnion pin. The FTM is, therefore, shown with a negative sign in the table. The pin loads were determined by dividing the TTM by the effective moment arm. The effective moment arm for both overspeed cases was 7.20 cm (2.835 in).

3.5 Hub Loads

The blade loads are transferred to the hub through the blade retention. Some of the loads, such as the centrifugal load, are absorbed by the hub. Other loads are transmitted through the hub tailshaft to the engine shaft. Ideally, the same loads should be used to analyze the mating components at these interfaces, but this was not possible at the hub/blade retention interface.

The hub analysis was started long before the blade loads were finalized. The hub spring rate was needed to determine the blade loads, so the loads used to analyze the hub were based on preliminary calculations. The orientation of these loads and the hub arm finite element model can be seen on Figure 3.7. The hub was analyzed for high and low cycle fatigue at the 0.2 Mn, take-off climb condition and for over-stressing at 140% overspeed. Only the centrifugal load was applied to the hub for the overspeed analysis. The following loads were used in the hub analysis.

Centrifugal Force - Fc = 384,307 N (86,400 lbs)

Out-of-Plane Moment - Moop = 1,349 $\pm$ 1,960 N-M (11,937 $\pm$17,350 in-lbs)

In-Plane Moment - Mip = 1,384 $\pm$ 2,514 N-M (12,248 $\pm$ 22,251 in-lbs)

140% Overspeed - Fc = 753,224 N (169,340 lbs)

The centrifugal load and the out-of-plane moment load above are not consistent with the loads used in the retention analysis. The blade centrifugal load, as calculated by BESTRAN, has been adjusted to include all the retention and pitch change hardware (see the Blade Retention Loads section). One addition to the BESTRAN centrifugal load was the pull of the blade trunnion. The blade trunnion weight was estimated at 37.81 N (8.50 lbs) for the initial centrifugal load calculation, but the final trunnion weighs only 14.10 N (3.17 lbs). This revision, in conjunction with a minor change to the taper bore, reduced the centrifugal load above to 368,695 N (82,890 lbs) (see the Blade Retention Loads summary - Section 3.2).

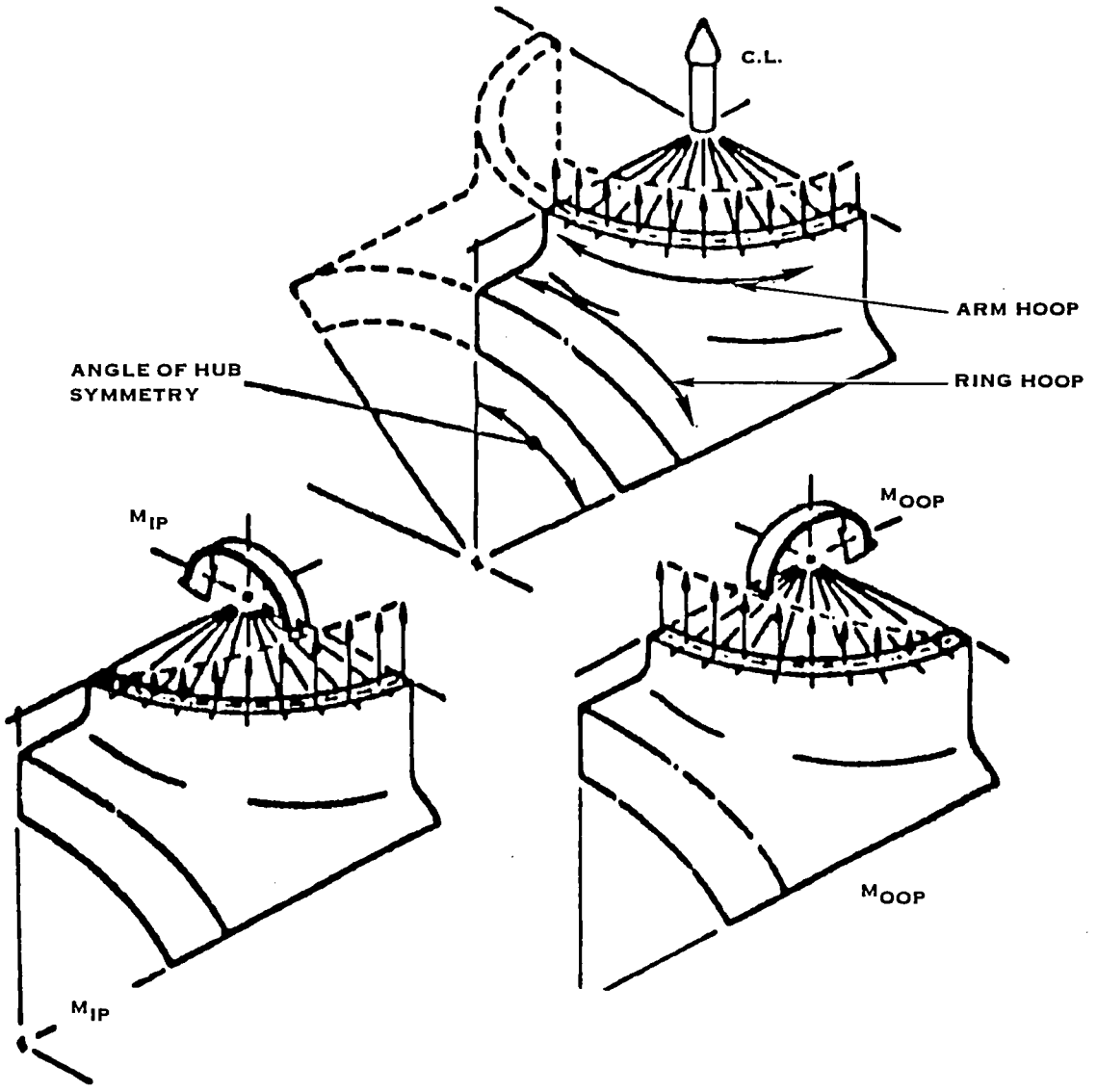

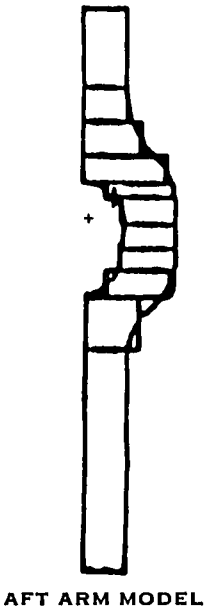

AFT ARM MODEL

FIGURE 3.7 HUB LOADING

On previous designs, the direction of the moment produced by the trunnion pin force was small and opposite to that of the centrifugal restoring moment. The net result was a reduction in the steady bending moment on the hub and retention. Neglecting this moment usually adds conservatism to the analysis. It was erroneously assumed that the Prop-Fan blade would behave in the same manner. However, it did not, and the pin force moment was additive.

Moreover, the magnitude of the trunnion pin force was much higher than that encountered on normal propellers. This occurred because the centrifugal twisting moment for swept blades is much higher than that of straight blades. Adding the moment due to the pin force, therefore, had a significant impact on the OOP bending moment. As discussed in the Blade Retention Loads section, the pin load increased the steady out-of-plane bending moment from 1,349 N-M (11,937 in-lbs) to 4,178 N-M (36,981 in-lbs). Future designs could be improved by reversing the direction of actuation or restacking the blade to significantly reduce this load.

Past experience has also shown that the shear loads are usually not important in the hub analysis. However, the pin forces have never been as large as they are on the Prop-Fan blade. Shear forces of this magnitude Foop = 32,341 $\pm$ 4,163 N (7,271 $\pm$ 936 lbs) and Fip = 8,638 $\pm$ 5,725 N (1,942 $\pm$ 1,287 lbs), would increase the barrel arm stresses to a small extent.

If the hub stresses had not had such a significant margin of safety (see Figure 5.2), the increase in stress due to the neglected loads could have been a problem. The hub stresses were due primarily to the centrifugal load. The effect of the additional steady moment was evaluated by resolving it into an equivalent centrifugal load, using a 2M/R distribution. 2 M/R is a 2 ball approximation of a bearing which relates overturning moment to an equivalent axial force. This increased the load from 384,307 N (86,400 lbs) to *442,224 N (99,421 lbs), [368,695 + 2(4,178-1,349) / 7.70 x 10 (2m/r equivalent where r=7.70cm)] a 15% increase. The hub stress varied linearly with load. At the most highly stressed point, the steady load could be increased by 25% and still meet the infinite life stress limit. The increase in stress due to the inclusion of the pin load was, therefore, well within the stress limits. See Section 6.0 for a complete discussion of the system stresses.

As anticipated, the hub stresses were low because the hub has been sized by spring rate requirements. The spring rates were not sensitive to the magnitude of the applied loads, so they were not affected by the trunnion pin load. The bending rates of seven individual components were combined as springs in parallel to determine the total in and out-of-plane bending spring

rates. These spring rates (see the following table), were then degraded using empirically determined factors (0.77 in-plane and 0.89 out-of-plane) to the values found in the Blade Loads section.

Prop-Fan Hub Spring Rates

	In-Plane ($\times 10^{-6}$)	Out-of-Plane ($\times 10^{-6}$)
Blade	18.64 N-M/RAD (165.0 IN-LB/RAD)	18.64 N-M/RAD (165.0 IN-LB/RAD)
Blade/Race	24.52 N-M/RAD (217.0 IN-LB/RAD)	24.52 N-M/RAD (217.0 IN-LB/RAD)
Race	98.97 N-M/RAD (876.0 IN-LB/RAD)	98.97 N-M/RAD (876.0 IN-LB/RAD)
Ball Bearing	3.12 N-M/RAD (27.65 IN-LB/RAD)	3.12 N-M/RAD (27.65 IN-LB/RAD)
Barrel Arm	76.26 N-M/RAD (675.0 IN-LB/RAD)	76.26 N-N/RAD (675.0 IN-LB/RAD)
Barrel Bridge	41.80 N-M/RAD (370.0 IN-LB/RAD)	---- ----
Barrel Rings	8.02 N-M/RAD (71.0 IN-LB/RAD)	7.57 N-M/RAD (67.0 IN-LB/RAD)
Total	1.50 N-M/RAD (13.27 IN-LB/RAD)	1.70 N-M/RAD (15.04 IN-LB/RAD)
Degraded	1.15 N-M/RAD (10.22 IN-LB/RAD)	1.51 N-M/RAD (13.41 IN-LB/RAD)

3.6 Tailshaft Loads

The hub tailshaft provides the coupling between the engine shaft and the hub. It transfers the blade thrust, torque and 1P bending moment to the shaft. The tailshaft also absorbs a portion of the centrifugal load. This radial load is transmitted through the web connecting the tailshaft to the barrel arms. To simulate this radial load in the finite element model, a constant radial deflection field was applied to the web (see Figure 3.8). Web deflections were calculated during the hub arm and bridge analysis.

Cone seats are used to lock the hub on the engine shaft. The cones eliminate the radial and axial clearances between the shafts. This ensures the smooth transfer of loads from the hub to the engine shaft. A large nut is threaded on the engine shaft to provide the necessary wedging force. The nut is pre-

loaded to maintain a tight fit at the cone seats and react the blade thrust loads. The following loads and deflections were used for the 0.20 Mn, take-off climb condition (see Figure 3.8 for the proper load orientation).

Blade Thrust = 32,995 N (7,418 lbs)

Shaft Torque = 25,159 N-M (222,700 in-lbs)

1P Shaft Moment = 8,643 N-M (76,500 in-lbs)

Web Radial Deflection = 0.0036 cm (0.0014 in)

Preload = 298,906 N (67,200 lbs)

These loads were supplied by a number of sources. The blade thrust and torque loads were supplied by the Aerodynamics group. The Prop-Fan thrust and torque loads were approximately equal to the thrust and torque produced by the 54460 propeller. The 54460 is an existing Hamilton Standard propeller that has been in service for many years. Because of the similarities in the loads, the Prop-Fan tailshaft was made identical to the 54460 tailshaft. The shaft nut preload used in the analysis was also equal to the 54460 load. The 1P shaft moment was calculated by the vibrations analysis group and was approximately one-half of the 54460 shaft moment. This is mostly due to the smaller diameter of the Prop-Fan, 9 ft. vs. 13.5 ft., and the resulting smaller moment arm for the cyclic loads. The 1P shaft moment reflects the difference in the aerodynamic loads caused by a non-uniform flow field such as occurs when the prop axis is inclined during a climb condition. Flow disturbances can also arise from Prop-Fan installation geometry, i.e. proximity to the fuselage, or operation in front of a swept wing. The moment is applied as a cyclic moment because the shaft rotates in a steady moment field.

3.7 Spinner Loads

An aircraft propeller vibrates in three primary modes: (1) the whirl mode, (2) the symmetrical mode and (3) the reactionless mode (see Figure 3.9). All of these modes can occur in one revolution and the type of excitation that occurs for a given P-order (integer multiple of propeller rotational speed), is a function of the number of blades. The magnitude of the excitation is dependent on the P-order, but the 1P excitation is by far the strongest of the excitations.

The Prop-Fan vibrations are transferred to the spinner through the spinner bulkheads. The rear bulkhead is bolted to the aft surface of the hub arms. A total of sixteen bolts are used; two per hub arm. Additional radial O-rings are mounted on the OD of the actuator dome.

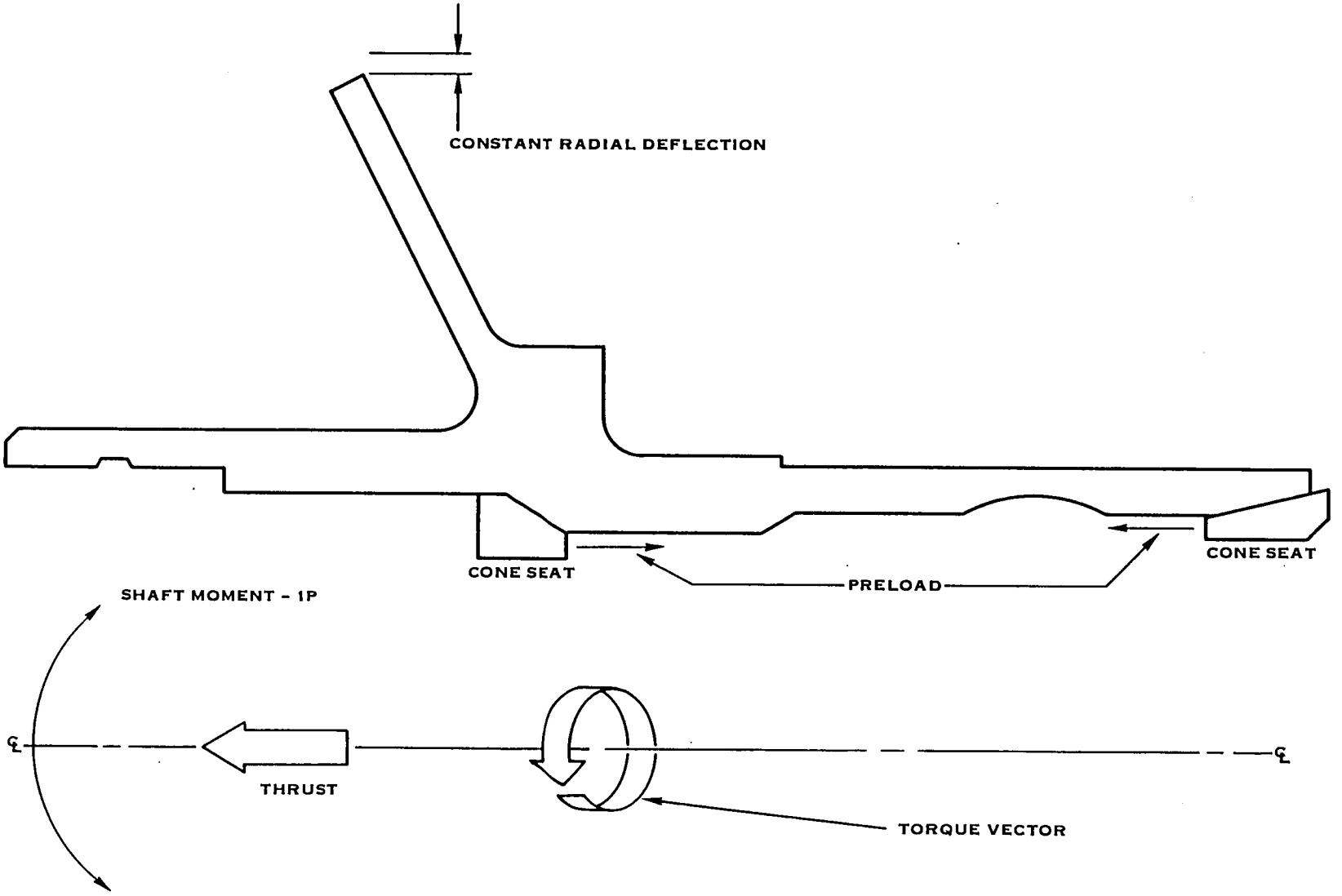

FIGURE 3.8 TAILSHAFT LOADING (ON CROSS-SECTION)

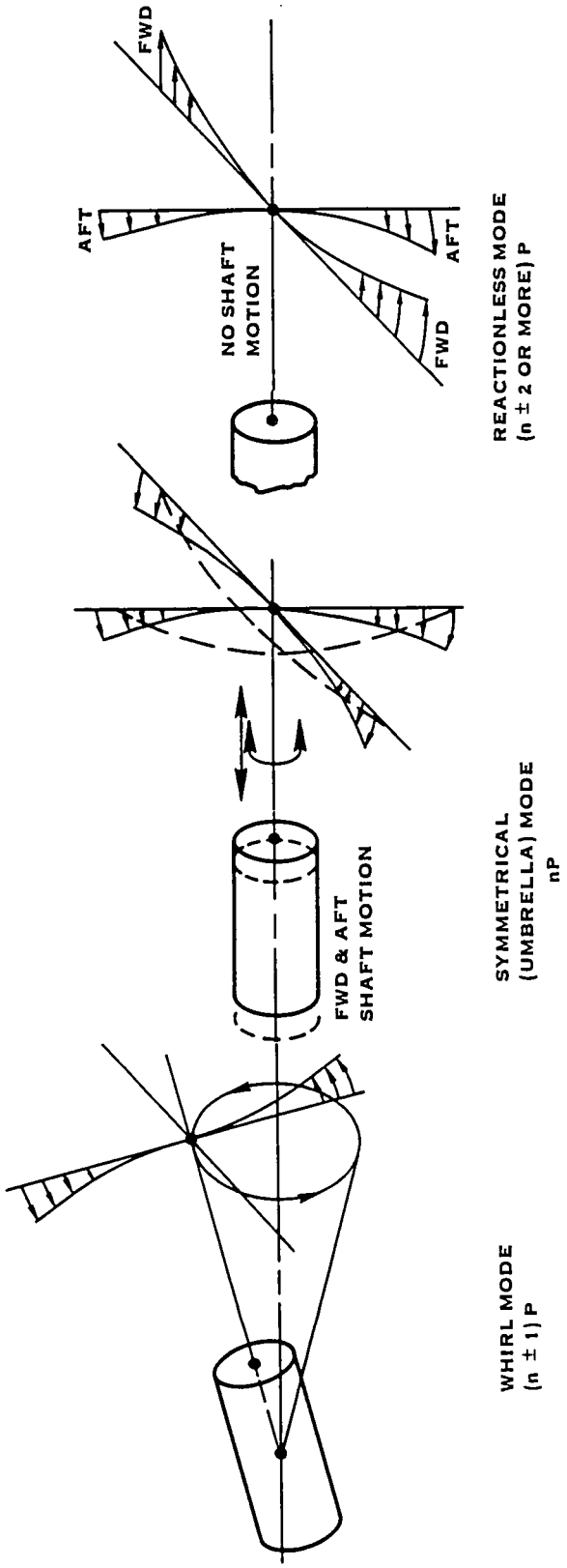

FIGURE 3.9 PROPELLER MODES OF VIBRATION

The propeller vibrations excite the spinner in two important modes. The two modes of interest are the fore-and-aft mode and the lateral mode (see Figure 3.10). The magnitudes of the spinner accelerations are dependent on the flight condition and the mass and stiffness of the Prop-Fan/engine mounting/ wing system. Since most of these parameters were undetermined at the time of the design, a worst case acceleration, based on experience, was chosen for analytical purposes. Therefore, these loads cannot be compared directly to the loads used to design the other components. The spinner was analyzed for a lateral acceleration of 12.7 g's and a fore-and-aft acceleration of 10 g's.

The accelerations are based on previous piston engine experience. The data collected from these tests has been degraded for turbine engine applications. The old piston engines did not run as smoothly as todays engines and the spinner accelerations were produced by the engine (N-order excitations). The Prop-Fan spinner is driven by aerodynamic or P-order excitations, which are not as strong as the N-order excitations. Spinner acceleration data is currently being collected for turbine engine applications now in service, and it is expected that acceleration loads under flight conditions will be lower than those assumed for the Prop-Fan.

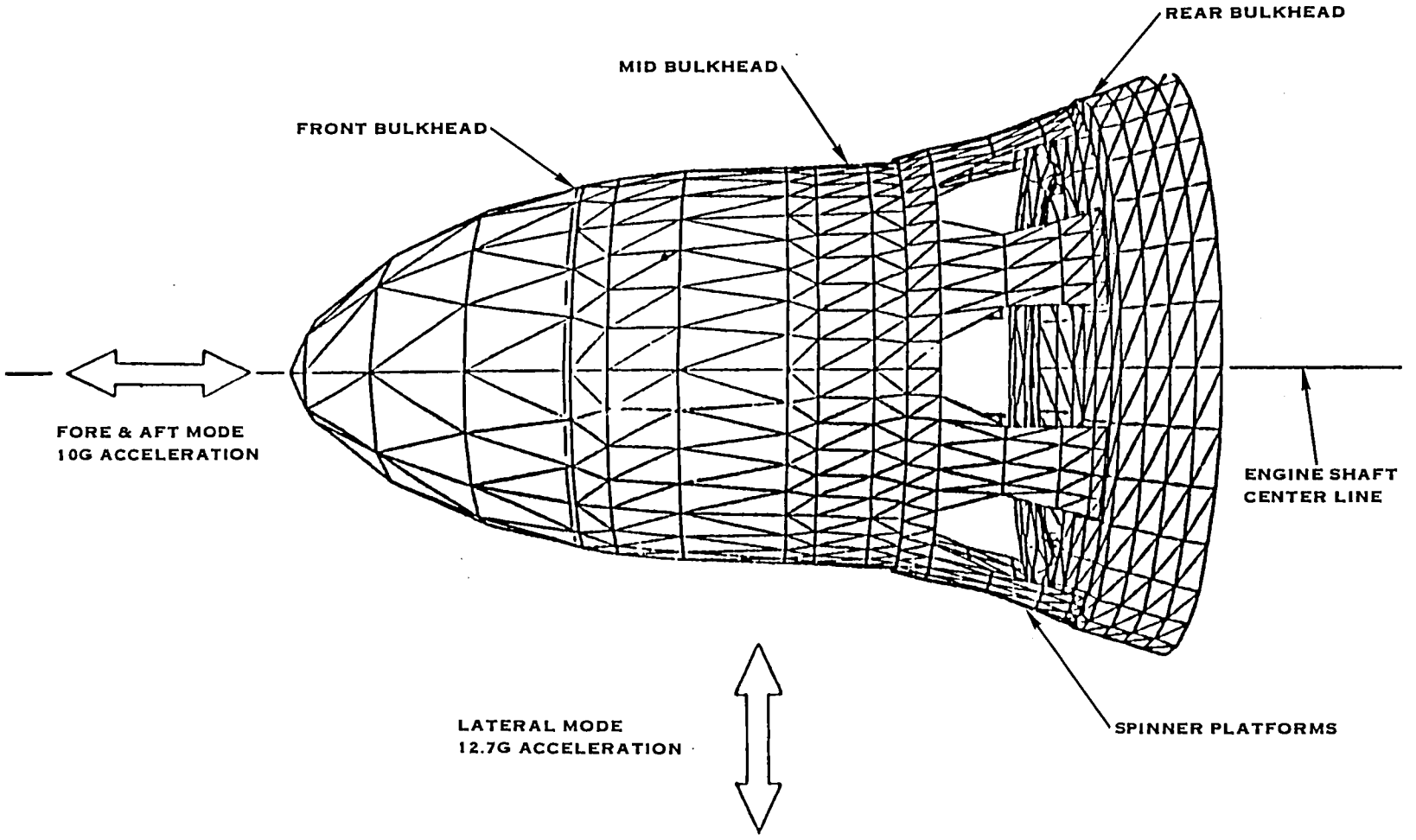

FIGURE 3.10 SPINNER VIBRATORY MODES AND ACCELERATIONS

4.0 Fatigue Allowable Methodology

Hamilton Standard's many years of experience in establishing safe unlimited fatigue allowables for critical aircraft propeller structures is unsurpassed and is directly applicable to Prop-Fans.

The methodology used to establish fatigue allowables is illustrated in Figures 4.1 & 4.2. Propeller blades, in addition to experiencing high steady centrifugal and aerodynamic loads, are subjected to high cyclic vibratory loads which are a major fatigue life consideration. Over a billion cycles of significant vibratory stress during the useful life is not uncommon. Through experience, it was recognized that laboratory fatigue specimen test results alone cannot provide adequate definition of the fatigue strength of a full-scale structure due to such things as size difference, processing variations and hardware geometry. Hamilton Standard has conducted numerous and extensive fatigue tests on full-scale propeller blades and hubs, as produced and after various service exposure times. Blades tested have been both solid and hollow structures encompassing metal alloys as well as fiberglass-reinforced plastic. These test results have not only provided valuable assessments of the fatigue strength of the specific structures being tested, but have provided, when coupled with specimen fatigue data and service experience, an invaluable basis for extrapolation to provide fatigue allowables for new designs. The application of the newer fracture mechanics methodologies by themselves can lead to unconservative fatigue allowables for unlimited life in service environments. The hardware for this program has been designed for unlimited fatigue life using life allowables developed from this vast data base of test and experience. Since all safety factors are accounted for in the establishment of the design allowables, designers work directly to these limits.

ALL FACTORS ARE CAREFULLY CONSIDERED AND INTRGRATED IN THE DEVELOPMENT OF AN APPROPRIATE FATIGUE ALLOWABLE

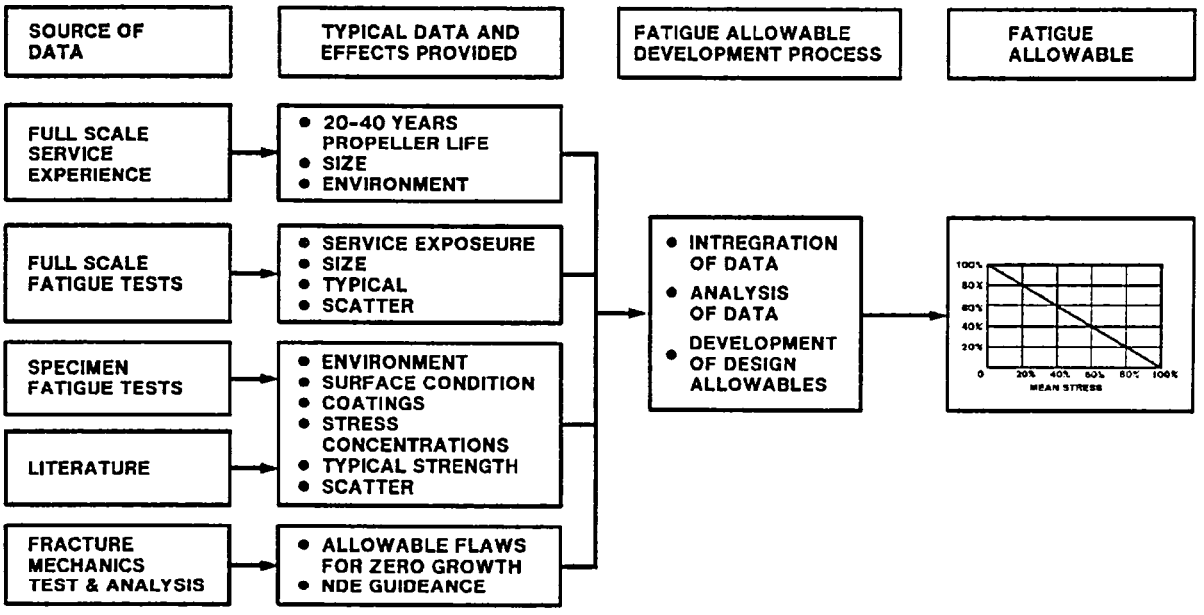

FIGURE 4.1 FATIGUE ALLOWABLE METHODOLOGY

TYPICAL FATIGUE ALLOWABLE THAT ILLUSTRATES THE IMPORTANT DIFFERENCE BETWEEN THE HAMILTON STANDARD APPROACH AND "SPECIMEN ONLY" APPROACH TO FATIGUE ALLOWABLES FOR UNLIMITED LIFE

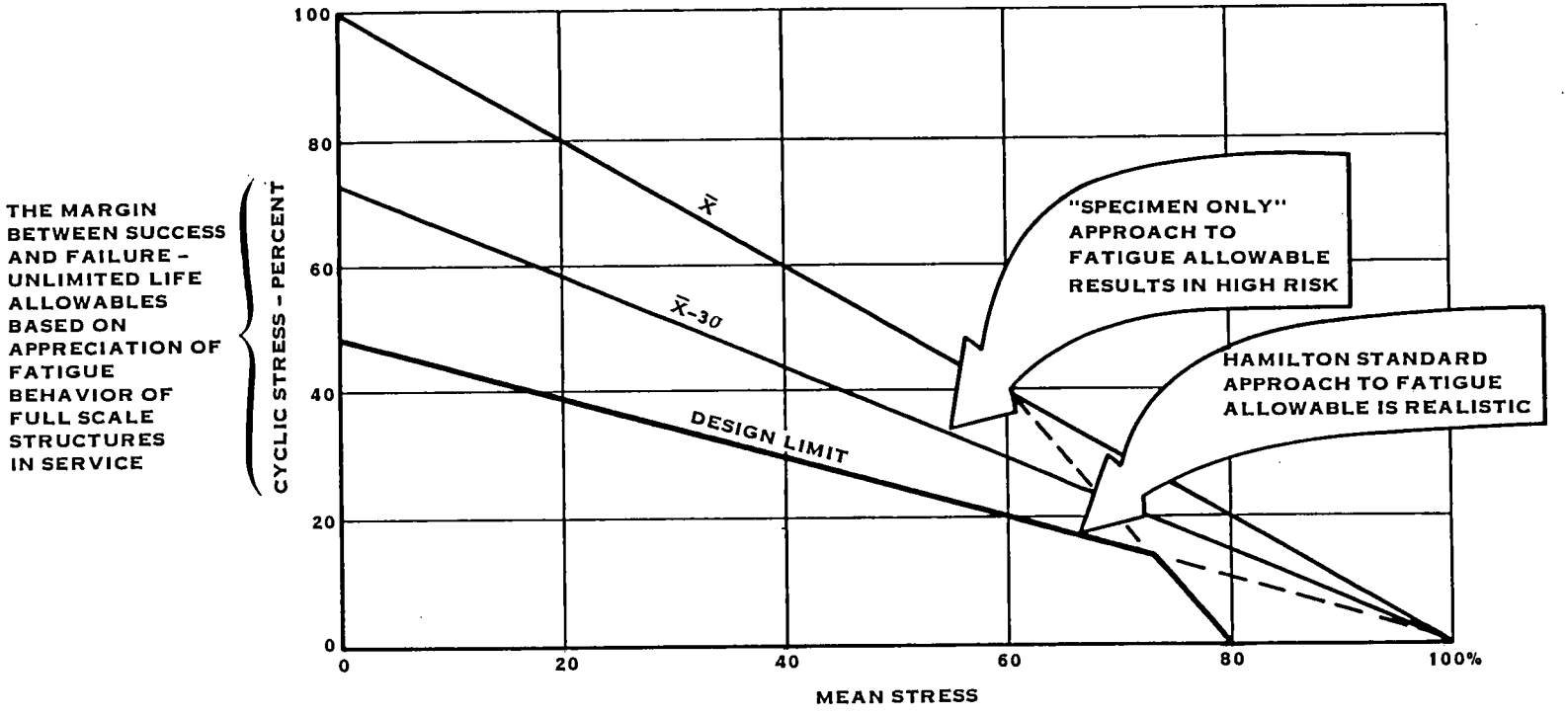

FIGURE 4.2 TYPICAL FATIGUE ALLOWABLE (MODIFIED GOODMAN DIAGRAM)

5.0 System Stress Summary

This report is concerned primarily with the design results at the system interfaces and, as such, the discussion is limited to the peak system stresses in these areas. For a complete component stress summary, see the pertinent design report (i.e. Blade Report, Spinner Report, etc.). Special attention is devoted to the hub and blade retention in this section, because of the inconsistencies in the design loads at this interface.

5.1 Hub Arm Stresses

The hub arm stresses were calculated using the loads listed in the Hub Loads section. The maximum surface tensile stress occurred at the center of the ball raceway (see Point A, Figure 5.1). The combined effects of the bending moments and the centrifugal load produced a high cyclic fatigue stress of 42,400 $\pm$ 8,116 N/cm^2 (61,499 $\pm$ 11,772 psi) at this location. The stress at Point A reflected the combined effects of the front ring hoop stress, the barrel arm hoop stress and the barrel arm bending stress. As discussed in the Hub Load section, the loads used to calculate these stresses did not account for all the forces on the barrel. Inclusion of the trunnion pin force increased the equivalent, steady centrifugal load and consequently, the hub arm stress by approximately 15%. The stress then becomes 48,790 $\pm$ 7,904 N/cm^2 (70,768 $\pm$ 11,464 psi). As shown on the hub Goodman Diagram (Figure 5.2), this stress (Point A') is well below the HCF design limit.

The low cycle surface tensile stress at Point A' is 28,453 $\pm$ 28,453 N/cm^2 (41,270 $\pm$ 41,270 psi). Low cycle fatigue (LCF), sometimes referred to as "stop-start" cycles, is associated with alternating between an unstressed state and the maximum stress state. For the low cycle fatigue stresses, the steady and cyclic stresses were combined to determine the maximum tensile or compressive stress. For LCF evaluation, the steady and cyclic stresses were each assumed equal to half of this maximum, and were then plotted on a modified Goodman Diagram, as shown on Figure 5.3, for comparison to the material allowable limits. For the low cycle fatigue conditions, each of the hub components must withstand at least 50,000 stress cycles under this combined stress. The fatigue life at this stress level is 220,000 cycles and is acceptable since 50,000 cycles is the required life. The 140% overspeed stress, at Point A', Figure 5.2, is 74,961 N/cm^2 (108,727 psi).

5.2 Retention Stresses

The retention stress analysis was concerned with two types of stress (1) the surface Hertzian contact stress at the interface of the races and balls (Point B, Figure 5.1) and (2) the subsurface, octahedral, shear stress (Point C, Figure 5.1). The contact stresses were evaluated on the basis of high cycle fatigue (HCF) and low cycle fatigue (LCF). For the octahedral shear stresses, only the HCF portion of the analysis was of interest.

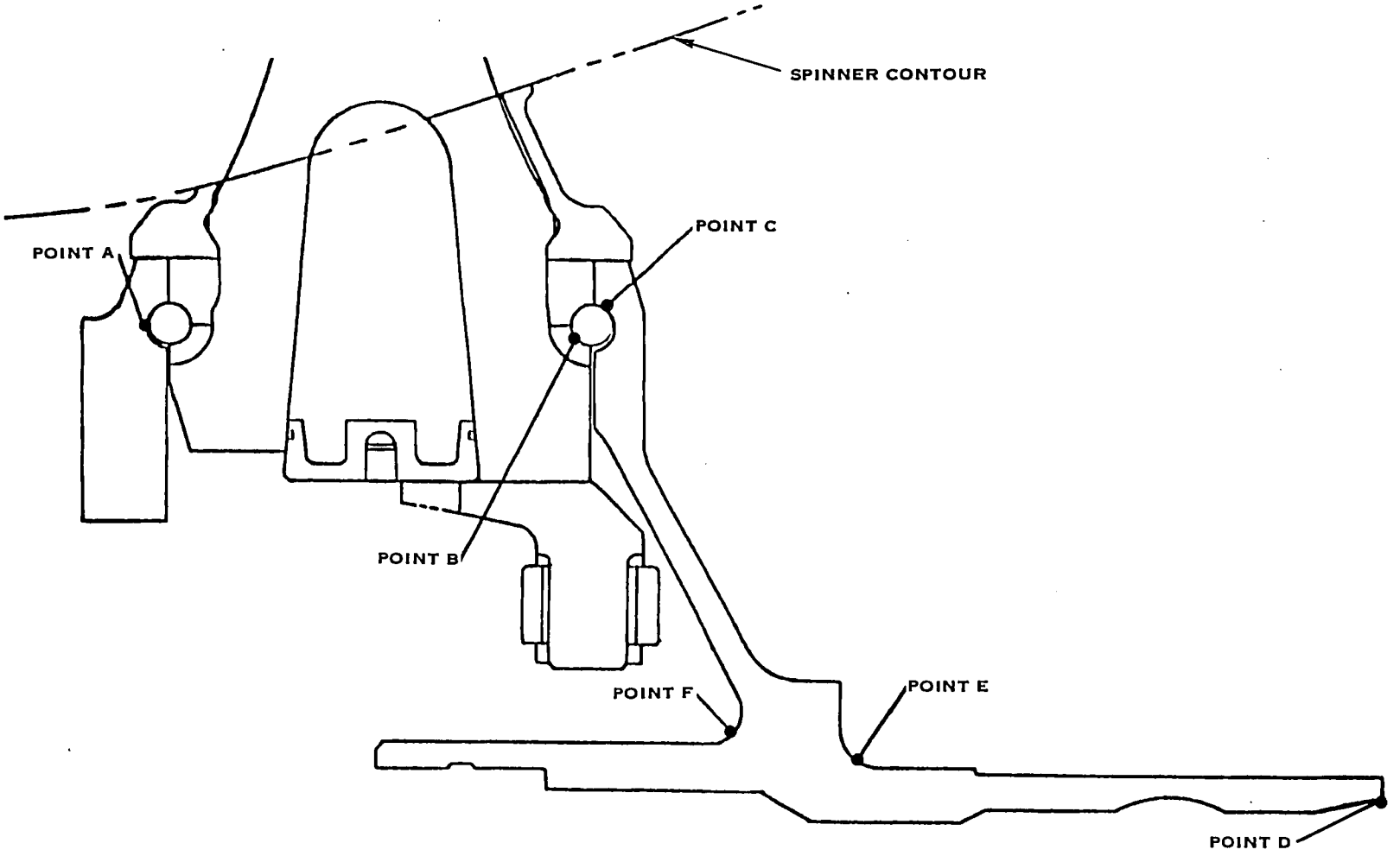

FIGURE 5.1 HUB & RETENTION PEAK STRESS LOCATIONS

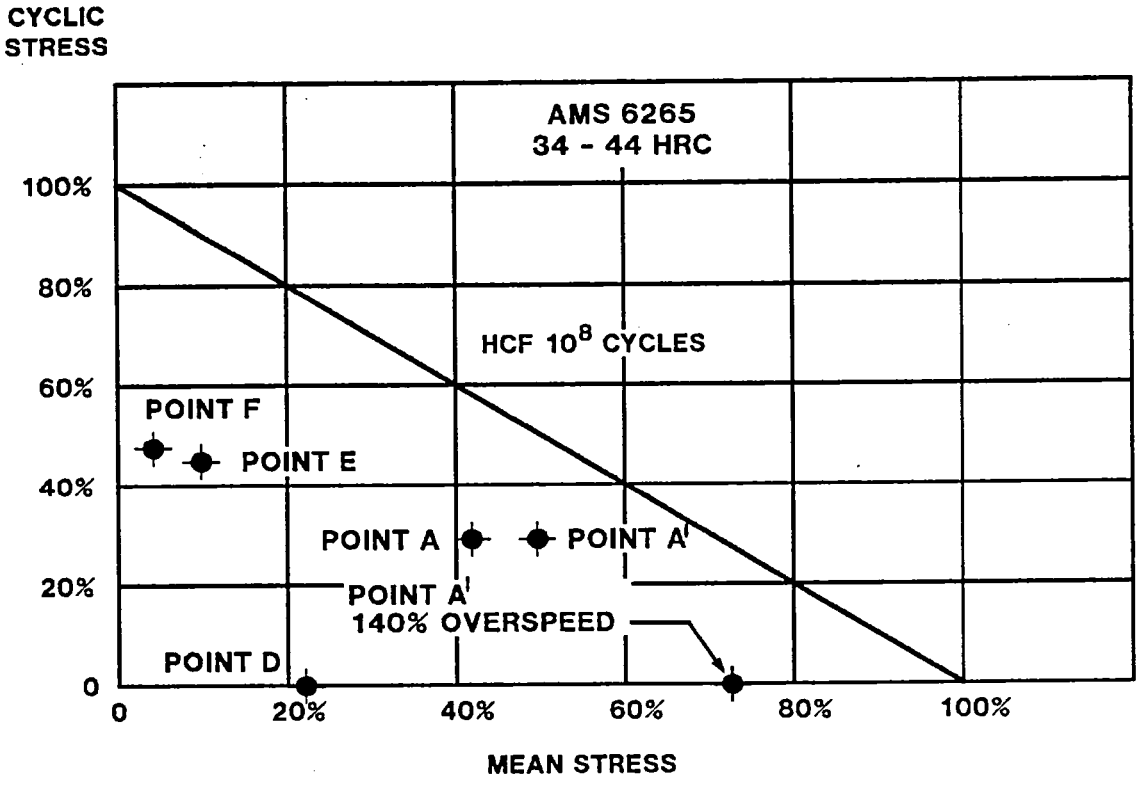

FIGURE 5.2 HUB & TAILSHAFT SURFACE TENSILE STRESSES
(HCF & OVERSPEED)

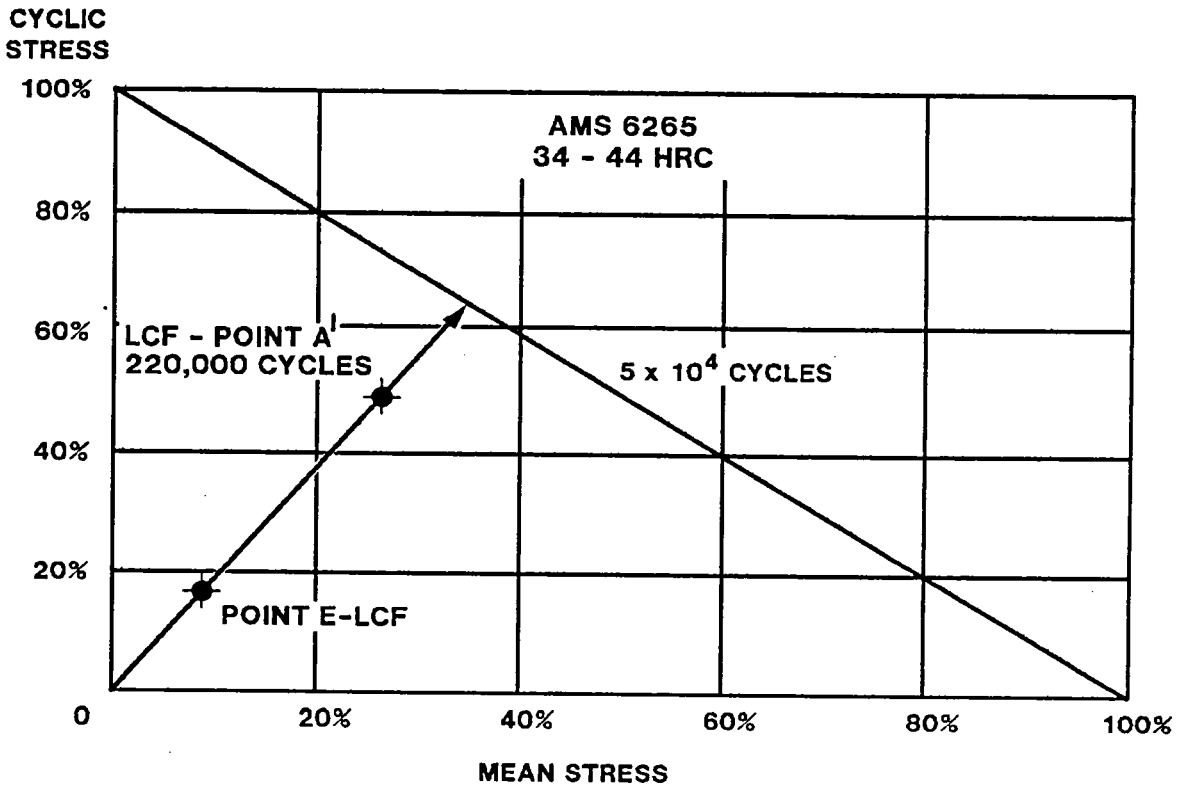

FIGURE 5.3 HUB & TAILSHAFT SURFACE TENSILE STRESSES (LCF)

5.2.1 HCF Retention Stresses

The HCF portion of the retention analysis included the effects of the trunnion force. The centrifugal load and all the steady and cyclic moments and shear loads were also included (see the Blade Retention Loads section for the appropriate loads). The surface, HCF, Hertzian contact stress for the 0.2 Mn, take-off climb condition, at Point B, is 442,414 $\pm$ 10,617 N/cm^2 (641,700 $\pm$ 15,400 psi) and, as can be seen on Figure 5.4, is within the infinite life design limit.

5.2.2 LCF Retention Stresses

All the loads used in the HCF retention stress analysis were not included in the LCF stress calculation. The trunnion pin effects and all the moment and shear loads were neglected in this portion of the analysis. The results obtained using only the centrifugal load for the LCF calculation have, over our fifty years of propeller experience, correlated very well with the data collected from actual propeller service. Therefore, to be consistent with past experience, only the centrifugal load was used. This includes some conservatism because the stresses reflect a worst case tolerance condition. The LCF stress for the 0.2 Mn take-off climb condition is 206,832 $\pm$ 206,832 N/cm^2 (300,000 $\pm$ 300,000 psi). As shown on Figure 5.5, the low cycle fatigue life for this stress level is 10,000 cycles.

5.2.3 Overspeed Retention Stresses

The surface Hertzian contact stresses at the two overspeed cases, 125% and 140% overspeed, were evaluated for two blade angle settings. As discussed in the Retention Load section, it was assumed that both overspeeds could occur at either Flat Pitch or at the Design Cruise blade angle, 57.57 degrees. Under the first assumption, only the centrifugal load was applied to the retention. Under the second assumption, all the steady loads were included in the analysis. The inner retention race stress, calculated using centrifugal load only, is 472,266 N/cm^2 (685,000 psi) at 125% Overspeed and 510,186 N/cm^2 (740,000 psi) at 140% RPM. The stresses at 125% and 140% overspeed, applying all the steady loads, were 498,207 N/cm^2 (722, 625 psi) and 530,069 N/cm^2 (768,840 psi), respectively. These stresses are shown on Figure 5.4.

5.2.4 Retention Octahedral Subsurface Shear Stresses

The octahedral subsurface shear stress calculation was most important on the integral barrel race (Point C, Figure 5.1). This area of the barrel is carburized. The resulting increase in hardness and strength is a function of the depth measured from the race surface, and results in essentially three hardness zones (see insert on Figure 5.6). Zone A extends from the surface to a minimum depth of 0.104 cm (0.041 in), with a minimum hardness of 59 HRC. Zone B, 50 HRC min., extends to a minimum depth of 0.203 cm (0.080 in.). The core hardness is that of the parent material, 34 HRC min. The subsurface shear stress was calculated at each hardness zone.

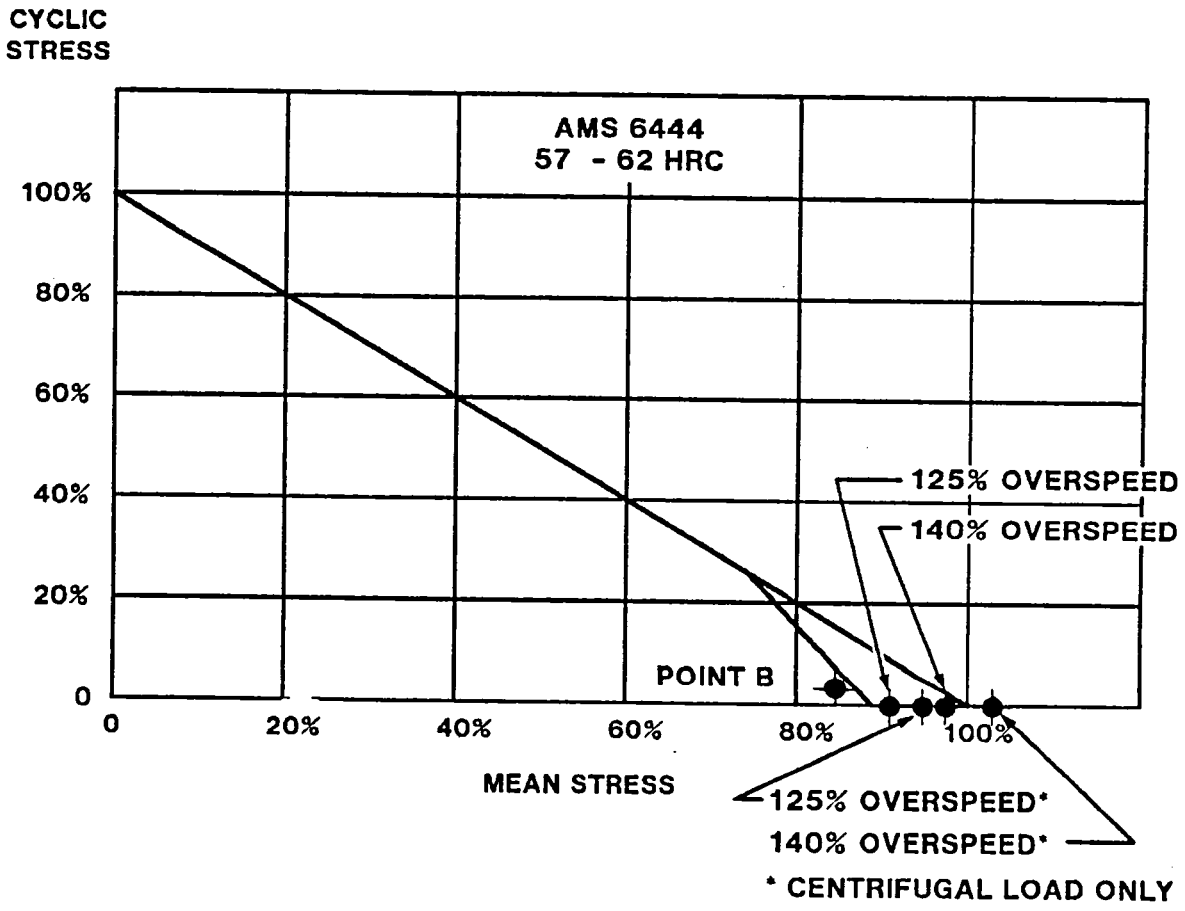

FIGURE 5.4 BLADE RETENTION SURFACE HERTZIAN CONTACT STRESSES (HCF & OVERSPEED)

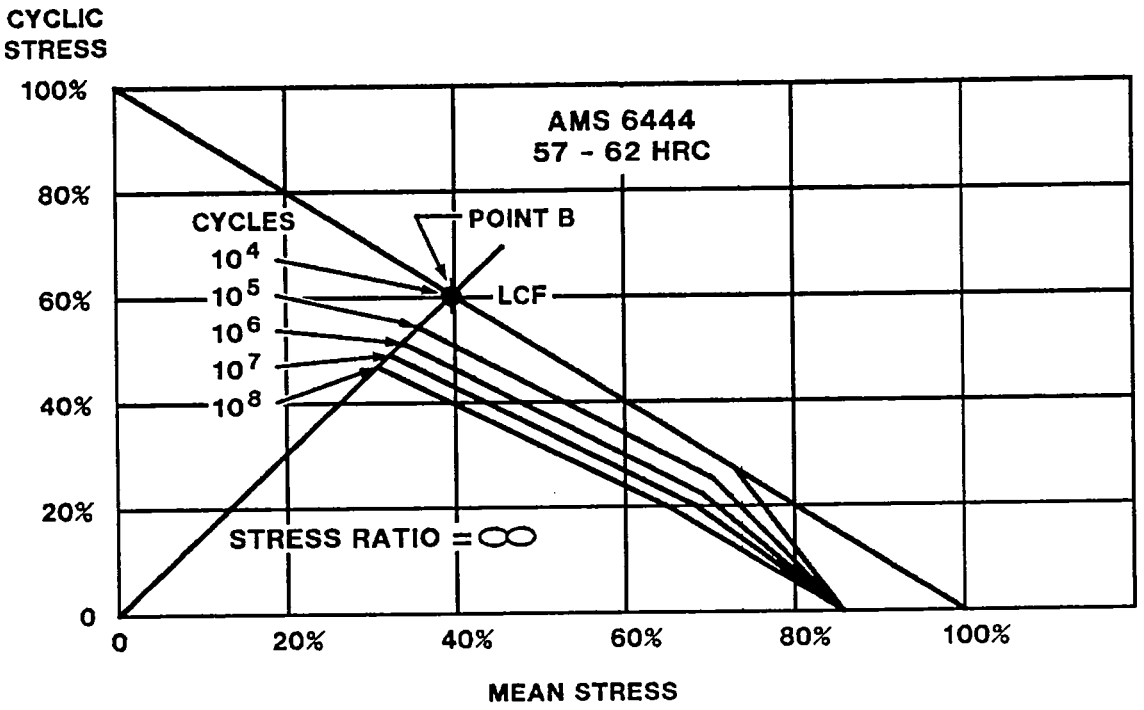

FIGURE 5.5 BLADE RETENTION STRESSES

Figure 5.6 shows the results of these calculations. The 10^8 cycles line for 34 - 44 HRC, represents the allowable for the core material. To meet this design limit, the carburized region must penetrate to approximately 0.297 cm (0.117 in). The 50 HRC zone, Zone B, is guaranteed to a depth of 0.203 cm (0.080 in), but may extend to 0.254 cm (0.100 in). The transition zone between Zone B and the core will be approximately 0.102 cm (0.040 in) deep. The core will, therefore, begin below the cross over shown on Figure 5.6, at a depth between 0.305 cm (0.120 in) and 0.356 cm (0.140 in). The stress calculated at 0.297 cm (0.117 in) is 40,846 $\pm$ 2,437 N/cm^2 (59,245 $\pm$ 3.535 psi).

Therefore, the octahedral, subsurface shear stresses are acceptable in all respective hardness zones.

5.3 Blade Trunnion Stresses

The highest blade trunnion stresses are shown on Figures 5.7 - 5.10. The maximum HCF stress (see Figure 5.7) is below the infinite life, unpeened allowable for AMS 6415 steel. This stress, 42,401 $\pm$ 16,030 N/cm^2 (61,500 $\pm$ 25,350 psi), occurred at section G-G (see Figure 5.8). The other HCF trunnion stress shown, 42,866 $\pm$ 16,064 N/cm^2 (62,175 $\pm$ 23,300 psi) occurred in the trunnion pin fillet radius, point I on Figure 5.9. The trunnion is peened in this area and could be compared against a higher allowable than that shown on Figure 5.7. Both stresses reflected the appropriate stress concentration factors in fatigue, K_f, and were within the HCF design limit. The maximum low cycle fatigue stress is 29,939 $\pm$ 29,939 N/cm^2 (43,425 $\pm$ 43,425 psi) for an adequate fatigue life of 118,000 cycles (see Figure 5.10).

The blade trunnion overspeed stresses are also shown on Figure 5.9. The 125% overspeed stress includes a K_f of 1.65, for a maximum stress of 110,264 N/cm^2 (159,932 psi). The 140% RPM stress is 83,945 N/cm^2 (121,757 psi). This stress does not reflect the stress concentration factor.

5.4 Actuator Stresses

The pertinent actuator stresses occurred at the yoke fillet radius (Point I on Figure 5.8) and in the roller wear plate (Point J). The fillet stress was primarily a tensile bending stress, while the wear plate was an octahedral subsurface shear stress. The HCF stress in the fillet area is 56,534 $\pm$ 12,410 N/cm^2 (82,000 $\pm$ 18,000 psi) and the LCF stress is 34,472 $\pm$ 34,472 N/cm^2 (50,000 $\pm$ 50,000 psi). The HCF and LCF stresses are shown on Figures 5.9 and 5.10, respectively. The appropriate K_f values have been applied to these stresses. The HCF stress was below the infinite life allowable. The fatigue life for this LCF stress level is 76,000 cycles, which is greater than the 50,000 cycle requirement. As discussed in the Actuator Loads section, the actuator trunnion was also analyzed at the proof-test load, which was more conservative than either overspeed load. The trunnion fillet stress, at this load, is 82,733 N/cm^2 (120,000 psi) and is also shown on Figure 5.9.

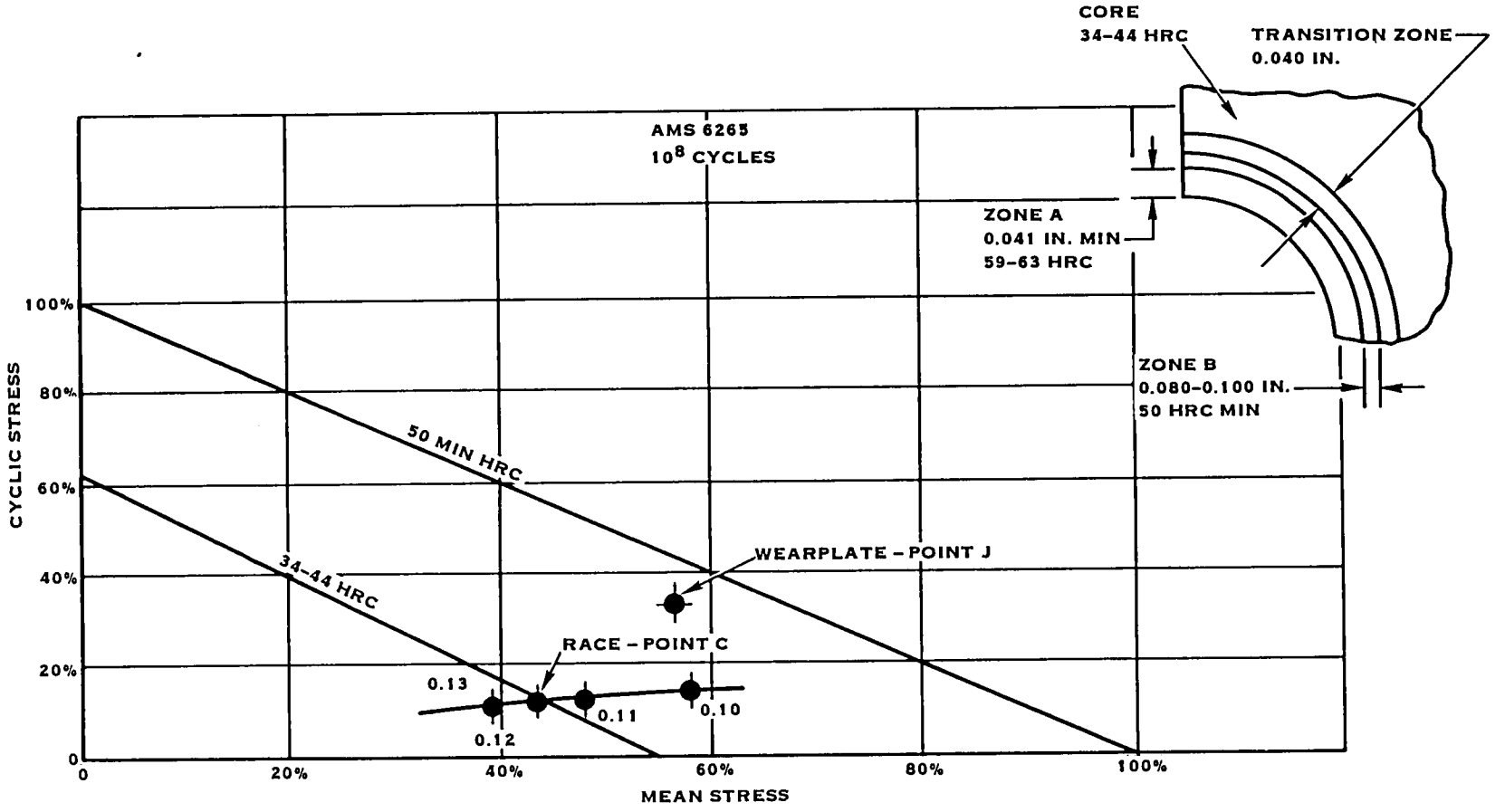

FIGURE 5.6 OCTAHEDRAL SUBSURFACE SHEAR STRESS (HUB RACEWAY & ACTUATOR WEAR PLATE)

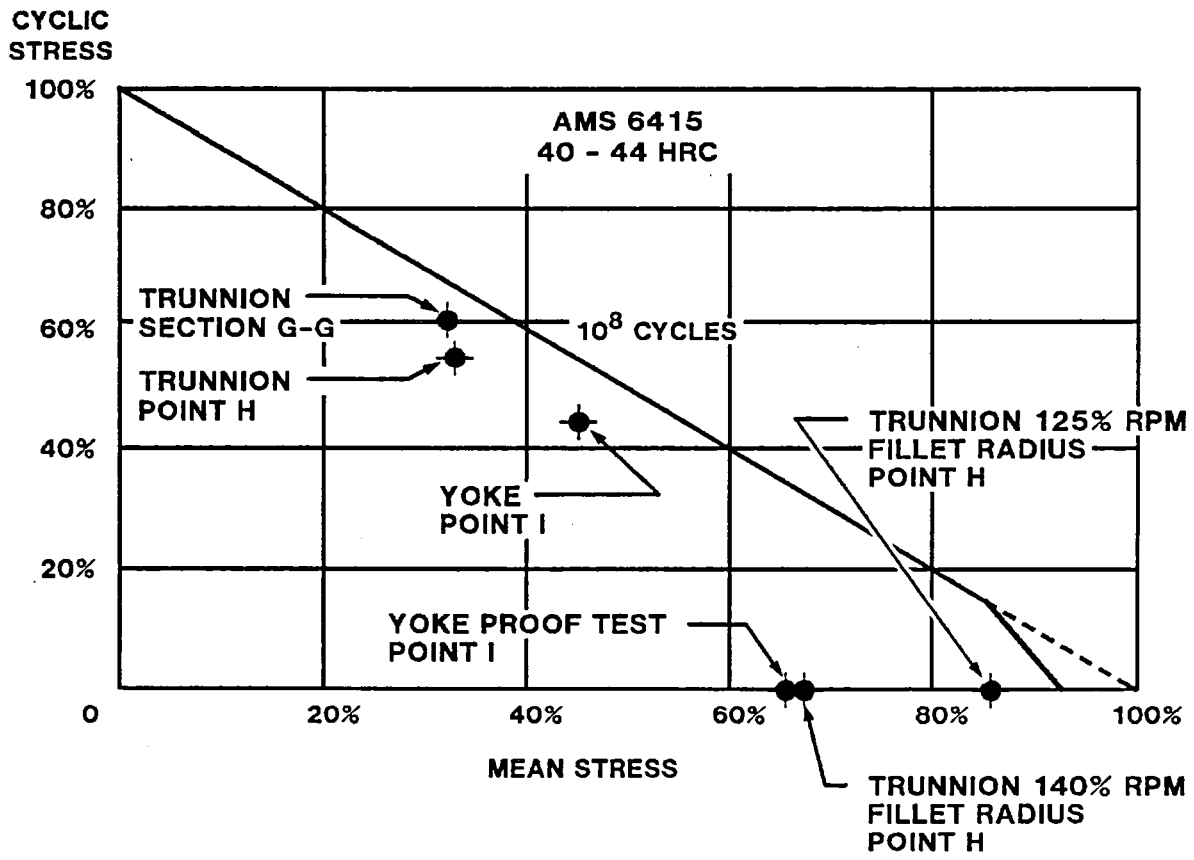

FIGURE 5.7 BLADE TRUNNION & ACTUATOR YOKE STRESSES
(HCF & OVERSPEED)

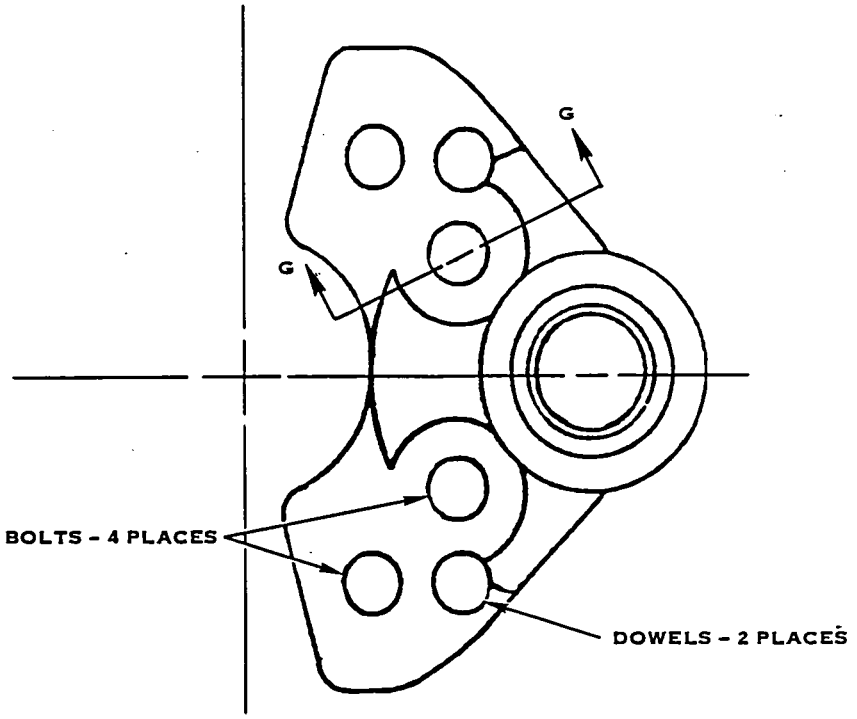

FIGURE 5.8. TRUNNION PEAK STRESS LOCATION

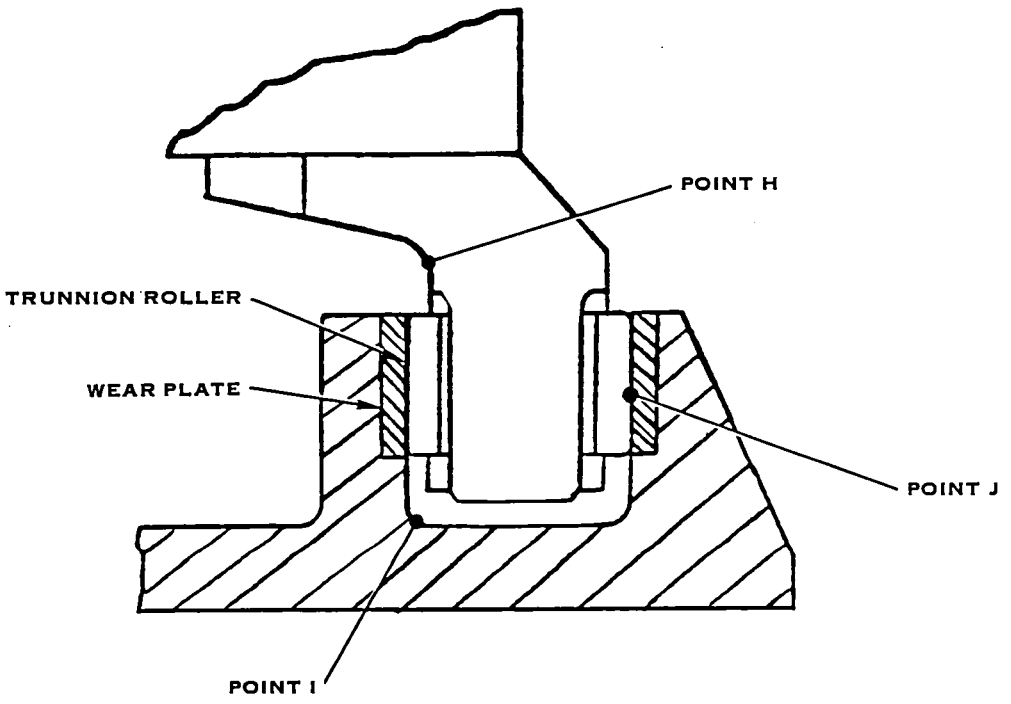

FIGURE 5.9. TRUNNION/ACTUATOR INTERFACE (PEAK STRESS LOCATIONS)

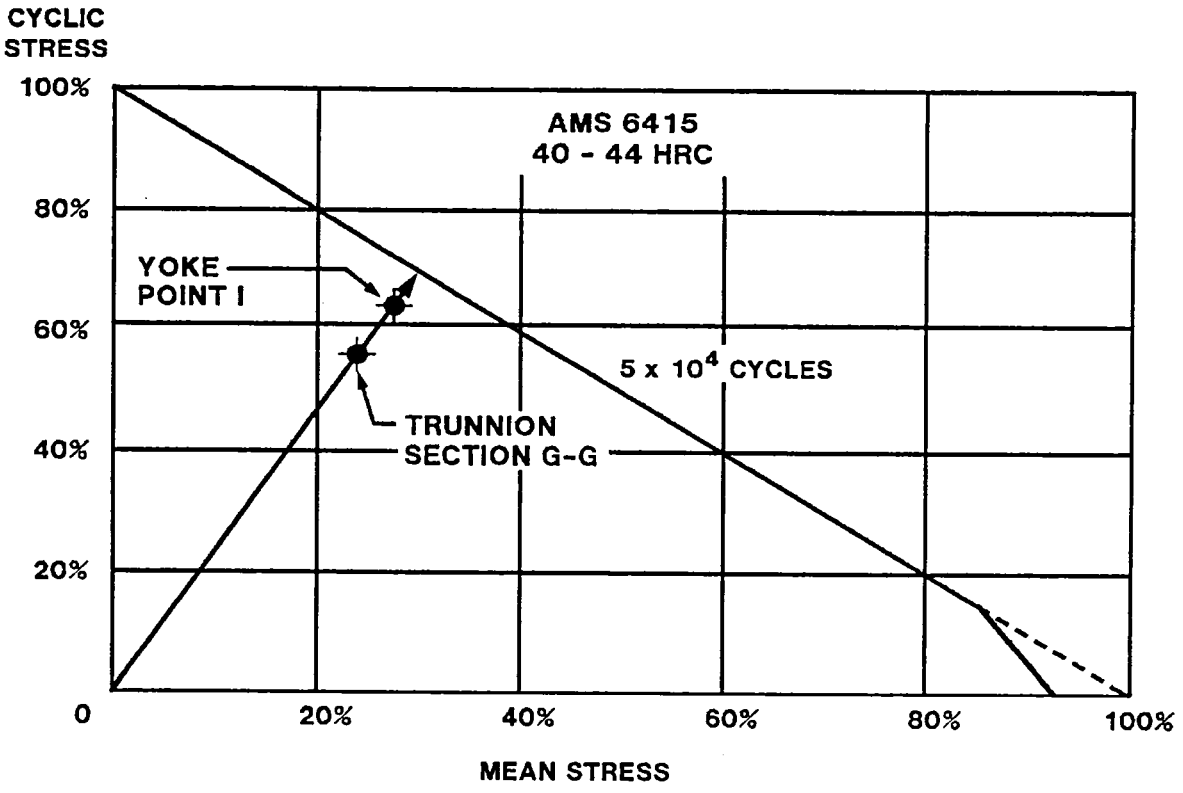

FIGURE 5.10 BLADE TRUNNION & ACTUATOR YOKE STRESSES (LCF)

The wear plate, HCF, octahedral subsurface shear stress is 51,708 ± 7583 N/cm^2 (75,000 ± 11,000 psi) at the minimum case depth of 0.203 cm (0.080 in). The shear infinite life allowable for this material, AMS 6265, is shown on Figure 5.6. The stress at the minimum case depth is within the design limit for the hardness specified at this depth. The LCF shear stress at Point J is 25,852 ± 25,852 N/cm^2 (37,500 ± 37,500 psi) for a fatigue life greater than the 10,000 cycle requirement.

5.5 Tailshaft Stresses

The tailshaft stresses are shown along with the other hub stresses on Figures 5.2 and 5.3. The stress at point D (Figure 5.1) was a hoop tensile stress. This stress, 19,994 ± 34 N/cm^2 (29,000 ± 50 psi), was produced by the high preload on the cone seats. The stresses at Point E and Point F, 6,688 ± 12,893 N/cm^2 (9,700 ± 18,700 psi) and 207 ± 13,651 N/cm^2 (300 ± 19,800 psi) respectively, are primarily bending stresses. The max LCF stress occurred at point E and is shown on Figure 5.3. The stress is 9,790 ± 9,790 N/cm^2 (14,200 ± 14,200 psi) for a LCF life greater than 10^8 cycles. This life is more than adequate since the life requirement is 50,000 cycles. The appropriate K_f values were applied to all these stresses. The location of the points of interest can be found on Figure 5.1.

5.6 Spinner Stresses

The spinner stresses for both the fore-and-aft mode and the lateral mode are very low. The max steady stress occurred in the spinner platforms (see Figure 5.11) at 100% speed with a 10g fore-and-aft acceleration. The stress at this condition is 2,685 ± 345 N/cm^2 (3,894 ± 500 psi). The maximum cyclic stress, 1,151 N/cm^2 (1,670 psi) occurs in the aft bulkhead where the steady stress is 834 N/cm^2 (1,210 psi). These stresses correspond to a lateral, 12.7g acceleration at 1460 rpm. The stresses for all the spinner components at these two conditions can be seen on Figures 5.11 and 5.12. These stresses are acceptable since they are well below the design allowables.

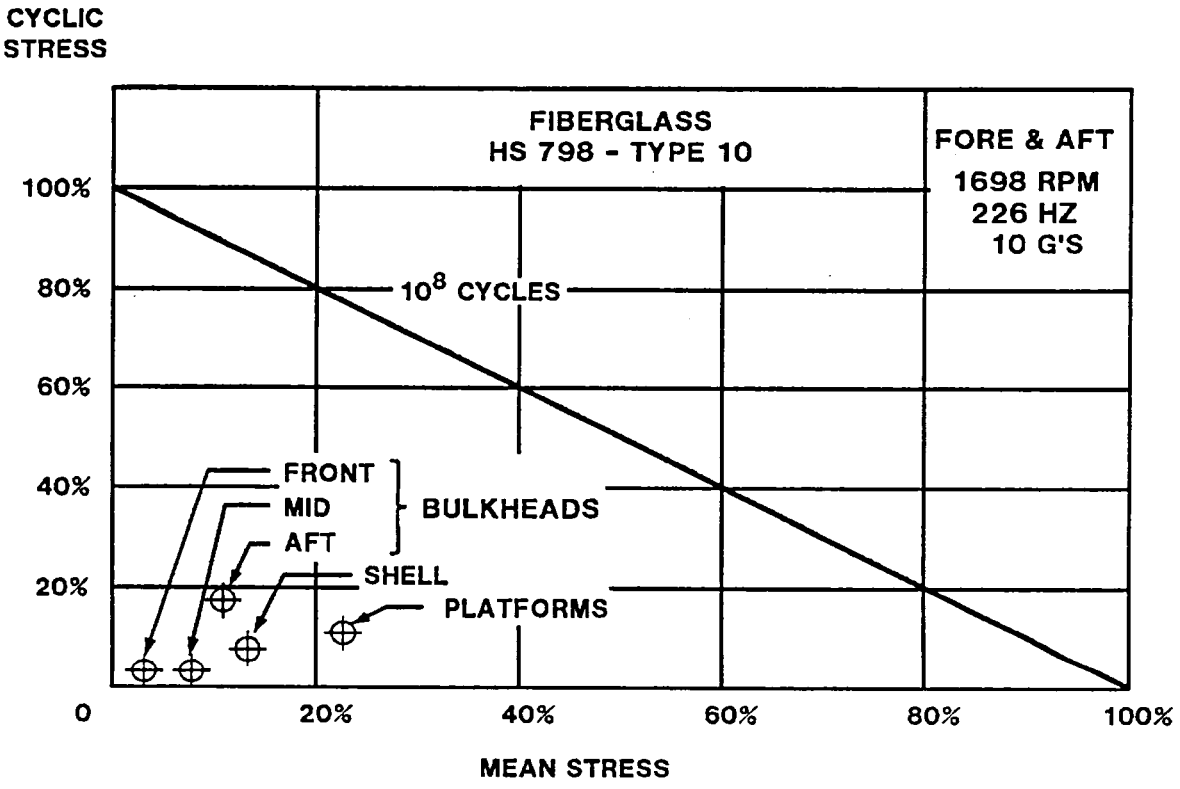

FIGURE 5.11 SPINNER STRESSES (FORE & AFT)

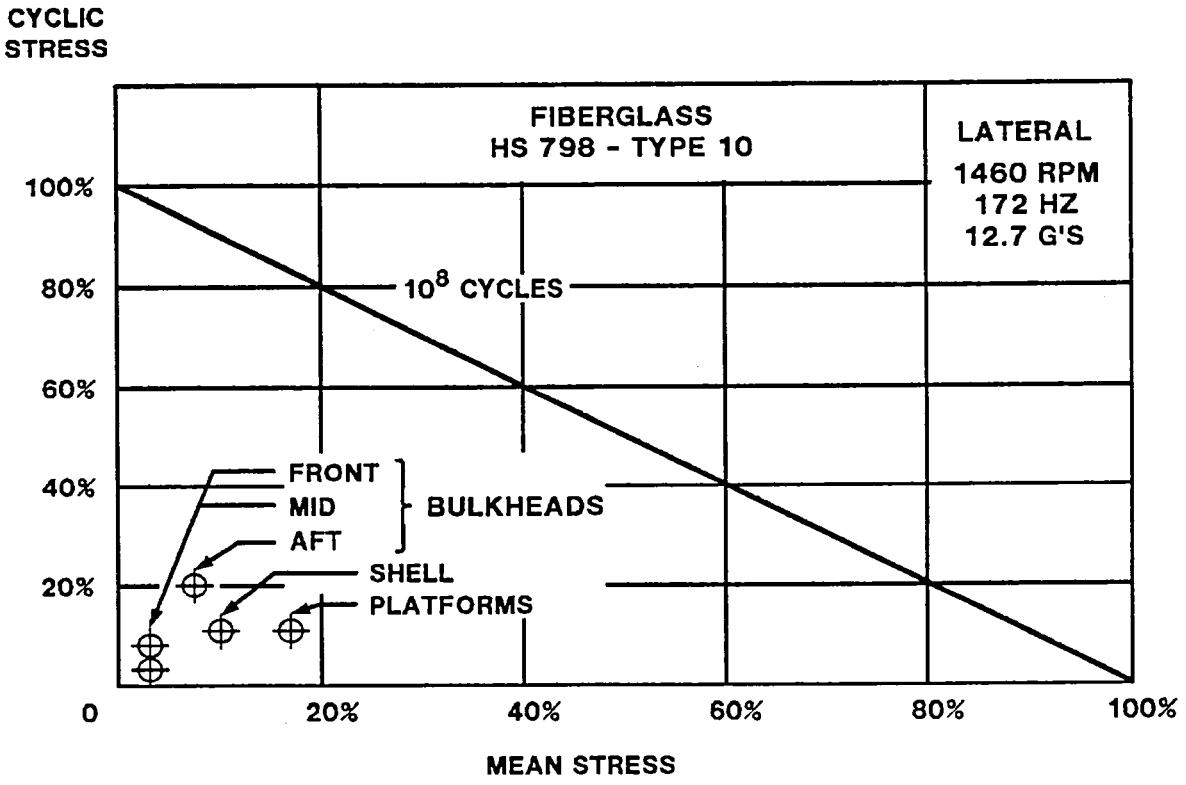

FIGURE 5.12 SPINNER STRESSES (LATERAL)

6.0 Comparison of Final Design to Design Specifications

The following section compares the final system to the internally generated Design Specifications (reference document 267X - 1; Design Requirements For SR-7L Propeller; revised 4-11-83). Only those sections where the specific component design requirements (Section 5.0 of document 267X - 1) were not met, will be discussed.

6.1 Blade Requirements (Section 5.1)

Several requirements stated in this section were not fully satisfied. The first area of concern was the stall flutter analysis (Section 5.1.4). The stall flutter parameter was quoted in terms of blade angle. Stall flutter sometimes occurs as power is increased, which corresponds to increasing blade angle. The design condition in question was the static thrust condition where the blade angle setting is 33°. The flutter blade angle as predicted by a semi-empirical analysis method developed at Hamilton Standard was only 31 degrees (see Figure 6.1), indicating that the Prop-Fan could not develop the required power before onset of flutter. However, a second purely empirical method for predicting flutter (the Steinman Analysis), shown in Figure 6.2, indicated that the stall flutter parameter, +1.35, was well above the flutter region and no flutter will occur at 33° so that the required power can be developed. The two predictions were inconsistent and inconclusive. There has been no experimental verification of the first method and the Steinman Analysis is based entirely on straight blades, so the final determination will have to be made through testing. Flutter tendencies subside as forward speed increases so that this situation should not pose a problem to the Prop-Fan test program.

The next area of concern deals with the Blade Critical Speed Margins (Section 5.1.5). For a 2P excitation, the ground operation margin should be 20%, but for the 0.2 Mn, take-off climb condition it was only 19%. The other design case that violates the critical speed margin requirements was the 100% speed design cruise. The 3P excitation should have a 7.5% margin, but the margin was only 5.7% for this case. These frequencies and the margin violations are shown on Figure 6.3.

6.2 Disc/Retention Requirements (Section 5.2)

The problem areas in this segment of the propeller system are the retention races. The Design Specifications document states that the steady stress at 125% overspeed must be below the 0.2% yield strength and the 140% overspeed stress must be below the ultimate strength. Under either assumption (centrifugal load only or all steady loads applied), the 125% overspeed stresses did not meet this criteria. Under the first assumption the 140% RPM criteria was

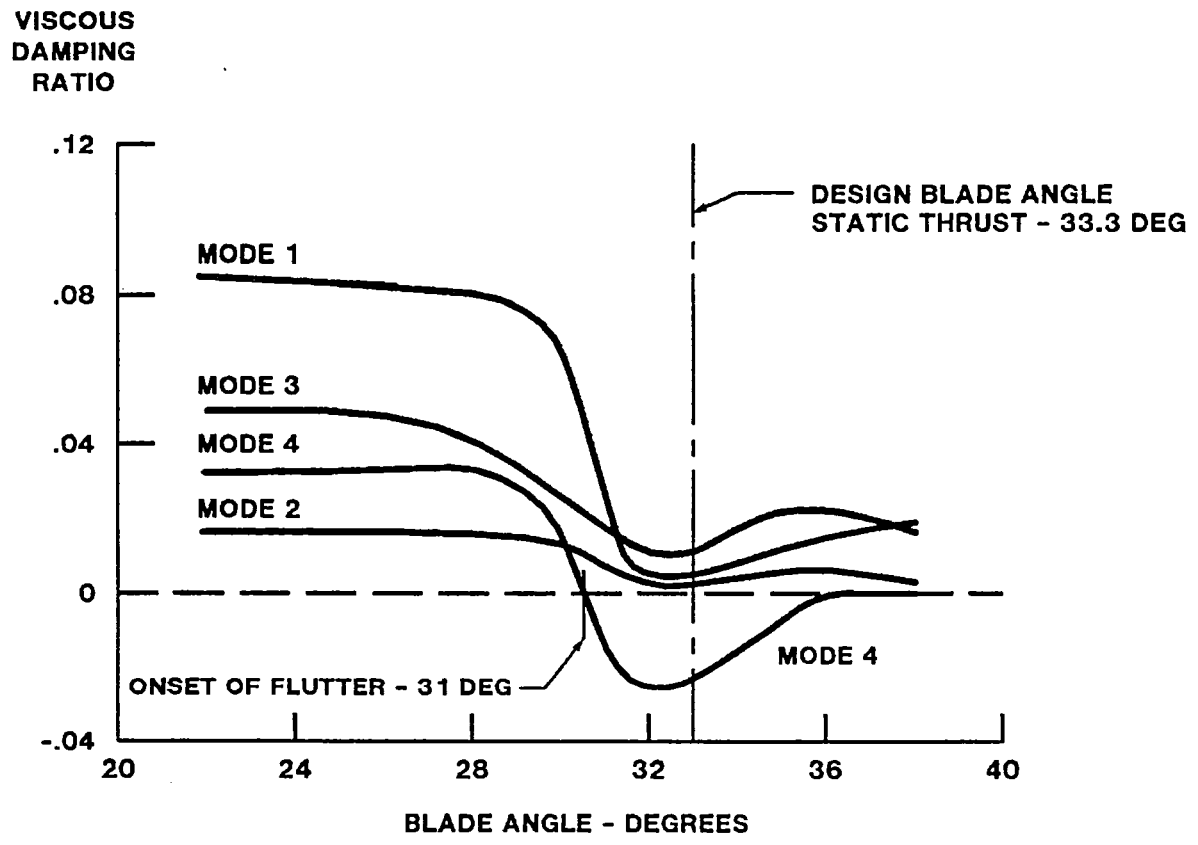

FIGURE 6.1 STALL FLUTTER (H.S. METHOD)

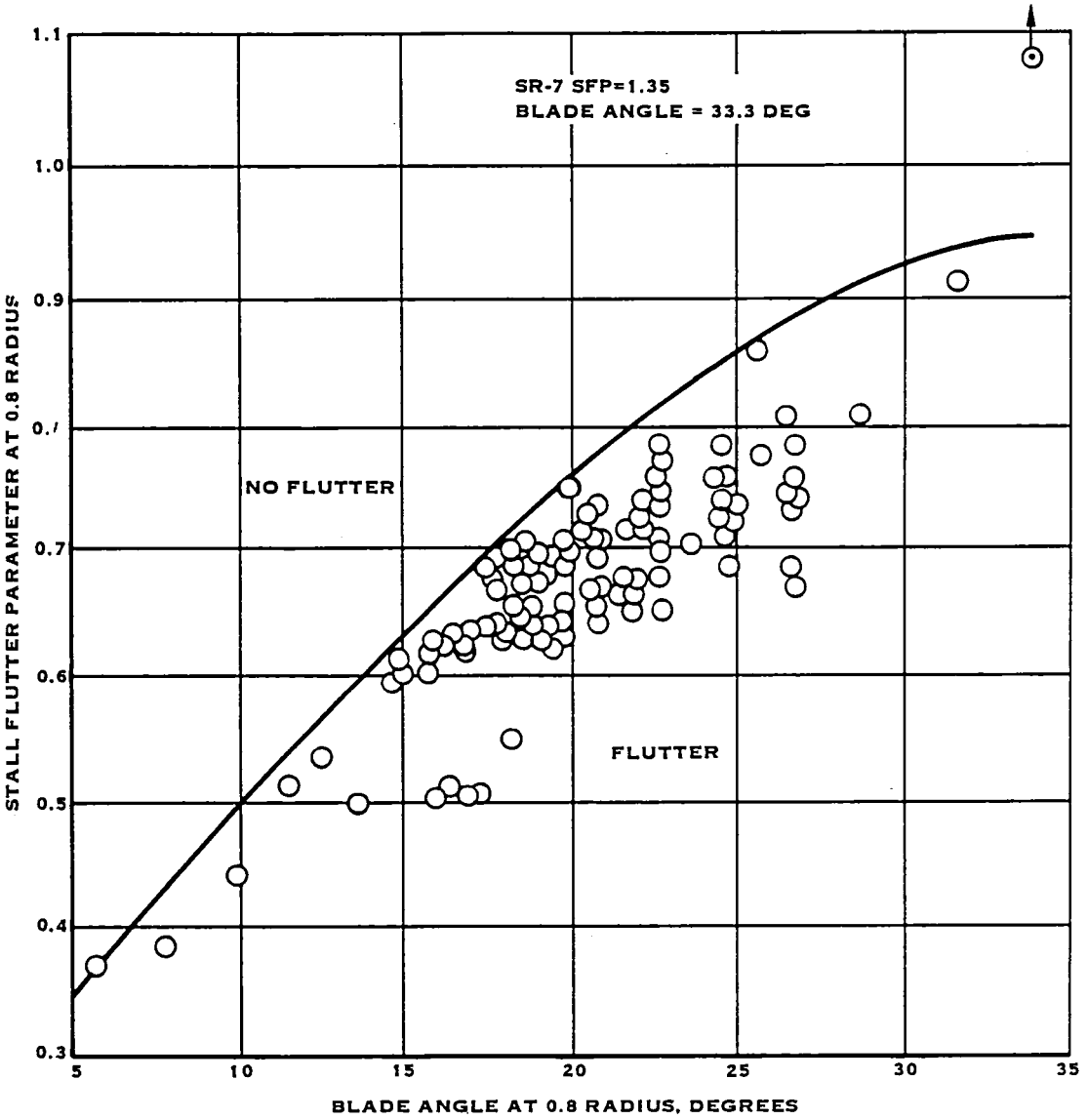

FIGURE 6.2 STALL FLUTTER (STEINMAN METHOD)

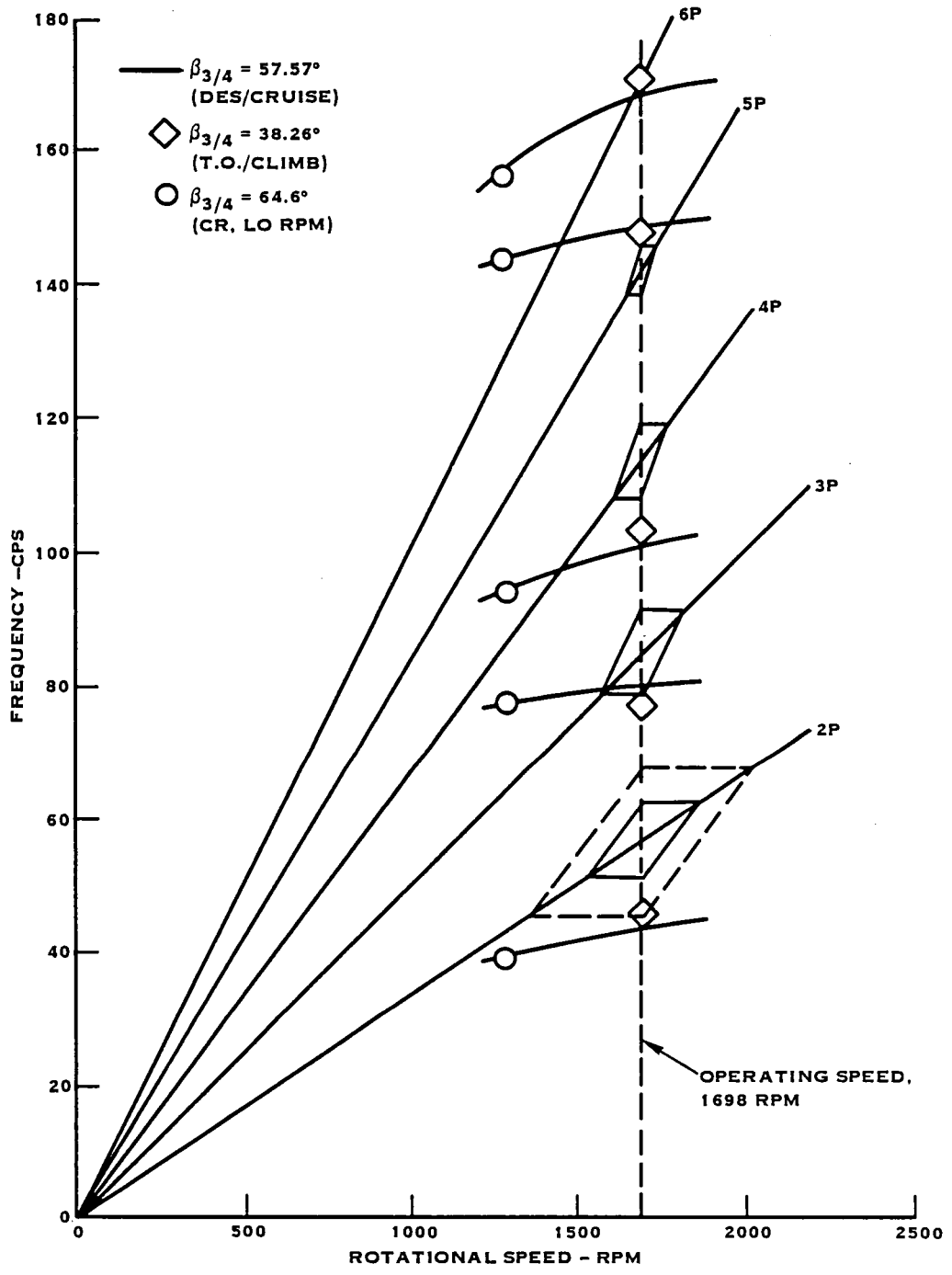

FIGURE 6.3 BLADE CRITICAL SPEED MARGINS

met. However, the 140% overspeed stress with all steady loads applied, exceeds the ultimate strength. Furthermore, the LCF life of the races did not meet the design specification for the 0.2 Mn take-off climb condition. Section 5.2.6 of the Design Specification requires 50,000 cycles, but the calculated life of the races is only 10,000 cycles. Although the retention did not meet the 50,000 cycle LCF requirement, the design is adequate for the Prop-Fan program. These components are either repairable or replaceable.

7.0 Hardware Compatibility

The first step in the Design/Drafting loop is the creation of the layouts. As the designers created their layouts, they communicated amongst themselves to define the system interfaces and envelopes. When the layout is complete, it is put through a series of design reviews. After receiving final approval, the layout is sent to drafting. The layout is the vehicle used to formally communicate design requirements to drafting.

Drafting takes the layout and creates the detail drawings. If a problem arises, drafting works with design to resolve the problem without compromising the design. Before the drawing is released, it is checked to ensure that all the design requirements have been satisfied and that the proper fits and clearances have been maintained. If the adjacent hardware has not been detailed, a Cavity Sketch Layout (CSL) is created to define the mating interfaces and the checking is then completed. The detail drawings are thoroughly reviewed again and signed by design, drafting, materials and project engineering. As a final check, a system assembly layout is created. Special attention is devoted to all system interfaces.

8.0 Failure Mode and Effects Analysis

The Failure Mode and Effects Analysis (FMEA) that follows was used by Hamilton Standard to evaluate the potential reliability of the Large-Scale Advanced Prop-Fan (LAP).

The primary objective of this "functional" FMEA was to highlight critical failure areas so that susceptibility to such failures could be removed from the system during the design phase. In this analysis, each potential functional failure was considered in light of the probability of occurrence and evaluated as to the probable effect on safety and mission success.

Since the LAP is a research and development unit to explore the structural and acoustic characteristics of highly loaded, thin, swept blades at high Mach numbers, the philosophy was to have failures in the actuation system result in either blade pitch lock or feather.

The conclusions reached are based upon experience with similar products. Representatives from the reliability, design and project functions have reviewed this FMEA and concur that it properly describes the LAP at this stage of development.

The opinions expressed in this FMEA/FHA represent best estimates based on information presently known to Hamilton Standard. Hamilton Standard reserves the right to revise such estimates as additional information becomes available.

This analysis shall not be construed as a warranty or guarantee of the equipment described nor constitute the basis of liability to Hamilton Standard in contract or otherwise.

In the FMEA the definition of "Hazard Category" and "Hazard Probability" were taken from MIL-STD-1629A and are listed below for reference.

Hazard Category:

Category I - Catastrophic - A failure which may cause death or system loss (i.e., aircraft, missile, ship, etc.)

Category II - Critical - A failure which may cause severe injury, major property damage, or major system damage which will result in mission loss.

Category III - Marginal - A failure which may cause minor injury, minor property damage, or minor system damage which will result in delay or loss of availability or mission degradation.

Category IV - Minor - A failure not serious enough to cause injury, property damage, or system damage, but which will result in unscheduled maintenance or repair.

Hazard Probability:

Level A - Frequent. A high probability of occurrence during the item operating time interval. High probability may be defined as a single failure mode probability greater than 0.20 of the overall probability of failure during the item operating time interval.

Level B - Reasonably Probable. A moderate probability of occurrence during the item operating time interval. Probable may be defined as a single failure mode probability of occurrence which is more than 0.10 but less than 0.20 of the overall probability of failure during the item operating time.

Level C - Occasional. An occasional probability of occurrence during item operating time interval. Occasional probability may be defined as a single failure mode probability of occurrence which is more than 0.01 but less than 0.10 of the overall probability of failure during the item operating time.

Level D - Remote. An unlikely probability of occurrence during item operating time interval. Remote probability may be defined as a single failure mode probability of occurrence which is more than 0.001 but less than 0.01 of the overall probability of failure during the item operating time.

Level E - Extremely Unlikely. A failure whose probability of occurrence is essentially zero during item operating time interval. Extremely unlikely may be defined as a single failure mode probability of occurrence which is less than 0.001 of the overall probability of failure during the item operating time.

UNITED TECHNOLOGIES HAMILTON STANDARD

FAILURE MODE & EFFECT ANALYSIS

SYSTEM LAP 108 Prop-Fan

SUBSYSTEM Control Housing

DRAWING NO. L-14325-3

REPORT

DATE 6/29/84 PAGE 1 OF 9

PREPARED BY T. Sutak/R. Schwartz

FILE REF 6970A, 6971A

ITEM	PART OR ASSEMBLY DESCRIPTION	MODE OF FAILURE	EFFECT OF FAILURE ON THE SYSTEM	HAZ. CAT.	HAZ. PROB.	REMARKS
1.0	Main Pump	Low or No Pump Output	Supply Pressure decreases. Main and Standby Regulating Valve shifts to maintain supply pressure. Standby Pump Check Valve opens. System continues to function normally on Standby Pump. Maximum slew rate of propeller is reduced. Response to transients may be slowed. Control operating temperature increases slightly.	IV	C	A Standby Pump provides operating pressure in the event of a Main Pump failure.
2.0	Standby Pump	Low or No Pump Output	System continues to function normally on Main Pump. Low output from Standby Pump causes flow switch to close illuminating a warning light. Maximum slew rate of propeller is reduced. Response to transients may be slowed.	IV	C	In the event of a Main and Standby Pump failure, the propeller can be feathered by the Auxiliary Pump which is actuated by the airframe mounted emergency feather button.
3.0	Scavenge Pump	Low or No Output	Normal oil leakage or drainage collecting in Atmospheric Sump will not be returned to Pressurized Sump. Sump pressurization will be lost. Main or Standby Pump cavitation is possible. Maximum slew rate of propeller is reduced. Response to transients may be slowed. If total loss of supply oil occurs, propeller will pitchlock.	IV	C	
4.0	Auxiliary Pump	Low or No Pump Output	Loss of ground handling capability. No feather capability in case of loss of primary hydraulics.	IV	D	
5.0	Auxiliary Scavenge Pump	Low or No Pump Output	Sump cannot be pressurized for ground handling operations. Normal oil leakage or drainage will not be returned to the pressurized sump. Auxiliary Pump cavitation is possible. No feather capability in case of loss of primary hydraulics.	IV	D	
6.0	Auxiliary Motor	No or Low Torque Output	Little or no Auxiliary Pump output. Little or no Auxiliary Scavenge Pump output. Loss of ground handling capability. No feather capability in case of loss of primary hydraulics.	IV	C	

UNITED TECHNOLOGIES HAMILTON STANDARD

FAILURE MODE & EFFECT ANALYSIS

SYSTEM LAP 108 Prop-Fan
SUBSYSTEM Control Housing
DRAWING NO. L-14325-3

REPORT
DATE 6/29/84 PAGE 2 OF 9
PREPARED BY T. Sutak/R. Schwartz
FILE REF 6970A, 6971A

ITEM	PART OR ASSEMBLY DESCRIPTION	MODE OF FAILURE	EFFECT OF FAILURE ON THE SYSTEM	HAZ. CAT.	HAZ. PROB.	REMARKS
7.0	Sump Relief Valve	Valve fails open	Sump pressurization is lost. Main and Standby Pump cavitation is possible. Maximum slew rate of propeller is reduced. Response to transients may be slowed.	IV	D	
		Valve fails closed	Sump and actuator pressure increases. Seal or sump failure occurs. System pressure is lost. Propeller pitchlocks.	III	E	The Sump Relief Valve is a ball type check valve. A failure of this type is considered extremely unlikely. System pressure acts to open valve.
8.0	Main Pump Check Valve	Valve fails closed	Main Pump pressure increases. Main Pump or seal failure occurs.	IV	E	System pressure acts to open valve. This type of failure is considered extremely unlikely.
		Valve fails open	Operation other than feather, system operates normally. Ground handling and Auxiliary Pump feathering capability is lost.	IV	D	
9.0	Standby Pump Check Valve	Valve fails closed	Standby Pump pressure increases. Standby Pump or seal failure occurs.	IV	E	System pressure acts in a direction to open the valve. This type of failure is considered extremely unlikely.
		Valve fails open	Operation other than feather, system operates normally. Ground handling and Auxiliary Pump feathering capability is lost. Standby Pump operating temperature increases.	IV	D	
10.0	Auxiliary Pump Check Valve	Valve fails closed	Auxiliary Pump cannot supply oil to pitch change actuator for ground handling operations or feathering. Propeller may still be feathered with primary hydraulics.	IV	E	Auxiliary Pump pressure acts to open valve.
		Valve fails open	Supply pressure leaks to drain. Maximum slew rate of propeller is reduced. Response to transients may be slowed. Propeller may pitchlock.	IV	D	

UNITED TECHNOLOGIES HAMILTON STANDARD

FAILURE MODE & EFFECT ANALYSIS

SYSTEM LAP 108 Prop-Fan
SUBSYSTEM Control Housing
DRAWING NO. L-14325-3

REPORT
DATE 6/29/84 PAGE 3 OF 9
PREPARED BY T. Sutak/R. Schwartz
FILE REF 6970A, 6971A

ITEM	PART OR ASSEMBLY DESCRIPTION	MODE OF FAILURE	EFFECT OF FAILURE ON THE SYSTEM	HAZ. CAT.	HAZ. PROB.	REMARKS
11.0	Auxiliary Scavenge Pump Check Valve	Valve fails closed	Auxiliary Scavenge Pump pressure increases. Auxiliary Scavenge Pump or seal failure occurs.	IV	E	Auxiliary Scavenge Pump pressure acts in a direction to open the valve. The Auxiliary Scavenge Pump Check Valve is a ball type check valve. This type of failure is considered extremely unlikely.
		Valve fails open	Sump pressurization is lost. Cavitation of Main, Standby, or Auxiliary Pump is possible.	IV	D	
12.0	High Pressure Relief Valve	Valve fails open	Maximum slew rate of propeller is reduced. Response to transients may be slowed.	IV	D	
		Valve fails closed	Operation other than feather: System operates normally.	III	E	The High Pressure Relief Valve acts as a backup pressure regulating device for the Main and Standby Regulating Valve.
			Feather Operation: System experiences abnormally high pressures. Seal or structural damage is possible.	III	E	Propeller must continue to rotate after feather position is reached for failure to occur. A failure of this type is considered unlikely.
13.0	Main Filter	Filter clogs	Filter Bypass Valve opens. Control continues to function on unfiltered oil.	III	D	All critical downstream components have individual screens of finer mesh than that used in the Main Filter. Additionally, the pumps are equipped with inlet screens.
14.0	Standby Filter	Filter clogs	Filter Bypass Valve opens. Control continues to function on unfiltered oil.	III	D	All critical downstream components have individual screens of finer mesh than that used in the Standby Filter.
15.0	Filter Bypass Valve	Valve fails closed	If filters are clear: No effect on system. If filters are clogged: Pump damage or structural failure is possible.	IV	E	

UNITED TECHNOLOGIES HAMILTON STANDARD

FAILURE MODE & EFFECT ANALYSIS

SYSTEM LAP 108 Prop-Fan
SUBSYSTEM Control Housing
DRAWING NO. L-14325-3

REPORT
DATE 6/29/84 PAGE 4 OF 9
PREPARED BY T. Sutak/R. Schwartz
FILE REF 6970A, 6971A

ITEM	PART OR ASSEMBLY DESCRIPTION	MODE OF FAILURE	EFFECT OF FAILURE ON THE SYSTEM	HAZ. CAT.	HAZ. PROB.	REMARKS
16.0	Heat Exchanger Bypass Valve	Valve fails open	Propeller oil temperature increases. Seal and bearing degradation possible. Potential Transfer Bearing seizure. Propeller may pitchlock or feather dependent upon bearing damage location.	III	D	
		Valve fails closed	If extreme low oil temperatures exist, excessive flow restriction in the heat exchanger can occur. Supply pressure increases until High Pressure Relief Valve opens.	IV	E	The system will operate at the High Pressure Relief Valve setting. As oil temperature increases, it will begin to flow through heat exchanger. Supply pressure is monitored for failure detection.
17.0	Delta Pressure Valve	Upstream orifice clogs (P supply)	Supply pressure decreases. Propeller pitchlocks.	IV	D	The system is equipped with a Main and Standby filter. In addition, the orifices have their own screens.
		Downstream orifice clogs (P drain)	Backup pressure increases. Main and Standby Regulating Valve shifts to bypass less flow. Supply pressure increases until High Pressure Relief Valve opens.	IV	D	The system is equipped with a Main and Standby filter. In addition, the orifices have their own screens. The system will operate at the High Pressure Relief Valve setting. Supply pressure is monitored for failure detection.
18.0	Main and Standby Regulating Valve	Seized (No Supply pressure bypass position)	System pressure increases to cracking pressure of High Pressure Relief Valve.	IV	C	The system will operate at the High Pressure Relief Valve setting.
		Seized (Supply pressure bypass position)	Main and Standby Pump output is bypassed to drain. Propeller will pitchlock.	IV	C	
19.0	Servo Governor	Valve seizes in increase pitch position or Speeder Spring/Speed Set Linkage failure causes valve to go to increase pitch position.	Propeller will feather.	IV	E	This is a rotating valve and thus a seizure is extremely unlikely. The linkage and spring are conservatively designed.
		Valve seizes in decrease pitch position or loss of fly weights or Governer drive.	Blade pitch moves to decrease pitch position. Propeller overspeeds.	IV	E	This is a rotating valve and thus a seizure is extremely unlikely. The aircraft supplied electrical overspeed governor will activate the Feather Solenoid and maintain RPM at overspeed setting. Pilot may feather the propeller.

UNITED TECHNOLOGIES HAMILTON STANDARD

FAILURE MODE & EFFECT ANALYSIS

SYSTEM LAP 108 Prop-Fan
SUBSYSTEM Control Housing
DRAWING NO. L-14325-3

REPORT
DATE 6/29/84 PAGE 5 OF 9
PREPARED BY T. Sutak/R. Schwartz
FILE REF 6970A, 6971A

ITEM	PART OR ASSEMBLY DESCRIPTION	MODE OF FAILURE	EFFECT OF FAILURE ON THE SYSTEM	HAZ. CAT.	HAZ. PROB.	REMARKS
20.0	Feathering Solenoid	Solenoid will not actuate open	Feather valve will not move to feather position hydraulically.	IV	C	Propeller can be moved to the feather position manually via the feather cam.
		Solenoid will not actuate closed	Propeller cannot be moved from the feather position. No windmill start possible.	IV	C	System pressure acts to close the solenoid valve.
		Solenoid leaks to Atmospheric sump	Pitch change oil at supply pressure leaks to Atmospheric Sump. If leakage is slight, no effect on system. If leakage is severe, maximum slew rate of propeller is reduced. Response to transients may be slowed.	IV	C	
21.0	Feather Valve	Seized (Unfeathered Position)	Main Pump output continues to flow to Servo Governor. Standby Pump output continues to flow to Main and Standby Regulating Valve. Constant speed governing continues. Propeller cannot be feathered.	II	D	
		Seized (Feathered Position)	Inability to unfeather propeller for windmill start.	III	D	
		Mechanical linkage broken/jammed	Propeller cannot be feathered manually.	III	D	Propeller may still be feathered by actuating the Feather Solenoid.
22.0	Atmospheric Breather	Total clogging	Front and Rear Lip Seal failure due to high pressure possible. Propeller may pitchlock.	IV	D	
23.0	Seals	Overboard seal leakage	If leakage is severe, propeller will pitchlock.	IV	D	Leakage will be visible during normal walk around check.
		Pressurized Sump to Atmospheric Sump leakage.	Sump pressurization is lost. Main and Standby Pump cavitation is possible. Maximum slew rate of propeller is reduced. Response to transients may be slowed.	IV	D	

UNITED TECHNOLOGIES HAMILTON STANDARD

FAILURE MODE & EFFECT ANALYSIS

SYSTEM LAP 108 Prop-Fan

SUBSYSTEM Control Housing

DRAWING NO. L-14325-3

REPORT

DATE 6/29/84 PAGE 6 OF 9

PREPARED BY T. Sutak/R. Schwartz

FILE REF 6970A, 6971A

ITEM	PART OR ASSEMBLY DESCRIPTION	MODE OF FAILURE	EFFECT OF FAILURE ON THE SYSTEM	HAZ. CAT.	HAZ. PROB.	REMARKS
23.0	Seals (cont'd)	Supply or Standby flow to either Pressurized or Atmospheric sump.	Maximum slew rate of propeller is reduced. Response to transients may be slowed. If leakage is severe, supply pressure will decrease and propeller may pitchlock.	IV	D	System Supply pressure is monitored.
		Supply Pressure leaks to Governor Metered Pressure.	If leakage is minor: maximum slew rate of propeller is reduced. Shift in operating RPM occurs. Response to transients may be slowed. If leakage is severe: blade pitch moves to decrease pitch position. The propeller overspeeds.	IV	D	The aircraft supplied electrical overspeed governor will activate feather solenoid and maintain RPM at overspeed setting. Pilot may feather the propeller. Where probability is higher (i.e. dynamic seals) Supply and Metered pressure are separated by drain pressure.
		Metered Pressure leaks to drain	If leakage is excessive, the propeller will feather. Shift in operating RPM occurs. Response to transients may be slowed.	IV	D	
		Supply Pressure leaks to Delta P valve signal	Main and Standby Regulating Valve function is lost. System continues to function normally on the High Pressure Relief Valve.	IV	D	
24.0	Delta Pressure Regulating Valve	Valve Seizes (Supply Pressure ported to Metered Pressure)	Metered pressure rises to Supply pressure. Propeller overspeeds.	IV	D	Valve generates sufficient force to overcome 20 lbs of resistance. The aircraft supplied electrical overspeed governor will activate feather solenoid and maintain RPM at overspeed setting. Pilot may feather the propeller.
		Valve Seizes (Metered Pressure ported to Sump)	Metered pressure is ported to sump. Servo moves to increase pitch.	IV	D	
		Valve seizes in null position	Excessive forces are applied to the actuator linkage.	III	E	

UNITED TECHNOLOGIES HAMILTON STANDARD

FAILURE MODE & EFFECT ANALYSIS

SYSTEM LAP 108 Prop-Fan
SUBSYSTEM Pitch Change Actuator
DRAWING NO. L-14325-3

REPORT
DATE 6/29/84 PAGE 7 OF 9
PREPARED BY T. Sutak/R. Schwartz
FILE REF 6970A, 6971A

ITEM	PART OR ASSEMBLY DESCRIPTION	MODE OF FAILURE	EFFECT OF FAILURE ON THE SYSTEM	HAZ. CAT.	HAZ. PROB.	REMARKS
25.0	Actuator Valve	Valve seizes in null position	Actuator Valve and pitch change actuator remain in position at time of failure. Propeller remains in fixed position.	IV	D	
		Valve seizes in position other than null	Actuator moves in direction of last called for signal until valve moves or actuator linkage failure occurs. If failure is in decrease pitch direction: propeller will pitchlock. If failure is in increase pitch direction: propeller will feather.	III	D	Very large actuator force is available to move Actuator Valve.
26.0	Ballscrew/Quill Shaft	Ballscrew/Quill Shaft fails open	Servo output does not drive Actuator Valve. Dependent upon vibration levels, and friction, Actuator Valve may move to increase pitch, decrease pitch, or null position. If increase or decrease direction, blade angle changes slowly. The blade angle is limited by the low pitch stop in the decrease pitch direction.	III	D	Actuator Valve seal friction acts to hold valve in position. Propeller speed is controllable by reduction in engine power level and aircraft speed.
27.0	Pitchlock Screw	Pitchlock Screw fails open	Servo output does not drive Actuator Valve. Dependent upon vibration levels, and friction, Actuator Valve may move to increase pitch, decrease pitch, or null position. If increase or decrease direction, blade angle changes slowly. The blade angle is limited by the low pitch stop in the decrease pitch direction.	IV	E	There is a high probability of loads overcoming valve seal friction. Propeller speed is controllable by reduction in engine power level and aircraft speed.
28.0	Actuator Valve Drive Rod	Actuator Valve drive rod fails open	Servo output does not drive Actuator Valve. Dependent upon vibration levels, and friction, Actuator Valve may move to increase pitch, decrease pitch, or null position. If increase or decrease direction, blade angle changes slowly. The blade angle is limited by the low pitch stop in the decrease pitch direction.	IV	E	There is a low probability of loads overcoming Actuator Valve seal friction. Propeller speed is controllable by reduction in engine power level and aircraft speed.
29.0	Servo	Seizes	Servo becomes locked in position. Propeller will remain fixed in position at time of failure.	IV	D	

UNITED TECHNOLOGIES HAMILTON STANDARD

FAILURE MODE & EFFECT ANALYSIS

SYSTEM LAP 108 Prop-Fan

SUBSYSTEM Pitch Change Actuator

DRAWING NO. L-14325-3

REPORT

DATE 6/29/84 PAGE 8 OF 9

PREPARED BY T. Sutak/R. Schwartz

FILE REF 6970A, 6971A

ITEM	PART OR ASSEMBLY DESCRIPTION	MODE OF FAILURE	EFFECT OF FAILURE ON THE SYSTEM	HAZ. CAT.	HAZ. PROB.	REMARKS
30.0	Pitch Control Actuator	Actuator seizes	Actuator remains fixed in position at time of failure. No pitch change possible, propeller remains at fixed pitch.	IV	D	
		Fails open	Propeller goes to low pitch. Propeller overspeeds, blade angle is uncontrollable.	II	E	Pitch Control Actuator is designed as a primary structure and as such, this failure is considered unlikely.
31.0	Anti-torque Quill	Fails open	Actuator will rotate with respect to blade trunions until blades disengage. Propeller overspeeds, blade angle is uncontrollable.	II	E	Pitch Control Actuator is designed as a primary structure and as such, this failure is considered unlikely.
32.0	Dome/Actuator	Fails open (loss of Barrel lubricating oil)	Loss of lubricating oil for ball-screw bearings, trunion rollers, and sliding components. Wear increases.	IV	E	External leakage is visually detected on normal walk around check.
33.0	Seals and Transfer Tubes	Supply to Governor Metered Pressure leakage	Propeller goes to decrease pitch. Propeller will overspeed.	II	E	All dynamic seals for Supply to Governor Metered pressure are separated by drain pressure. The aircraft supplied electrical overspeed governor will activate feather solenoid and maintain RPM at overspeed setting. Pilot may feather the propeller.
		Governor Metered Pressure to Pressurized Sump leakage	Shift in operating RPM occurs. Maximum slew rate of propeller is reduced. Response to transients may be slowed. If leakage is severe, propeller will feather.	IV	C	
		Actuator Metered Pressure leaks high to low	Maximum slew rate of propeller is reduced. Response to transients may be slowed. If leakage is severe, propeller will pitchlock.	IV	C	
		Any leakage to Barrel cavity	Maximum slew rate of propeller may be reduced. Response to transients may be slowed. If leakage is severe, control may run dry, propeller will pitchlock. Barrel pressure increases with blade seal leakage possible.	IV	C	Oil level in Barrel and Control should be checked periodically.

UNITED TECHNOLOGIES HAMILTON STANDARD

FAILURE MODE & EFFECT ANALYSIS

SYSTEM LAP 108 Prop-Fan

SUBSYSTEM Pitch Change Actuator

DRAWING NO. L-14325-3

REPORT

DATE 6/29/84 PAGE 9 OF 9

PREPARED BY T. Sutek/R. Schwartz

FILE REF 6970A, 6971A

ITEM	PART OR ASSEMBLY DESCRIPTION	MODE OF FAILURE	EFFECT OF FAILURE ON THE SYSTEM	HAZ. CAT.	HAZ. PROB.	REMARKS
34.0	Transfer Bearing	Seizure (Supply Pressure leaks to drain)	Maximum slew rate of propeller is reduced. Response to transients may be reduced.	IV	C	
		Seizure (Supply Pressure leaks to Metered Pressure)	Propeller moves toward decreased pitch. Propeller rpm increases.	IV	C	Propeller speed is controllable by reduction in engine power level and aircraft speed. Propeller may be feathered by the feather valve.
		Seizure (Metered Pressure leaks to drain)	Propeller feathers	IV	C	
35.0	Barrel	Fracture (cracks through the wall)	Loss of blade retention and trunion lubricating oil	II	E	Barrel is designed as a primary structure and as such this failure is considered unlikely. External leakage will be visible during normal walk around check.
36.0	Blade Retention	Fracture of Balls/Races or Spalling	Maximum slew rate of propeller is reduced. Response to transients may be slowed.	III	E	
37.0	Trunion	Fracture	No response to pitch change inputs for affected blade.	III	E	Remaining blades will respond to pitch change inputs.
38.0	Propeller Blade	Separation of shell	Loss of blade performance.	III	E	Propeller can be moved to the feather position.
		Spar separation	Loss of blade retention and trunion lubricating oil.	II	E	Blade Spar is designed as a prime structure and as such this failure is considered unlikely.

9.0 Conclusion

The main purpose of this report is to review the loads and stresses at the system interfaces. As explained in the introduction, some of the loads used to size the component interfaces were "best estimates" based on preliminary analysis and previous experience. Some of the estimated loads used in the analysis were higher than the final loads, while other estimates were lower. Where the final loads were lower, the stress analysis was conservative and there is, obviously, no problem. Where the final loads were greater than the estimated loads, the re-evaluated stresses still indicated that all the system components have adequate life for the program. The retention components that do not meet the LCF requirements or the overspeed requirements, are either repairable or replaceable.

This report also reviews the coordination efforts performed to confirm that the system interfaces are dimensionally compatible. The designers provided an early check in the layout phase that was verified in the detailing and checking phases. At the time this report was being written, the final system assembly drawing was in process; no dimensional problems (fits, clearances etc.) had been found to date.

In evaluating the results of the design, it is important to remember the intent of the program. The 9 ft. diameter Prop-Fan was designed to demonstrate the feasibility of a large scale (nearly full size) Prop Fan. It was intended to show that the shape of the earlier model blades could be scaled up to meet the performance requirements while still meeting stability and stress requirements. The highlights of the component design interface reviewed above indicate that the Prop-Fan final design will meet the objectives.

10.0 APPENDIX

10.1 Design Requirements for SR-71 Propeller; 267X-1

DESIGN REQUIREMENTS

FOR

SR-7L PROPELLER

267X-1

May 6, 1983

Revised 12-1-83

Revised 4-11-84

Prepared by: _____

Approved by: _____

_____

_____

LIST OF FIGURES

1. Velocity vs. Altitude

2. Power vs. Altitude

3. Temperature vs. Altitude

4. Blade Design Cases

5. Blade Analysis Cases

6. Spinner Contour

7. CTM vs. Blade Angle

8. ATM vs. Blade Angle

9. Input Lever Schedule

10. T-56 Installation Sketch

1.0 INTRODUCTION

In recent years, considerable attention has been directed toward reducing aircraft fuel consumption. Studies have shown that the inherent efficiency advantage that turboprop propulsion systems have demonstrated at 0.65 Mn may now be extended to the higher cruise speeds of today's turbofan powered aircraft. To achieve this goal, propeller designs require advancements such as thin high-speed airfoils and aerodynamic sweep.

A series of small-scale (24.5 inch diameter) model tests have been conducted in both UTRC and NASA wind tunnels and on a modified NASA airplane. These tests have shown that propellers with 8-10 swept blades, high tip speeds and high power loadings can offer increased fuel efficiencies at speeds up to 0.8 Mn. The next logical step is to test this advanced propeller concept (Prop-Fan) in a larger scale.

NASA contract NAS3-22394 (Propeller Blade Structure Design Study) covers the detail design (thru layout) of a large-scale blade (SR-7L) and a preliminary design of a Prop-Fan suitable for flight test in a future program. NASA contract NAS3-23051 (Large-Scale Advanced Prop-Fan Program) covers the detailing of the large-scale blade, completion of the design of the Prop-Fan, fabrication of hardware and testing of the isolated assembly at Wright Field and in the Modane wind tunnel in France. The hardware will then be used in a follow-on program where it will be run with an engine on a static test stand, in a low speed wind tunnel and on a research aircraft.

This document sets forth the requirements for the design of the SR-7L Prop-Fan.

1.1 Scope

This specification defines the requirements for the testbed Prop-Fan system (SR-7L) for the Large-Scale Advanced Prop-Fan program (LAP).

1.2 Classification

The testbed Prop-Fan shall consist of blades, disc/retention, actuator, trunnion, constant speed control, and spinner. The assembly shall mount on a 60A spline shaft. It is intended for testing at Wright Field and in a high speed wind tunnel on powered test rigs. It will also be tested statically, in a low speed wind tunnel and on a testbed airplane with an engine.

1.3 Features

- o Constant speed governing
- o Mechanical in-place pitchlock (14SF type)
- o Feather via mechanical input signal
- o Feather via electrical input signal
- o Ground adjustable low pitch stop
- o Fixed angle reverse capability
- o Electrical aux feather/unfeather motor
- o Instrumentation slipring
- o Single lever input
- o Individual replacement of blades
- o Aerodynamic spinner

2.0 APPLICABLE DOCUMENTS

2.1 HS Proposal 81A12

2.2 LAP Program Plan

2.3 LAP Work Plan

2.4 MIL-STD-810C

2.5 MIL-H-5606

2.6 L-14325-1 and -2 Prop-Fan concept

2.7 Design Requirements for Advanced Turboprop Blades (SR-7) dated February 1983

2.8 MIL-P-26366 (vibration environment)

2.9 FAR-25 (deicing)

2.10 FAR Advisory Circular 33-1B dated 4/22/70 (FOD)

3.0 PROPELLER DESCRIPTION

3.1 General -- This section defines the general requirements for the SR-7L Prop-Fan.

3.2 Description

Type:	Tractor
No. of blades:	8
Blade:	SR-7-21 (aero version 100)
Diameter:	9.00 ft (108 inches)
Direction of rotation:	Counterclockwise (left-hand blade)

Note: Unless otherwise specified, all blade angles are specified at the 3/4 station (40.5 inch radius), per aerodynamic conic.

4.0 GENERAL REQUIREMENTS

4.1 Velocity vs. altitude: See Figure 1.

4.2 Power: See Figure 2.

4.3 Tip Speed & RPM: The normal max tip speed is 800 fps (1698 RPM) and is defined as 100% RPM. Provision shall be made to test up to 105% or 840 fps (1783 RPM). The min RPM ro be tested is 600 fps (1273 RPM). As a design goal this range shall be provided without hardware changes.

4.4 Operating Condition -- The Prop-Fan shall be designed to operate satisfactorily within the temperature versus altitude limits defined in Figure 3. The system shall be capable of rotating after soaking for a period of three hours in ambient air temperatures of -65°F to +130°F. Operation is permitted as soon as engine oil temperature reaches normal engine operating limits. Maximum

4.4 (cont'd)

temperature of oil provided shall be 170°F.

4.5 Environment Conditions — The Prop-Fan shall be designed to satisfy the requirements of MIL-STD-810C for humidity, fungus, salt, spray, sand and dust.

4.6 Operating Fluid: MIL-H-5606

4.7 Oil Management — The pitch change actuator and control shall have a self-contained oil system.

The hub shall have a separate oil supply to lubricate the retention bearing races, the actuator anti-torque spline and the trunnion bearings.

The capacity of the oil tank in the control is 18 quarts.

The actuator requires 12 quarts while operating. When the propeller shuts down (at feather), 6 quarts will drain back to the control.

4.8 Deicing: Deicing heaters shall be incorporated in the blades. There shall be no provisions for deicing ring or brush block and connections at this time.

4.9 Max Loading:

a) Overspeed Limit — All elements of the rotating propeller will be designed to withstand 125% overspeed or 150% centrifugal load with no inelastic deformation.

All elements of the rotating propeller will be designed to withstand 140% overspeed or 200% centrifugal load. This includes the blade, retention, disc, and blade angle control mechanism. Local inelastic deformation will be permitted in all of these elements at this overspeed but the propeller shall be capable of feathering after exposure to 140% overspeed, but may not be operational.

4.9 b) Proof Pressure: 1.5 times normal pressure (1.5 x 1130 = 1700 psi)

c) Burst Pressure: 2.25 times normal pressure (2.25 x 1130 = 2550 psi)

4.10 Weight -- The blades and blade retention shall be designed to have weight characteristics that are representative of anticipated Prop-Fan systems for future aircraft applications.

For the rest of the system there is no weight target. This design shall be start-of-the-art and aimed at low development risk.

5.0 SPECIFIC REQUIREMENTS

5.1 Blade

5.1.1 Configuration -- Based on SR-7L version 21 (aero version 100). (Reference PDR conducted 2/25/83.)

5.1.2 Deicing -- Heater incorporated in inboard leading edge (ref. FAR-25). The heater will not be wired for use in the Prop-Fan but may be subjected to icing tests by NASA.

5.1.3 FOD Protection -- Metal sheath on outboard leading edge.

5.1.4 Flutter Margin

5.1.4.1 Stall -- Free of flutter at 100% of take-off power at 100% design speed (800 fps) at Mn = 0 to 0.2 for forward thrust and at 20% of takeoff power at 100% design speed at Mn = 0 to 0.2 for reverse thrust.

5.1.4.2 Hi-speed -- Free of flutter over the flight envelope (reference Figure 1) and range of power loadings up to 105% of deaign rotational speed (840 fps) and at 14,000 ft. altitude, the calculated flutter Mach number must be greater than 0.8 at a test rig horsepower and RPM equivalent to the design power coefficient and advance ratio to allow testing in the Modane wind tunnel.

5.1.5 Critical Speed Margins -- No 1P critical speeds shall be permitted in the operating speed range and the minimum margin shall be 40% of maximum operating speed. For 2P excitation, the ground operation critical speed margin at 800 fps shall be a minimum of 20% of Prop-Fan speed and 2P integer crossover. The flight margin shall be a minimum of 10% Prop-Fan speed and 2P integer crossover. This margin shall be reduced inversely as the exciting order is increased from 3P up to 5P. In determining these margins, the effect of blade angle on frequencies shall be determined.

5.1.6 Stress Margins -- The combined steady and cyclic stresses shall be plotted on modified Goodman Diagrams for the materials of construction. The strength boundaries shall represent a high probability of survival derived from experimental data on specimens and full-scale structures. As a minimum, the boundaries shall represent $\bar{X} - 3.5\ \sigma$ lines. The start-stop stress range shall be reflected against a boundary for a life of $50X10^3$ cycles. The high cycle combined stresses shall be reflected against a boundary for $100X10^6$ cycles or infinite life.

The maximum elastic (nominal x k_T) stressing due to 125% overspeed and the nominal stressing due to a 140% overspeed shall be kept below the 0.2% offset yield strength for homogenous metal materials. The change in elastic module shall be kept below 5% for fiber reinforced resin material regarding these same overspeed requirements.

5.1.7 Aerodynamic Excitations -- The equivalent design Excitation Factor (EF) shall be 4.5. The basic EF due to 1P only is 3.3.

5.1.8 FOD Criteria -- The foreign objects are classified into three categories as follows: minor, moderate, and major impacts. Major and moderate impacts correlate with Group I and II definitions in FAR Advisory Circular 33-1B

5.1.8 (cont'd)

dated April 22, 1970. Minor impacts include sand, small stones, and birds up to about 4 ounces. Moderate impacts include two-inch hailstones and birds up to two pounds. Major impacts include a single bird up to four pounds. The damage criteria are as follows:

Minor Impacts - No damage allowed to basic blade structure. Operation will continue without impediment.

Moderate Impact - Damage can include loss of material or airfoil distortion. Operation shall continue at 75% power minimum for 5 minutes. No metal fragments shall be lost which can penetrate the aircraft fuselage pressure shell. Roughness shall be tolerable and as a guide, rotor unbalance force shall be kept below 5,000 pounds.

Major Impacts - Damage can include loss of material or airfoil distortion. Ability to feather the propeller must be maintained. A Shutdown must be accomplished without catastrophic effects on the airframe structure. As a guide, the rotor unbalance force shall be kept below 25,000 lbs. No metal fragments shall be lost which can penetrate the aircraft fuselage pressure shell.

5.1.9 Life and Reliability Goals -- The blade shall be designed for the following goals:

Maximum Continuous Stress Level	Infinite life
Replacement Life	35,000 hours
Mean Time Between Unscheduled Blade Removals (8 blade set) (Inherent)	50,000 hours

5.1.10 Lightning Protection -- Lightning protection shall be incorporated in the blade.

5.1.11 Design Cases -- See Figure 4

5.1.12 Analysis Cases -- See Figure 5

5.2 Disc/Retention

5.2.1 Mounting -- Shaft type, same as 54460 propeller.

5.2.2 Slip Ring -- Provision for mounting an instrumentation slip ring (provided by the Instrumentations Group) on the back of the disc.

5.2.3 Spinner -- Provision for attaching a spinner (reference Figure 6).

5.2.4 Control -- Provision for mounting a control on the tail shaft (reference 54460).

5.2.5 Stress Margin -- The maximum elastic (nominal X stress concentration factor) stressing due to a 125% overspeed and the nominal stressing due to a 140% overspeed shall be kept below the 0.2% yield strength for homogeneous metal material.

5.2.6 Life -- The disc shall have a life of 50,000 start/stop cycles. The retention bearing shall have a life of 50,000 cycles of low cycle fatigue and unlimited life under maximum centrifugal, maximum steady bending and maximum vibratory bending anywhere in the flight envelope.

5.2.7 Retention Bearing -- The retention bearing shall be capable of replacement or the disc shall include provisions for up to three (3) regrinds with a maximum total stock removal of 0.04.

5.2.8 Speed Pickup -- Provisions for the rotating portion of a speed pickup shall be made. This signal shall also be conpatible with synchrophasing. The device shall be the same or similar to 54460 hardware.

5.2.9 1P Shaft Moment -- The maximum 1P shaft moment is predicted to be 76,500 in.lbs at the following condition:

1698 rpm
6000 SHP
M_{η} = 0.2 (132 KEAS S.L. S.D.)
EF = 3.3

5.3 Pitch Change Actuator/Trunnions

5.3.1 General Requirements -- Any malfunction of the pitch change actuator will cause the system to pitchlock or feather. The actuator shall be modular to the extent that is practical for the test program.

5.3.2 In-place Pitchlock -- An in-place pitchlock shall be provided to limit the max loss of blade angle to approximately 1 degree below the governor scheduled blade angle. The minimum pitchlock gap shall allow the pitch change system to slew at a rate of approximately 9 degrees/sec.

5.3.3 Ground Adjustable Low Pitch Stop -- A ground adjustable low pitch stop is provided for reverse blade angle ground testing. The stop shall be set to limit in-flight blade angle from going below $+40^{\circ}\beta$. The stop shall be adjustable between $-10^{\circ}\beta$ and $+40^{\circ}\beta$ for reverse testing. The low pitch stop shall be readily adjustable without dismantling the pitch change system.

5.3.4 Feather -- The pitch change system shall be capable of feathering the propeller to an angle of 87.5 degrees $\pm$ 2.5° with an accuracy of 0.1°.

5.3.5 Reverse -- The actuator shall provide the travel necessary to give a reverse blade angle of -10° set by the adjustable low pitch stop. The actual minimum blade angle will be established by blade-to-blade interference. There is no beta control to the reverse angle.

5.3.6 Actuator Sizing

5.3.6.1 Aerodynamic Sizing Criteria

CTM (Centrifugal twisting moment):	See Fig. 7
ATM (Aerodynamic twisting moment):	See Fig. 8
FTM (Frictional twisting moment):	$CL \times \frac{PD}{2} \times .005$
CL (Centrifugal Load):	82,900 lbs. at 1698 rpm
TTM (total twisting moment):	CTM + ATM + FTM

A contingency allowance of 20% shall be added to the ATM and CTM of Figs. 7 and 8.

5.3.6.2 The pitch change system shall be capable of increasing blade angle with a 10 psi margin over the operating range of Figure 1 at 110% rpm (1868 rpm) and 0 SHP.

5.3.6.3 The pitch change system shall be capable of changing blade angle at 9 deg/sec over the operating range of Figure 1 at 100% rpm (1698 rpm) at 80% (4800) SHP.

5.3.7 Life -- The minimum design fatigue life shall be 10,000 start/stop cycles, with a flight cycle time of 1.5 hours.

5.3.8 Instrumentation -- Provision to measure both high and low pitch pressure during operation shall be provided. (Pressure sensors to be provided by the Instrumentation Group.) Provision to measure blade angle shall be provided.

5.3.9 Time Constant -- The actuator loop time constant shall be 0.25 sec at no load.

5.4 Control

5.4.1 Configuration -- Based on 739000-1 (54460/E2).

5.4.2 Control Schematic

a) Present 54460 Control (SK90621)

b) Modified schematic for LAP (L-14325-3)

5.4.3 Governing Range -- 1273 to 1783 rpm (600 to 840 fps) (75 to 105%)

5.4.4 Operating Pressure

Supply - 1050 to 1130 psig
HPRV setting - 1150-1375 psi
Pump Pulsation - 1150 $\pm$ 175 psi

5.4.5 Pump Flow

62.2 qts/min at 100% rpm, 1125 psi, 170°F

46.6 qts/min at 75% rpm, 1125 psi, 170°F

5.4.6 Leakage

5.4.6.1 Control - 1.5 qts/min at 100% rpm, 170°F

5.4.6.2 Transfer Bearing - 3.7 qts/min at 100% rpm, 170°F

5.4.6.3 Pitch Change - Null 13 qts/min at 100% rpm, 170°F
- slewing 1.1 qts/min at 100% rpm, 170°F

5.4.7 Net Flow - 55.9 qts/min slewing at 100% rpm, 170°F

5.4.8 Cooling Requirements - Cooling for the control shall be provided by an airframe supplied heat exchanger. The heat exchanger must remove 550 btu/min from the control hydraulic oil. Circulation of the control oil through the heat exchanger shall be provided by an airframe supplied pump. Fittings for hydraulic lines to and from the heat exchanger shall be located at the rear of the control per L-14325-20.

Oil outlet temp of heat exchanger:	170^{O}F max
Pump outlet pressure:	30 psi max (@ 170^{O}F)

5.4.9 Input Lever - The control shall have a single lever input for feather and speed set. The shaft can be driven by either a mechanical input or electric motor. The drive is aircraft supplied. The input lever torque is 65 in.lbs. max.

5.4.9.1 Schedule — Figure 9 shows the condition lever schedule.

5.4.10 Feather -

Electrical -- A solenoid actuated by the engine overspeed governor and/or a feather button shall be provided.

Mechanical — The input lever shall be the mechanical input for feather.

5.4.11 Overspeed protection — An aircraft-supplied overspeed system shall activate the feather solenoid whenever the propeller speed exceeds 110% of 800 FPS.

5.4.12 Beta control -- There are no provisions for Beta control.

5.4.13 Unfeather — The auxiliary motor shall be used to unfeather the Prop-Fan.

5.4.14 Reverse -- Provision to run in reverse with the adjustable low pitch stop set to the desired reverse angle shall be provided.

5.4.15 Synchrophasing — Provisions to incorporate synchrophasing shall be provided within the constraints of ease of assembly and low development risk the hysteresis and backlash between the governor and the actuator shall be minimized.

5.4.16 Dynamic Response — Governor gain. 2.4^{O}/sec/% RPM at null.

5.4.17 Aux Motor & Pump — An electrical motor-driven pump is provided to assist in feathering, airstart, and for ground handling.

5.4.17 (cont'd)

- o Pressure: 1375 PSI
- o Flow: 14 qts/min
- o Voltage: 208 VAC, 3 phase, 400 cycles
- o Amperage: 15 normal, 30 at relief valve
- o Duty cycle: 5.5 HP for 10 sec
  4.5 HP for 10 sec
  15 min off

5.4.18 Life — The minimum design fatigue life shall be 10,000 start/stop cycles with a flight cycle time of 1.5 hours.

5.4.19 Instrumentation — Provision shall be made to measure supply, governor metered pressure, and stationary transfer bearing and sump temperature. (The sensors will be provided by the Instrumentation Group.)

5.4.20 Brush Block — Provision shall be made to mount an instrumentation brush block (provided by the Instrumentation Group) on the existing brush block mounting pad.

5.4.21 Speed Pickup — Provision for the stationary portion of a speed pickup shall be made. This signal shall also be compatible with synchrophasing. The device shall be the same or similar to 54460 hardware.

5.5 Spinner

5.5.1 Contour - Per Figure 6.

5.5.2 Material -

5.5.2.1 Forward - Fiberglass

5.5.2.2 Aft - Fiberglass

5.5.2.3 Bulkheads - Fiberglass

5.5.3 Deicing - Not required

5.5.4 Length - 44.5 in.

5.5.5 Blade Plug - A spinner to blade ring is required.

5.5.6 Removal/Installation — The spinner shall be designed for each of installation and removal of the forward spinner to facilitate system testing.

6.0 MAINTAINABILITY/RELIABILITY

6.1 M & R

There are no specific design requirements for maintainability and reliability. The hardware should be designed following good design practice and using state-of-the-art technique.

7.0 OTHER CONSIDERATIONS

7.1 There is the potential for a contract modification to add opposite rotation (clockwise) hardware to the program. During the design effort, ways to minimize the effect of incorporating opposite rotation should be considered. However, opposite rotation shall not be incorporated at this time.

7.2 The SR-7L will be tested on the static thrust rig at Wright Field to verify its static performance. For this test it is desirable to operate the Prop-Fan as a fixed pitch/ground adjustable unit. (The control will not be used.) Therefore, during the design of the SR-7L, Design should consider ways to incorporate a fixed pitch/ground adjustable actuator in the Prop-Fan, but this actuator shall not be designed at this time.

7.3 The SR-7L will be tested on the static thrust rig at Wright Field to explore the stall flutter boundary and in the Modane wind tunnel to explore the high speed flutter boundary. For these tests it is desirable to operate the Prop-Fan with direct blade angle control and not with speed control. To accomplish this it is envisioned that the blade angle could be varied using an external hydraulic supply directed to the high or low pitch chambers of the actuator through a commercial transfer bearing mounted on the front of the Prop-Fan. Design should consider ways to incorporate this capability in the hardware, but this hardware shall not be designed at this time.

7.4 The hardware designed in this program will be used in a future NASA Propeller Test Assembly (PTA) contract. The PTA contract will include static engine testing. At this time it is not known whether this test will be conducted on an indoor or outdoor test stand. The hardware will also be subjected to testing with an engine and wing in a low speed wind tunnel and with an engine on a testbed airplane.

8.0 PROPELLER INTERFACES

8.1 Propeller control installation drawing (Preliminary) (Ref. L14325-1 & L14325-2). This drawing defines the concept and interface between the propeller, the pitch change system, the control, and the gearbox.

8.2 Hub/Flange/Control Mounting — See Figure 10 (T56).

8.3 Slip Ring — A slip ring will be provided for instrumentation only. The brush block will mount on the control in place of the deicing brush block. The slip ring and brush block shall be supplied by the Instrumentation Group.

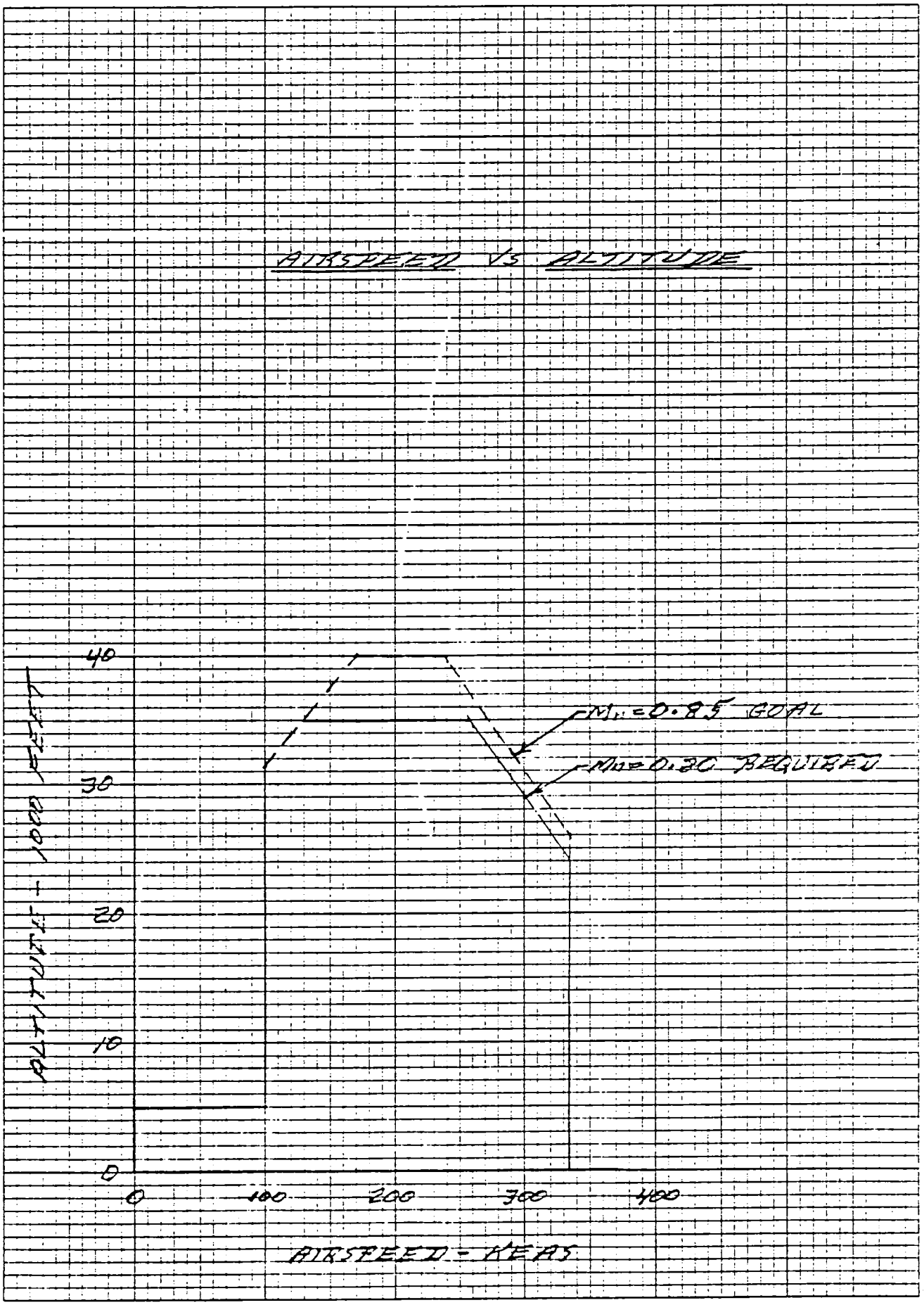

FIGURE 1

ENGINE POWER VS. ALTITUDE

SHP	Mn	Altitude	SHP/D^2	Tip Speed
6000	0-0.2	Sea Level	74.1	800 ft/sec
5400	0.5	10,000 ft.	66.7	800
4500	0.6	20,000	55.6	800
3820	0.8	30,000	47.2	800
3240	0.8	35,000	40.0	800
2025	0.8	35,000	25.0	600

FIGURE 2

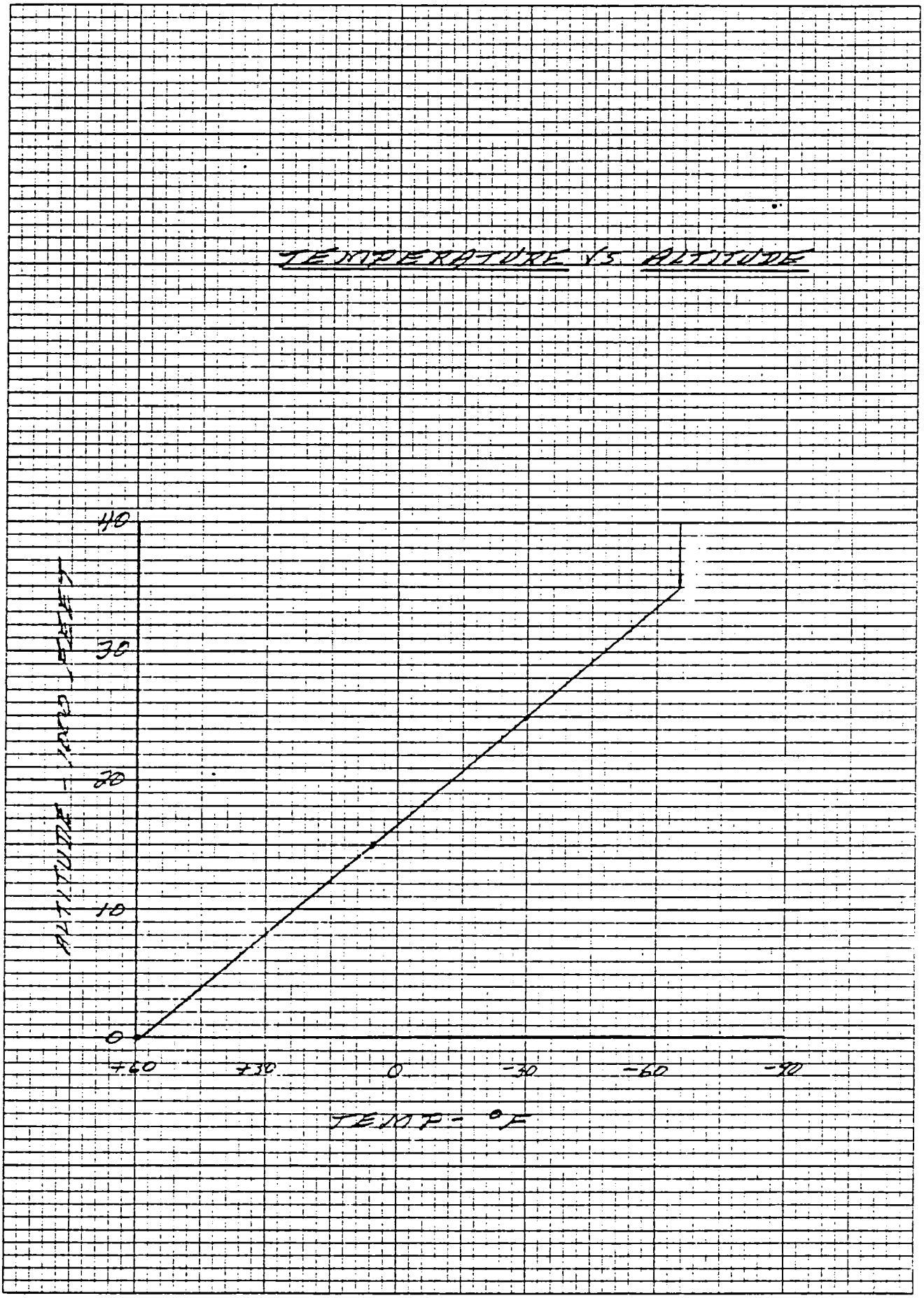

FIGURE 3

DESIGN CASES FOR SR-7L BLADE

CASE	CONDITION	Mn	ALTITUDE	HP	SHP/D^2	TIP SPEED	RPM	EF
1	Cruise	0.8	35,000 ft.	2592	32	800 fps	1698	4.5
2	Min Climb	0.2	Sea Level	6000	74.1	800 fps	1698	4.5
3	25% O'speed	0.8	35,000 ft.	0	0	1000 fps	2122	0
4	40% O'speed	0.8	35,000 ft.	0	0	1120 fps	2377	0

ANALYSES TO BE CONDUCTED

CASE	FLUTTER STALL	FLUTTER HI SPEED	CRITICAL SPEED MARGINS	STRESS MARGINS	FOD
1	No	Yes	Yes	Yes	No
2	Yes	No	Yes	Yes	Yes
3	No	No	No	Yes (steady)	No
4	No	No	No	Yes (steady)	No

FIGURE 4

Revised 9/15/83

SR-7L BLADE - CONDITIONS TO BE ANALYZED

1. Wind Tunnel*	0.8 Mn	14,000 ft.	1050 HP	13 SHP/D^2	800 fps	1698 rpm	4.5 EF
2. Static	0	Sea level	6000	74.1	800	1698	0
3. Reverse	0	Sea level	1200	14.8	800	1698	0
4. Cruise-lo rpm	0.8	35,000	2025	25	600	1273	4.5
5. Cruise-hi rpm & Mn	0.85	35,000	3280	40.5	840	1783	4.5
6. Climb	0.5	10,000	5400	66.7	800	1698	4.5
7. Dive	0.6	20,000	0	0	800	1698	0
8. Dive	0.8	35,000	0	0	800	1698	0

These conditions will be analyzed--however, the blade design will not be modified based upon the results.

* Conditions shown are for 8 blades. Will be done for 2 and 4 blades also.

Figure 5

Revised 9/15/83

ANALYSES TO BE CONDUCTED

Case	Flutter		Critical Speed Margins	Stress Margins	FOD
	Stall	Hi-Speed			
1	No	Yes	Yes	Yes	No
2	Yes	No	Yes	Yes (Steady)	No
3	Yes	No	Yes	Yes (Steady)	No
4	No	Yes	Yes	Yes	No
5	No	Yes	Yes	Yes	No
6	No	Yes	Yes	Yes	No
7	No	Yes	No	Yes (Steady)	No
8	No	Yes	No	No	No

Figure 5 (continued)

Revised 9/15/83

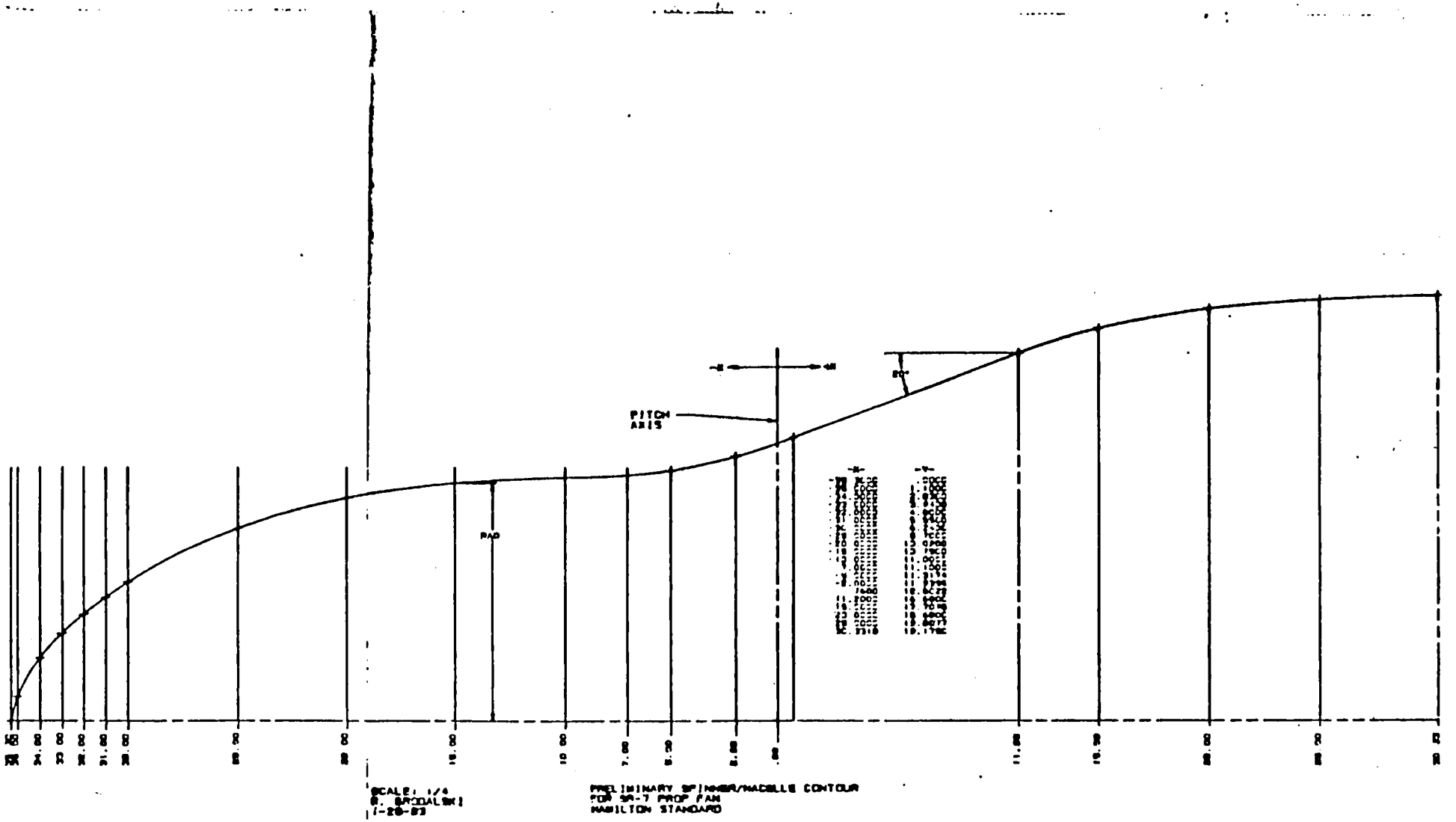
PITCH AXIS
PAD
SCALE: 1/4
PRELIMINARY SPINNER/NACELLE CONTOUR
FOR SR-7 PROP FAN
HAMILTON STANDARD

FIGURE 6

CFM VS BLADE ANGLE
5 3/4-100
BLADES 9 1/2 DIA
CFM PER BLADE
1698 RPM
CFM X 10^-3
-10
0
10
20
30
40
50
60
70
80
5
15
20
25
BLADE DEGREES

FIGURE 7

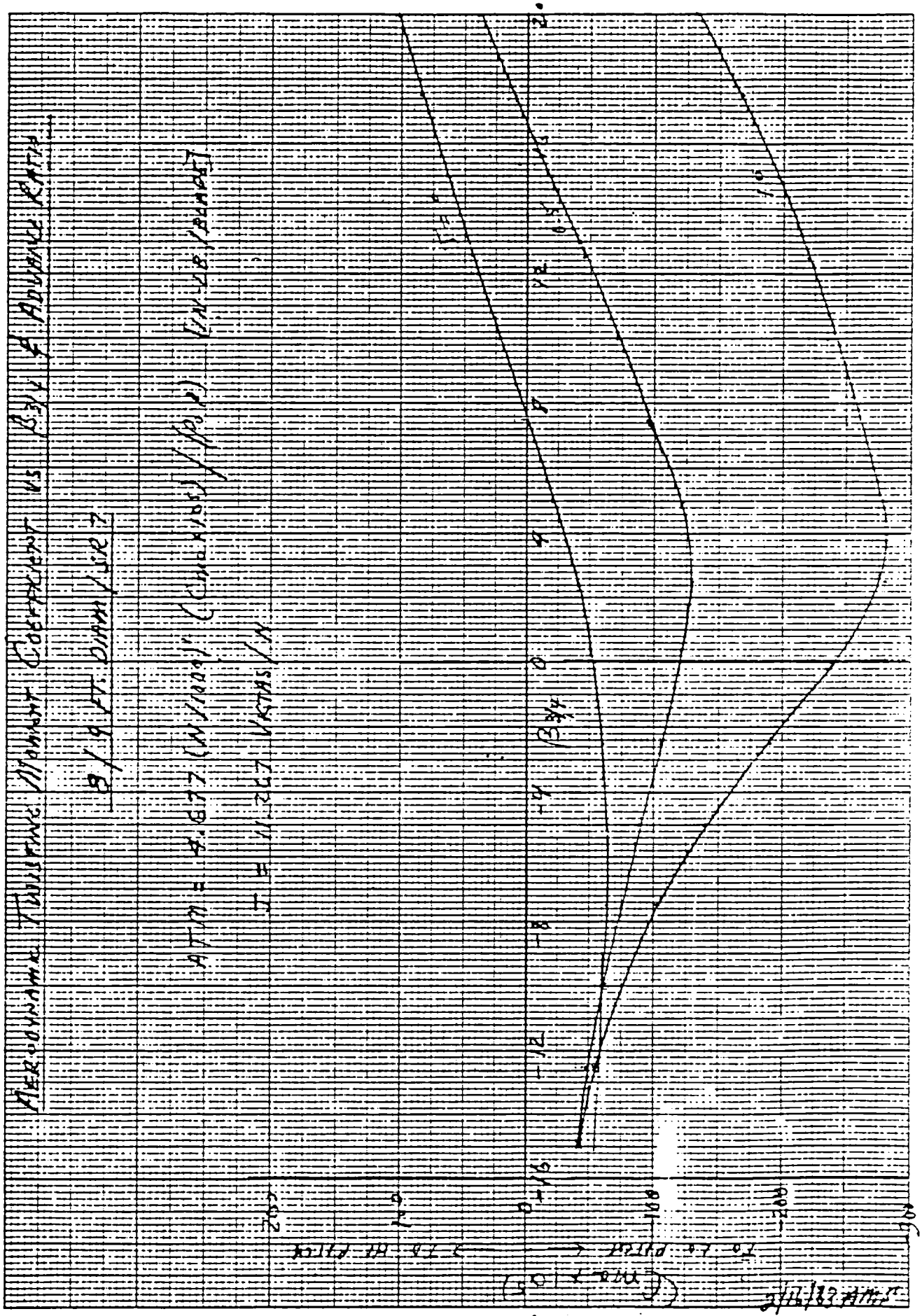

FIGURE 8

CALC. NO. 2956 C(1)

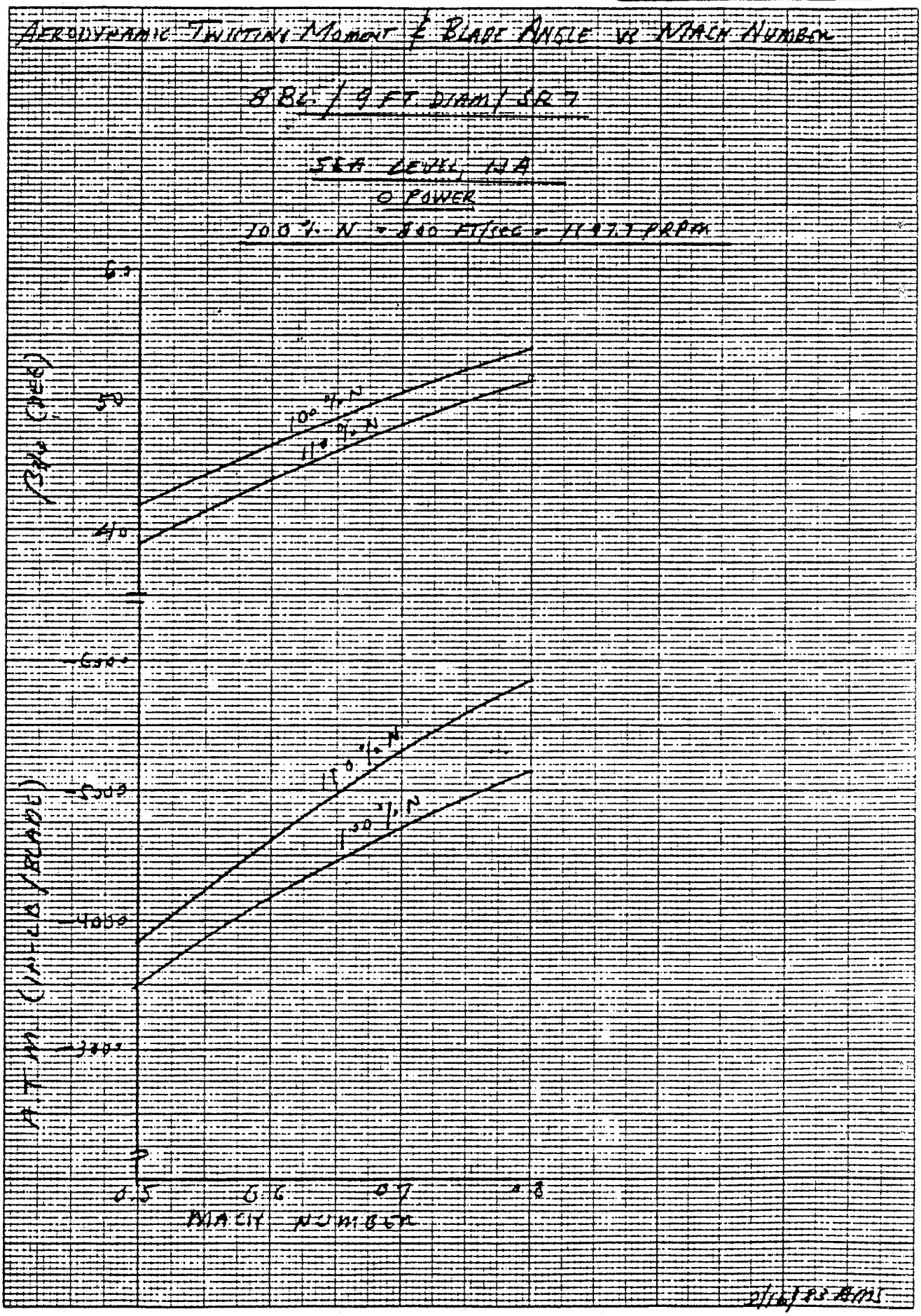

FIGURE 8 (cont'd)

INPUT LEVER SCHEDULE

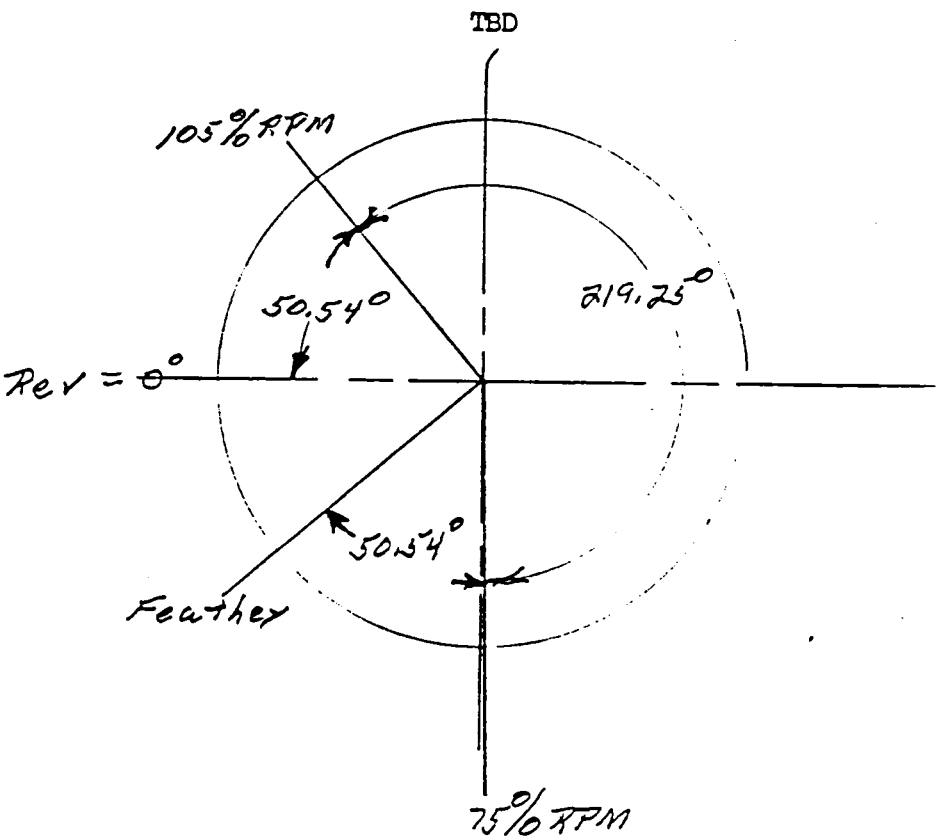

FIGURE 9

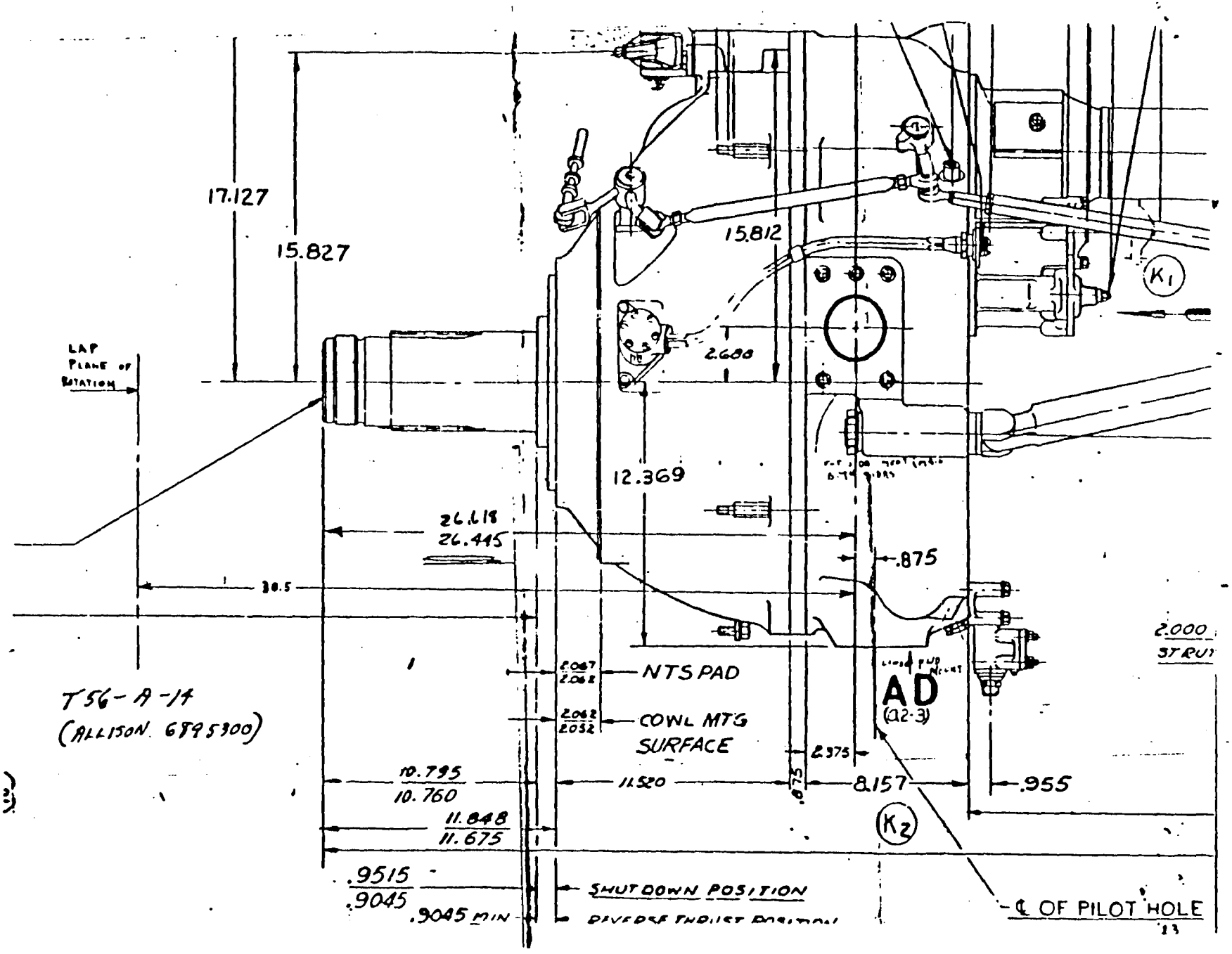
17.127
15.827
15.812
K1
LAP
PLANE OF
ROTATION
2.600
12.369
26.618
26.445
.875
30.5
2.000
STRUT
.067
2.062
NTS PAD
2.062
2.032
COWL MTG
SURFACE
AD
(12-3)
T56-A-14
(ALLISON 6B95900)
10.795
10.760
11.820
2.375
.875
8.157
.955
11.848
11.675
K2
.9515
.9045
.9045 MIN
SHUTDOWN POSITION
℄ OF PILOT HOLE

FIGURE 10